Uptake of nanoparticles by cells in experiments and models

The role of particle properties, test conditions and cell type

Katja Kettler

ISBN
978-94-028-1037-0

Design/lay-out
Promotie In Zicht, Arnhem

Print
Ipskamp Printing, Enschede

Uptake of nanoparticles by cells in experiments and models

The role of particle properties, test conditions and cell type

Proefschrift

ter verkrijging van de graad van doctor
aan de Radboud Universiteit Nijmegen
op gezag van de rector magnificus prof. dr. J.H.J.M. van Krieken,
volgens besluit van het college van decanen
in het openbaar te verdedigen op woensdag 13 juni 2018
om 10.30 uur precies

door

Katja Kettler
geboren op 5 januari 1986
te Duisburg, Duitsland

Promotoren
Prof. dr. ir. A.J. Hendriks
Prof. dr. ir. D. van de Meent

Manuscriptcommissie
Prof. dr. A.M.J. Ragas (Open Universiteit, voorzitter)
Prof. dr. A.M. Breure
Prof. dr. ir. W.J.G.M. Peijnenburg (Universiteit Leiden)

Paranimfen
Leonie Lautz
Renske Hoondert

Contents

1

General introduction

Definition of nanoparticles

Engineered Nanomaterials (ENMs) are used in increasing numbers of applications due to their physico-chemical properties [1, 2]. The increasing production volume and the increasing range of NM-containing products lead to increased likelihood of unintentional release. Determined negative side effects at cellular, as well as whole organisms level, after exposure have led to serious concerns about NM safety [3, 4].

The term 'nano' relates to the Greek word 'νᾶνος' (Latin 'nanus'), meaning "dwarf". Scientifically it is used as a prefix in the international system of units to describe a billionth or 10^{-9} of a unit, e.g. nanometer (nm). As an example, 1 nm is about the size of 3 gold atoms aligned in a row. The diameter of the DNA helix measures approximately 3 nm. By definition of the European commission, a material is considered a nanomaterial if any of its external dimension falls within the nanoscale of 1-100 nm or if the material has internal or surface structures within this size range [5]. Hansen et al. further distinguish classes of NMs based on the location of the nanoscale structure within a material [6]:

a) Nanostructured materials in 3 dimensions that make up the bulk material
b) Nanostructured surfaces
c) Free structures at nanoscale in at least 2 dimensions; they can be surface bound, suspended in solids, suspended in liquids or airborne

With their very small size NMs fall within the same size range as biomolecules. These include essential proteins necessary for cell growth, DNA, and viruses. NMs are much smaller than an average, eukaryotic cell with average sizes between 10- $30{\cdot}10^3$ nm, e.g. red blood cells. To differentiate between naturally occurring particles in the nanometer range and those intentionally produced, the definition is further extended. It includes the requirement that the decrease to nm scale goes along with a change in the material's property in comparison to the bulk material of the same chemical composition [6]. These are the so called Engineered NMs. As we are interested in the interaction of ENMs with biological systems, we focus on free nanostructures of category c within this study. More specifically, on those that are suspended in water or that are airborne. In addition, we limit our investigations to those NMs that fall within the nanoscale in all three dimensions to avoid possible overlaps with well-studied structures in the micrometer range, e.g. asbestos. We call free 3D nanostructures nanoparticles (NPs).

Nanoparticle properties and applications

NPs are used in increasing amounts and number of applications due to the described differences in physico-chemical properties in comparison to bulk material of the same chemical composition [5].

The physical properties of NPs are determined by their particulate nature at small size scales. They therefore represent a special form of solid matter. The difference in the material's properties in comparison to the bulk material of the same chemical composition is due to the increased surface area to volume ratio. A relatively larger part of the atoms or molecules making up the free 3D solids are surrounded by a liquid or air phase; in contrast to microparticles where a relatively large part of the atoms or molecules in a solid is surrounded by molecules or atoms of the same kind.

NPs show large variation with respect to their chemical composition due to different core materials and surface modifications. This, in turn, results in differences in their size, charge, hydrophilicity, and chemical and biological reactivity. The changes include, but are not limited to, electrical and optical properties, increased reactivity due to the increased surface area to volume ratio, solubility, melting temperature, and hardness [7-9]. These changes allow for many new applications, e.g. as catalysts, in the field of electronics, in optical systems, as well as in the medical field for therapy, imaging, and in diagnostics [10-14]. Also consumer products such as sportswear, deodorants or sprays for textiles and shoes are claimed to contain nanoparticles [15-18]. This huge variety in applications is possible due the large variation in the NPs itself. They can consist of different core materials (organic and inorganic) and have various surface coatings, leading to differences in their charge, hydrophobicity and lipophilicity.

Uptake mechanisms and biological effects

Many of the medical applications are based on the fact that the applied NPs are able to enter cells. The negative experiences with microparticles, such as asbestos, and the similar size of NP and biological entities taken up by cells, has resulted in serious concerns about possible negative side effects of NPs [19-26]. This leads unavoidably to the question about their biocompatibility after unintentional exposure. In this context biocompatibility refers to "being biologically compatible by not producing a toxic, injurious, or immunologic response in living tissue" [27]. In general, four different exposure routes for NPs exist: dermal uptake, ingestion, inhalation, and injection of nanomedicine. Inhalation is considered the main exposure route during production and handling of NPs, as well as during application of NP-containing sprays [16, 18].

Similar to microparticles, NPs have been shown to induce adverse effects at the cellular level by interacting with vital cell components, such as the cell membrane. In addition, NPs may reach and harm intracellular targets such as mitochondria, the nucleus and DNA. NPs may interact with mitochondrial respiration [28], deplete antioxidant species inside the cell [29], and bind to DNA [30]. Some NPs have been shown to enter cells and cause changes in their morphological structure, leading to decreased cell attachment and impaired cell division [31]. Mutagenesis, protein up/down regulation, apoptosis, oxidative stress and DNA damage are possible adverse outcomes [32, 33]. In contrast to traditional chemicals, NPs generally do not reach the cell interior through passive diffusion but via an active uptake process called endocytosis. NP uptake has been shown to take place via an energy dependent, therefore active, uptake mechanism. This has been shown through its strong decrease at low temperature, when cells are inactivated, or imaging of endocytic vesicles [34-39]. This biological mechanism enables eukaryotic cells to take up essential biomolecules from the environment, e.g. cholesterol-laden low-density lipoprotein and iron-laden transferrin. Endocytosis also includes phagocytosis, a mechanism employed by specialized cells of the immune system aimed at the destruction of foreign cells [40]. Through this mechanism NPs cross the cell membrane, the natural barrier separating the in- and exterior of a cell, allowing for the exclusion of substances [41]. The endocytosis mechanisms enable degradable NPs, such as metallic NPs, to induce stronger negative side effects than metal ions of the same concentration [21, 42]. Some degradable NPs are able to enter cells and release ions at the inside of a cell, resulting in further reactions [43, 44]. They gain access to the cellular machinery usually unavailable for the same chemicals in ionic form. NPs may, therefore, enter through a so called "Trojan horse effect" and increase the intracellular bioavailability [42]. Also non-degradable materials described as inert in their bulk from, such as gold, may cause negative side effects *in vitro* and *in vivo* when sized down to NPs. Uptake and possible accumulation in cells (or organisms) causes particular concerns due to the effect on internal cellular structures and hindering of processes purely through the physical presence (of chemically inert) NPs. Such secondary effects may trigger growth of defective living tissues on the long run [31]. NPs may cause injury by uptake and nonoxidant paradigms, so without the disturbance of the normal redox state of a cell. Such described hazardous effects on the cellular level might also lead to repercussion on the individual [45], populations [46] or even entire food webs through trophic transfer and biomagnification [47-52].

Risk assessment of NPs

A risk is defined as the product of exposure and hazard [53, 54]. Both factors for a risk are fulfilled in case of NPs due to increased likelihood of exposure and shown adverse effects *in vitro* and *in vivo* [55-57]. Given the large number of NP variations, extensive and detailed testing of all NP variants for their cellular uptake and subsequent toxicity (*in vivo*) separately seems unfeasible. Keeping pace with the development of new NPs and the need to predict their potential uptake and possible subsequent negative effects to human health and the environment, requires fast and inexpensive risk assessment. Models and the construction of quantitative structure activity relationships offer unique opportunities for risk assessment [58]. Therefore, models that allow for predictions of cellular uptake, based on easily measurable NP properties, are highly desirable. Models could allow to categorize NPs according to likelihood of uptake and prioritize them for specific testing in the early phase of development and before data begin to pile up. This would highly improve and speed up the risk assessment of these diverse and fast-developing products [7-9]. Risk assessment will benefit from increasing understanding of the mechanism of nanoparticle interactions with living cells, more specifically, NP properties and experimental factors influencing cellular uptake. Due to the unique endocytic uptake mechanism employed by NPs, this new type of emerging chemicals requires new models that take this active mechanism into account.

Objectives and outline of the thesis

The aim of this thesis is: First, to identify the (main) NP properties and experimental conditions that determine cellular NP uptake. Second, to assess their suitability for modelling and third, to construct a model to describe such a relationship.

First, a literature review was conducted in order to determine the physico-chemical NP properties, in combination with characteristics of the cellular and extracellular media, which govern cellular uptake of NPs (Chapter 2). Then, we explored the effect of NP size, which has been identified as the main determinant of NP uptake, and medium composition on uptake kinetics into two different types of cells (Chapter 3, Chapter 4). Next, a new method to determine the possible dissolution of the silver NPs (Ag NPs) during the time course of the experiments was developed (Chapter 5). This was followed by the comparison of NP uptake rates across studies and the attempt to construct property-effect relationships (Chapter 6). The collected data, possible contradictions and implications were critically discussed in a synthesis (Chapter 7).

Cited Work

1. B. Nowack and T.D. Bucheli, *Occurrence, behavior and effects of nanoparticles in the environment.* Environ. Pollut., **2007**. 150: p. 5-22.
2. C. Hendren, et al., *Modeling approaches for characterizing and evaluating environmental exposure to engineered nanomaterials in support of risk-based decision making.* Environ Sci Technol, **2013**. 47: p. 1190-1205.
3. G. Oberdörster, V. Stone, and K. Donaldson, *Toxicology of nanoparticles: A historical perspective.* Nanotoxicol., **2007**. 1 (1): p. 2-25.
4. A. Kunzmann, et al., *Toxicology of engineered nanomaterials: Focus on biocompatibility, biodistribution and biodegradation.* Biochim. Biophys. Acta, **2011**. 1810: p. 361-373.
5. European Commission, *Commission recommendation of 18 october 2011 on the definition of nanomaterial (text with eea relevance).* 2011: Brussels, Belgium.
6. S.F. Hansen, B.H. Larsen, and S.I. Olsen, *Categorization framework to aid hazard identification of nanomaterials.* Nanotoxicol., **2007**. 1 (3): p. 243-250.
7. T. Pal, T.K. Sau, and N.R. Jana, *Reversible formation and dissolution of silver nanoparticles in aqueous surfactant media.* Langmuir, **1997**. 13 (6): p. 1481–1485.
8. T.W. Ebbesen, et al., *Electrical conductivity of individual carbon nanotubes.* Nature, **1996**. 382: p. 54 - 56.
9. B.R. Powell, R.L. Bloink, and C.C. Eickel, *Preparation of cerium dioxide powders for catalyst supports.* Journal of the American Ceramic Society, **1988**. 71 (2): p. C-104–C-106
10. M.G. Lines, *Nanomaterials for practical functional uses.* Journal of Alloys and Compounds, **2008**. 449: p. 242-245.
11. N.L. Rosi, et al., *Oligonucleotide-modified gold nanoparticles for intracellular gene regulation.* Science, **2006**. 312: p. 1027-1030.
12. M. Lewin, et al., *Tat peptide-derivatized magnetic nanoparticles allow in vivo tracking and recovery of progenitor cell.* Nature Biotechnology, **2000**. 18: p. 410-414.
13. R. Weissleder, *Molecular imaging in cancer.* Science, **2006**. 312 (5777): p. 1168-1171.
14. P. Fortina, et al., *Applications of nanoparticles to diagnostics and therapeutics in colorectal cancer.* Trends Biotechnol., **2007**. 25 (4): p. 145-152.
15. T. Kuiken, et al. *The project on emerging nanotechnologies.* Consumer Products Inventory 2014 [cited 2014 July 28th]; Available from: http://www.nanotechproject.org/cpi/.
16. A. Oomen, et al., *Nanomaterial in consumer products: Detection, characterisation and interpretation.* 2011, RIVM. p. 96.
17. M.E. Vance, et al., *Nanotechnology in the real world: Redeveloping the nanomaterial comsumer products inventory.* Beilstein Journal of Nanotechnology, **2015**. 6: p. 1769-1780.
18. S. Wijnhoven, et al., *Nanomaterials in consumer products: Update of products on the european market in 2010.* 2011, RIVM. p. 78.
19. R. Foldbjerg, et al., *Pvp-coated silver np and silver ions induce ros, apoptosis and necrosis in thp-1 monocytes.* Toxicol Lett, **2009**. 190 (2): p. 156-163.
20. A. Haase, et al., *Toxicity of silver nanoparticles in human macrophages: Uptake, intracellular distribution and cellular responses* in *Journal of Physics: Conference Series*. 2011.
21. M.V.D.Z. Park, et al., *The effect of particle size on the cytotoxicity, inflammation, developmental toxicity and genotoxicity of silver nanoparticles.* Biomaterials, **2011**. 32 (36): p. 9810-9817.
22. R.P. Singh and P. Ramarao, *Cellular uptake, intracellular trafficking and cytotoxicity of silver nanoparticles.* Toxicol Lett, **2012**. 213 (2): p. 249-259.
23. J. Ji, et al., *Twenty-eight-day inhalation toxicity study of silver nanoparticles in sprague–dawley rats.* Inhalaton Toxicology, **2007**. 19: p. 857–871.
24. J. Seiffert, et al. *Pulmonary toxicity of instilled silver nanoparticles: Influence of size, coating and rat strain.* PloS One, **2015**. DOI: 10.1371/journal.pone.0119726.
25. R. Silva, et al., *Pulmonary effects of silver nanoparticle size, coating, and dose over time upon intratracheal instillation.* Toxicol Sci, **2015**. 144: p. 151-162.
26. F. Christensen, et al., *Nano-silver - feasibility and challenges for human health risk assessment based on open literature.* Nanotoxicology, **2010**. 4 (3): p. 284-95.

27. in *American Heritage Dictionary of the English Language*. 2016, Houghton Mifflin Harcourt: Boston.
28. T. Xia, et al., *Cationic polystyrene nanosphere toxicity depends on cell-specific endocytic and mitochondrial injury pathways*. ACS Nano, **2008**. 2 (1): p. 85-96.
29. E.J. Park, et al., *Oxidative stress and apoptosis induced by titanium dioxide nanoparticles in cultured beas-2b cells*. Toxicol Lett, **2008**. 180 (3): p. 222-229.
30. M. Semmler-Behnke, et al., *Biodistribution of 1.4- and 18-nm gold particles in rats*. Small, **2008**. 4 (12): p. 2108-2111.
31. N. Pernodet, et al., *Adverse effects of citrate/gold nanoparticles on human dermal fibroblasts*. Small, **2006**. 2 (6): p. 766 – 773.
32. K. Unfried, et al., *Cellular responses to nanoparticles: Target structures and mechanisms*. Nanotoxicology, **2007**. 1 (1): p. 52-71.
33. K.L. Aillon, et al., *Effects of nanomaterial physicochemical properties on in vivo toxicity*. Advanced Drug Delivery Reviews. 61 (6): p. 457-466.
34. J. Rejman, et al., *Size-dependent internalization of particles via the pathways of clathrin- and caveolae-mediated endocytosis*. Biochemical Journal, **2004**. 377: p. 159-169.
35. M.J.D. Clift, et al., *The impact of different nanoparticle surface chemistry and size on uptake and toxicity in a murine macrophage cell line*. Toxicol. Appl. Pharmacol, **2008**. 232: p. 418-427.
36. W. Jiang, et al., *Nanoparticle-mediated cellular response is size-dependent*. Nat Nanotechnol., **2008**. 3: p. 145-150.
37. B.D. Chithrani, A.A. Ghazani, and W.C.W. Chan, *Determining the size and shape dependence of gold nanoparticle uptake into mammalian cells*. Nano Letters, **2006**. 6 (4): p. 662-668.
38. H. Gao, W. Shi, and L.B. Freund, *Mechanics of receptor-mediated endocytosis*. Proc. Natl. Acad. Sci. USA, **2005**. 102 (27): p. 9469–9474.
39. G.J. Doherty and H.T. Mcmahon, *Mechanisms of endocytosis*. Annual Review of Biochemistry, **2009**. 78: p. 857-902.
40. S.D. Conner and S.L. Schmid, *Regulated portals of entry into the cell*. Nature, **2003**. 422: p. 37-44.
41. B.Y. Moghadam, et al., *Role of nanoparticle surface functionality in the disruption of model cell membranes*. Langmuir, **2012**. 28: p. 16318–16326.
42. N. Lubick, *Nanosilver toxicity: Ions, nanoparticles–or both?* Environ Sci Technol, **2008**. 42: p. 8617.
43. L. Limbach, et al., *Exposure of engineered nanoparticles to human lung epithelial cells: Influence of chemical composition and catalytic activity on oxidative stress*. Environ Sci Technol, **2007**. 41: p. 4158–4163.
44. S.N. Luoma, *Silver nanotechnologies and the environment: Old problems or new challenges?* 2008, The Pew Charitable Trusts.
45. A. Kunzmann, et al., *Toxicoloy of engineered nanomaterials: Focus on biocompatibility, biodistribution and biodegredation*. Biochimica et Biophysica Acta, **2011**. 1810 (3): p. 361-373.
46. M. Ploeg, et al., *Effects of c60 nanoparticle exposure on earthworms (lumbricus rubellus) and implications for population dynamics*. Environmental Pollution (Barking, Essex: 1987), **2010**. 159 (1): p. 198-203.
47. B.P. Jackson, et al., *Bioavailability, toxicity, and bioaccumulation of quantum dot nanoparticles to the amphipod leptocheirus plumulosus*. Environ Sci Technol, **2012**. 46: p. 5550–5556.
48. J.D. Judy, J.M. Unrine, and P.M. Bertsch, *Evidence for biomagnification of gold nanoparticles within a terrestrial food chain*. Environ Sci Technol, **2011**. 45: p. 776–781.
49. C. Pang, et al., *Bioaccumulation, toxicokinetics, and effects of copper from sediment spiked with aqueous cu, nano-cuo, or micro-cuo in the deposit-feeding snail, potamopyrgus antipodarum*. Environ. Toxicol. Chem., **2013**. 32 (7): p. 1561-1573.
50. K. Tervonen, et al., *Analysis of fullerene-c_{60} and kinetic measurements for its accumulation and depuration in daphnia magna*. Environ. Toxicol. Chem., **2010**. 29 (5): p. 1072-1078.
51. A. Wegner, et al., *Effects of nanopolysytrene on the feeding behavior of the blue mussel (mytilus edulis l.)*. Environ. Toxicol. Chem., **2012**. 31 (11): p. 2490-2497.
52. J.L. Bouldin, et al., *Aquepus toxicity and food chain transer of quantum dots in freshwater algae and ceriodaphnia dubia*. Environ. Toxicol. Chem., **2008**. 27 (9): p. 1958-1963.
53. U.S.D.O.H.H. Services, in *IUPCA Glossry*. 2013.
54. J. Duffus and H. Worth, *Hazard and risk*. 2003.
55. A. Shvedova, et al., *Exposure to carbon nanotube material: Assessment of nanotube cytotoxicity using human keratinocyte cells*. Journal of Toxicology and Environmental Health, **2003**. 66 (20): p. 1909-1926.

56. C.-M. Zhao and W.-X. Wang, *Biokinetic uptake and efflux of silver nanoparticles in daphnia magna.* Environ Sci Technol, **2010**. 44: p. 7699–7704.
57. A. Hinther, et al., *Nanometals induce stress and alter thyroid hormone action in amphibia at or below north american water quality guidelines.* Environ Sci Technol, **2010**. 44: p. 8314-8321.
58. B.F. Risikobewertung. *Use of qsar in chemical assessment - bfr.* 2017 [cited 2017 12.05.]; Available from: http://www.bfr.bund.de/en/use_of_qsar_in_chemical_assessment-10429.html.

2

Cellular uptake of nanoparticles as determined by particle properties, experimental conditions, and cell type

Published in

Environmental Toxicology and Chemistry, 2014. Vol. 33, No. 3, pp. 481–492

Katja Kettler[a], Karin Veltman[a], Dik van de Meent[a], Annemarie van Wezel[b], and A. Jan Hendriks[a]

[a] Department of Environmental Science, Institute for Water and Wetland Research, Radboud University, Nijmegen, The Netherlands
[b] KWR Watercycle Research Institute, Nieuwegein, The Netherlands

Abstract

The increased application of nanoparticles (NPs) is increasing the risk of NPs being released into the environment. Although many toxicity studies have been conducted, the environmental risk is difficult to estimate, because uptake mechanisms are often not determined in toxicity studies. Here we review the dominant uptake mechanisms of NPs in cells, as well as the effect of NP properties, experimental conditions and cell type on NP uptake. Knowledge about NP uptake is crucial for risk assessment, and essential to predict the behavior of NP, based on their physical-chemical properties. Important uptake mechanisms for eukaryotic cells are macropinocytosis, receptor-mediated endocytosis and phagocytosis in specialized mammalian cells. The studies reviewed demonstrate that uptake into non-phagocytic cells depends strongly on NP size, with an uptake optimum at an NP diameter of about 50 nm. Increasing surface charges, either positive or negative, have been shown to increase particle uptake in comparison to uncharged NPs. Another important factor is the degree of (homo-) aggregation. Results regarding shape have been ambiguous. Difficulties in the production of NPs, with one property changed at a time, call for the full characterization of NP properties. Only then it is possible to draw conclusions which property affected the uptake.

Keywords
nanoparticles, bioaccumulation, cellular uptake, endocytosis, particle properties

Introduction

Nanomaterials (NMs) are defined by common consensus as particles with dimensions from 1 nm up to 100 nm (nanotechnology), even though "there is no scientific evidence to support the appropriateness of this value" [1]. Their characteristics differ from those of macroscopic bulk material of the same chemical composition. In nanomedicine, NMs are defined as particles with dimensions up to 1000 nm [2]. NMs can be further divided into three categories as proposed by Hansen et al. [3], who pointed out that clarification of the terminology is needed and proposed a new categorization of NM based on the location of the nanostructure in the material. They differentiated between three main categories of NMs: "1. Materials that are nanostructured in the bulk, 2. Materials that have nanostructure on the surface, and 3. Materials that contain nanostructured particles (...) Category III contains nanoparticles, which we define as free structures that are nanosized in at least two dimensions." In the present study, we focus on nanoparticles (NPs) belonging to category III. Nanomaterials are manufactured because of their physical and chemical characteristics, including electrical, optical, transparency, hardness, and magnetic properties. NMs are being used in increasing amounts and applications [4, 5], including their use as fillers, coatings on surfaces, gas sensors, carriers for industrial catalysts, as well as in electronics, water treatment and environmental remediation [6, 7]. In addition, NMs are increasingly used in consumer products [8], as drug delivery systems for therapy [9-11], in imaging [12, 13], and in diagnostics [14-16]. Tuning the characteristic properties yields great advantages, such as a reduction of side effects by targeted administration, and improvement of the detection sensitivity [17, 18].

Despite these advantages, possible adverse effects of NMs need to be considered, preferably during the design phase, so that design options for functionality and safety go hand in hand. Adverse effects on human or environmental health may occur as a consequence of NMs being released into the environment, for example during the production, transport, usage or waste phases of consumer products [7, 19], leading to exposure of humans and the environment. Hazardous effects of NMs have been observed at the cellular level, including the generation of reactive oxygen species, lipid peroxidation, genotoxicity and mutagenesis, apoptosis or necrosis [20], mitochondrial dysfunction and changes in cell morphology [21], with potential repercussions for the individual [22]. Potential ecotoxicity has been shown in algae, plants, fungi [23], fish, cladocerans [24], and amphibians [7], as well as in bacterial communities [8, 25-27]. Also, NMs could have adverse effects on populations [28] and entire food webs, due to trophic transfer and biomagnification [29-34]. Larger impacts on the food web dynamics are possible even at sub-lethal concentrations, due to changes in the behavior of organisms [35, 36].

Unfortunately, most of the toxicity and ecotoxicity studies have been conducted without determining the uptake mechanism in detail, as was already mentioned by Zhao et al [19]. More knowledge about the NM properties and experimental conditions that

determine the transport and uptake across cell membranes will improve our understanding of their toxicity, and such information might be helpful in designing safer NMs. Toxic effects usually originate from the presence of the toxicant inside cells [37]. In addition, toxicity is determined by the entrance route and the final intracellular localization [17]. Hence, knowledge about NM uptake is crucial to risk assessment studies on NM toxicity.

It is known that the physical-chemical properties of NMs, in combination with characteristics of the cellular and extracellular media (e.g. protein/lipid adsorption patterns) govern the localization in the target cells [38, 39]. Understanding the effects of these various properties and characteristics will also be beneficial in pharmacology. Several reviews have been published on aspects of uptake in relation to NM properties and experimental conditions. Alexis et al. [40] described the factors determining blood residence times and organ-specific accumulation of NMs, while Ahsan et al. [41] focused on uptake by macrophages. Thevenot et al. [42] reviewed uptake for implant biocompatibility purposes. Verma et al. [43] addressed various NM properties but did not include the role of experimental conditions in detail. In addition, studies have reviewed the uptake of a specific NM such as gold [44, 45]. To the best of our knowledge, however, no overall review including the most important factors controlling the cellular uptake of various NPs has so far been published.

Here we (i) review uptake mechanisms of NPs in different cell types, and (ii) identify particle properties and experimental conditions that determine transport across cell membranes, describing the mechanisms that play an important role in NP uptake. Identification and understanding of the factors that determine NP uptake by cells is the first step towards predicting NP accumulation and toxicity based on easily measurable properties, such as size and zeta potential. Such predictions have already been achieved in risk assessment of conventional chemicals [46].

Ecotoxicity studies are often conducted using whole organisms, [19, 32, 33, 36] so mechanistic studies on NP properties and their effects on non-human cell lines are very scarce, and many of the cell lines mentioned in the method section are human cell lines. Translation of information obtained from human cell lines to cells from other organisms should, in principle, be possible. Pinocytosis, one of the fundamental, vital uptake mechanisms included under the broad name of endocytosis, is carried out by most [47, 48], essentially all eukaryotic cells [49, 50], as is clathrin-mediated endocytosis [51]. Receptor-mediated endocytosis is also known to be common to virtually all eukaryotic cells, except the mature erythrocyte [52]. Some researchers have gone a step further and stated that endocytosis, which is, for example, responsible for nutrient uptake into cells [53], exists at least across most [54, 55] if not all eukaryotic cells [56]. Thus, endocytosis is ubiquitous in all eukaryotic cells, enabling comparison of results from different cell lines. Humans can come into contact with NPs by direct exposure, e.g. during handling or use of NP-containing products, or indirectly through the food chain. Since biomagnification of NPs has been suggested [57, 58] and some evidence for accumulation within the

terrestrial food chain has been presented [30], this route of human exposure should be taken into consideration in modeling. Combining modeling and empirical studies allows for a cost- and time-effective risk assessment of NPs.

Methods

The literature search was conducted via Web of Science, Google Scholar and Scopus, using the following key words: nanoparticles, (size-dependent) cellular uptake, endocytosis, particle properties, biodistribution, virus and bacteria entry, macrophages, asbestos, fine dust. The search resulted in over 100 publications, though many of them concerned toxicity rather than accumulation. The papers cover a broad range of disciplines, including biomedical and chemical engineering, environmental science, materials chemistry, medicine, pathology, microbiology as well as particle and fiber toxicology. The articles address many different cell lines, both from exchanging and non-exchanging organs, such as HeLa, SNB19, STO, A375, A549, Jurkat, and different phagocytes. Nearly 30 different cell lines were used in the various studies. The articles also cover a broad range of NP types (approx. 10) such as latex beads, silica particles, hydrogels and various metal NPs (gold, silver, iron) with a variety of surface modifications. Information on the cell lines and NP types used can be found in Supplemental Data, Table S 2.1. Data presented in Table 2.2, Table 2.1, and Table S 2.1 are directly taken from the corresponding references. If the sizes are given for single nanoparticles and no measurement of aggregation was conducted, the concept of primary particle size is assumed to be valid. If no values were given for the surface area (SA) and volume (V), the data provided on the diameter and length of the particles were used to calculate them, assuming a spherical or cylindrical shape. The most important prerequisite for the selected studies was that one NP property had been changed at a time and the respective values are presented in the article as this allows the property responsible for a change in NP uptake to be identified. Due to the limited number of studies in which only one particle characteristic was changed at a time, the only further restriction placed on the literature used for the present study was the description of the pathway of uptake.

Table 2.1 Particle properties and their effect on nanoparticle (NP) uptake into phagocytic cells.

Determinant	Phagocytosis	Reference
Ligand	Increase	[59]
Hydrophilicity	Decrease	[60-63]
Mechanical flexibility	Rigid > soft, flexible	[64]

Table 2.2 Summary of particle properties and experimental conditions and their effect on nanoparticle (NP) uptake into cells[a]

Mechanism	Phagocytosis	Macropinocytosis
Size [nm]	Ligand-induced, particulate 500-1000	Non-specific 100-5000
Cell type	Specialized mammalian	Non-specialized eukaryotic
Sphere ø [nm]		
	20>200	
	300>150, 500>150	
Shape, ø and L [nm], V [µm^3], SA [µm^2]		ø 150,
		ø 150, L 450,
	2000>4000>8000 in vivo; 1800>2500>3000 in vitro (const. ø)	
	ø 80-150 = ø 80-150, L 400-1000	ø 100, L 450, V 35.3·10^{-4}, SA 15.7·10^{-2}>ø 100, L 240, V 18.9·10^{-4}, SA 9.1·10^{-2}>ø 100, V 5.2·10^{-4}, SA 3.1·10^{-2}
Charge/ ζ-potential [mV]		
Positive	Increase	
	35>25>15	
Negative	Increase	
	-40>-25>-15	
Pos. vs. neg.	Pos. > neg.	
Functional group		
NH_2		
COOH	Increase	
OH		Increase
Opsonization/ presence of serum	No change	
	Increase	
	Decrease	

[a] The size of the NPs is defined as the diameter; the surface area is given in µm^2 and the volume in µm^3. Volume and surface area (SA) are calculated assuming spherical shape or rod-shaped NPs. In the latter case, values are calculated with the formula for cylinders when only diameter and length are given in the literature, as $V=\Pi r^2L$; $SA=2\Pi rL+2\Pi r^2$; where r represents the radius of the particle, L the length (comparable to the height of a cylinder) in

	Receptor-mediated endocytosis		
	Clathrin-mediated	Caveolae-mediated	Reference
	Vesicles approx. 120	Vesicles approx. 80	[50, 76-80]
	50>100>200>500, 1000 not taken up		[73]
	Optimum at 50		[74, 81-86]
	150>300, 150>500		[75]
L 450, V $7.9{\cdot}10^{-3}$, SA $2.5{\cdot}10^{-1}$ >ø 200, L 200, V $6.3{\cdot}10^{-3}$, SA $1.9{\cdot}10^{-1}$			[87]
V $7.9{\cdot}10^{-3}$, SA $2.5{\cdot}10^{-1}$ >ø 100, L 300, V $2.4{\cdot}10^{-3}$, SA $1.1{\cdot}10^{-1}$ (AR= const)			
ø 74, V $212.2{\cdot}10^{-6}$, SA $17.2{\cdot}10^{-3}$ >ø 14, V $1.4{\cdot}10^{-6}$, SA $0{,}6{\cdot}10^{-3}$ >ø 14, L 40, V $6.2{\cdot}10^{-6}$, SA $2.1{\cdot}10^{-3}$ >ø 14, L 74, V $11.4{\cdot}10^{-6}$, SA $3.6{\cdot}10^{-3}$			[81, 88]
ø 50, V $6.6{\cdot}10^{-5}$, SA $7.9{\cdot}10^{-3}$ >ø 14, V $1.4{\cdot}10^{-6}$, SA $0{,}6{\cdot}10^{-3}$ >ø 20, L 30, V $9.4{\cdot}10^{-6}$, SA $2.5{\cdot}10^{-3}$ >ø 14, L 50, V $7.7{\cdot}10^{-6}$, SA $3.5{\cdot}10^{-3}$ >ø 7, L 42, V $6.2{\cdot}10^{-6}$, SA $0.6{\cdot}10^{-3}$			[82]
ø 80-150 >ø 80-150, L 400-1000			[89, 90]
Increase			[75]
35>25>15			[91]
	-15>-25>-40		[75, 92]
	-43.10>-16.26		[93]
Pos. > neg.			[40, 75, 93-95]
+32.2±8.19			
>-26±1			
-42.46>+41.59			
Increase			[40, 96-98]
		Increase	[96]
Decrease, increase			[99]
			[100]
			[101-103]
			[103]
Decrease, highest for most hydrophobic NP			[104]

the case of rod-shaped particles. The mechanisms are allocated based on information from the references in the last column. If no differentiation between macropinocytosis and receptor-mediated endocytosis is recorded, the results are not allocated to a specific mechanism, but the columns are merged. Higher uptake for a defined NP in comparison with another is denoted with >.

Results and discussion

Mechanisms for the uptake of particles into cells

Cell membranes tend to be impermeable to many large particles [65, 66]. Particles can only cross the membrane if they are at most 10-30 nm in size [67] (see the more detailed discussion below). The cell membrane acts as a barrier separating the external environment from the inside of the cell, allowing substances to be concentrated in cells or excluded from cells [68]. One mechanism to overcome this barrier is endocytosis. This mechanism is exploited by viruses [66, 69-71], which have therefore become a valuable tool to study endocytosis [69]. Endocytosis and diffusion have been proposed as mechanisms for the uptake into cells of NPs with similar sizes as viruses [63, 72-75].

Endocytosis is the uptake of particulate matter, such as proteins and other nutrients, into eukaryotic cells via enclosure by the cell membrane. It is also exploited by these cells for the clearance of cell debris and foreign cells from the body. Endocytosis has been defined as "the de novo production of internal membranes from the plasma membrane lipid bilayer" [76]. Several forms of endocytosis are distinguished, based on the substance to be internalized (see Figure 2.1).

Opsonized particulate substances and small solute volumes are internalized by a mechanism called phagocytosis [69]. Opsonins are small molecules that enhance binding in phagocytosis, e.g. antibodies [105]. Particles in large amounts of solute, on the other hand, are taken up by a process termed pinocytosis. Pinocytosis can be further divided into macropinocytosis [100] and receptor-mediated endocytosis (RME) [63, 73, 74, 82]. In view of the large differences between phagocytosis and non-phagocytosis, the results of the different studies have been discussed separately below according to the mechanism investigated.

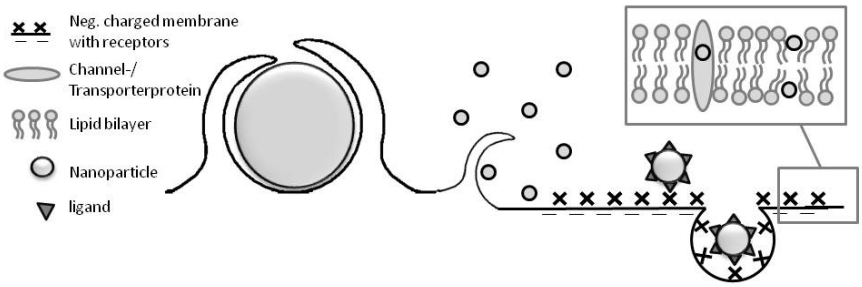

Figure 2.1 Proposed uptake mechanisms of nanoparticles (NPs). Depicted are from left to right: Uptake of a large particle by phagocytosis, liquid internalization with included particles by macropinocytosis, specific binding of ligands to cell surface receptors and subsequent receptor-mediated endocytosis, diffusion of NPs trough the lipid double layer forming the cell membrane, including transporter-/channel proteins.

Phagocytic cells are found in all kinds of organisms, ranging from unicellular organisms, where phagocytosis represents a form of feeding [106], to complex multi-cellular animals [107]. In animals, phagocytosis is part of the immune defense and is typically restricted to specialized cells, such as macrophages, monocytes and neutrophils. Phagocytic cells specialize in the uptake and degradation of foreign (infectious) cells, e.g. bacteria and cell debris and apoptotic cells belonging to the organism itself [108] with a diameter between 0.5 µm and 10 µm. Phagocytosis is a ligand-induced process [80]. In addition to phagocytosis, this cell type also uses pinocytosis. Non-phagocytic cells make use of endocytosis to take up small essential nutrients (e.g. cholesterol-laden low-density lipoprotein and iron-laden transferrin) [50]. Pinocytosis, the mechanism responsible for the uptake of soluble substances, can be divided into different processes according to the size of the vesicle and the protein involved in vesicle formation. The four mechanisms will be described subsequently.

Macropinocytosis: a non-specific mechanism by which fluid contents are taken up in the same concentration as in the surrounding medium [109]. The vesicle size is 100 nm to 5 µm [110]; *Clathrin-mediated endocytosis (CME):* receptor-mediated endocytosis with vesicle sizes of ~120 nm [50, 110]; *Caveolae-mediated endocytosis*: uptake by RME of vesicles of ~80 nm in size [110]; *Clathrin- and caveolin-independent endocytosis* with vesicles of approximately 50 nm. Several clathrin and caveolin independent pathways exist [50, 76, 79], but these are not discussed any further discussion here, as this uptake pathway was not examined in any of the studies discussed here.

The maximum dimensions of vesicles formed for each pathway are not definitive, but their dimensions are likely to be limited to allow internalization of confined cargo sizes [111]. The sizes of vesicles differ for each species and cell type and depend on the cargo size [73, 112], be it NPs or viruses [70, 71]. Therefore, a maximum NP size for internalization can be assumed to exist. Particles above a size limit of 200 nm will not be internalized via a single clathrin-coated vesicle [51] or can presumably hardly be internalized via classical endocytosis [111].

Macropinocytosis is a constitutive process occurring continuously and irrespective of the cell needs in highly ruffled regions of the plasma membrane. Ruffles trap the surrounding medium, including solutes, when their tip bends back towards the cell surface. Materials adsorbed onto the cell membrane can be taken up as well. This mechanism is called adsorptive macropinocytosis [79].

Receptor-mediated endocytosis is well studied and plays an important role in the study of non-phagocytic uptake. RME allows different types of ligands, such as toxins, cholesterol-carrying proteins, vitamins and iron transport proteins, as well as hormones and growth factors [113], to enter cells via the binding of specific receptors localized on the cell membrane [50]. RME allows the uptake of specific macromolecules from the surrounding medium in a concentrated form [79]. RME is also exploited by viruses to enter host cells, avoiding to leave evidence of entry (viral glycoproteins) on the outside of the cell for detection by the immune defense [66]. To be able to enter, viruses first bind to the

surface of a cell in order to concentrate on the cell surface or to induce transmission of cell signals for endocytosis [66]. Whether RME or another type of endocytosis takes place is determined, among other factors, by the particle size [69]. For particles, the rate of RME is determined by interplay of the decrease in free energy required to drive the cargo into the cell, the amount of available binding sites and the wrapping time [114]. Nanoparticle uptake by endocytosis is a complex interplay of the energy release by the number of bound receptors, the number of vesicles that can be formed from the membrane, receptor diffusion towards the attached particle and time to complete this process. For large NPs, allowing only one particle to be taken up per vesicle, attachment occurs to numerous receptors at a time, resulting in a major change in free energy. A larger contact area with the cell membrane for elongated particles will also lead to a larger decrease in the free energy [114], but at the same time to less available binding sites for other particles [81]. Large particles will require more time to complete wrapping [82, 114]. For small particles, several NPs can be taken up in one vacuole, but energy release is weaker because only single attachment sites exist. Since a local decrease in the Gibbs free energy is required to induce membrane wrapping a minimum size for a single particle at a given ligand density must exist, otherwise endocytosis is energetically impossible [115]. Uptake is only initiated after a certain number of receptors have been triggered. If the change in free energy is too small, membrane wrapping will not be induced [114].

In most studies reviewed, the NPs were larger than the reported size cutoff for diffusion. In addition, the uptake mechanisms were determined in each study and were reported to be phagocytosis or pinocytosis. Therefore, diffusion will only be discussed here shortly. Whether or not non-endocytic uptake mechanisms, such as diffusion or active transport, can also be exploited by NPs is under debate [67]. Diffusion is the movement of molecules from high to low concentration and takes place for small, hydrophobic, uncharged molecules such as oxygen or carbon dioxide. Lipid soluble substances, e.g. alcohols, are also able to diffuse through the membrane. Water-soluble molecules pass through the membrane passively via pores in a process called facilitated diffusion. The pores allow only molecules of a certain size range and electrical charge to cross the membrane. For molecules too large or too specialized, carrier molecules can aid to pass the membrane actively against the concentration gradient [49]. A study by Geiser et al. [72] showed that particles (78, 200 and 1000 nm) taken up by cells were not membrane bound, indicating transport via pores or diffusion as a potential route. However, charged molecules could not simply pass through the plasma membrane by diffusion and particles had to be 10-30 nm in size, the size of a channel pore, in order to allow movement via such channels [67]. Nanoparticle transport by transporters was considered unlikely due to the high specificity of the transporter structure. A plasma membrane that is not clearly distinguishable around NPs is not enough evidence for diffusion being accepted as a viable cellular uptake route for NPs [67]. In addition, a size cutoff of 1.47 nm diameter for organic chemicals [116] and 4.8 nm diameter for spherical proteins have been

reported [117, 118]. This diameter was calculated [117, 118] from the borderline for proteins to cross bacterial cell wall by diffusion given as 50 kDa [119]. The latter study concludes that only small uncharged hydrophilic molecules with mean radii below 2.5 nm were able to pass the wall of two bacterial species. Chain lengths of hydrophobic chemicals longer than 5.3 nm have been reported to lead to a lack of accumulation [120].

Nanoparticle properties influencing their uptake

Internalization of nanomaterials in cells is influenced by a large number of physical and chemical properties of the specific nanoparticle (Figure 2.2) and the circumstances in the exposure medium of the cells. The present study will focus on NP properties that are most broadly covered in mechanistic studies: NP size [63, 73-75, 81-85], shape [81, 82, 87-90], surface charge [75, 91-95, 121, 122], surface functional groups [40, 96, 97, 100, 123], NPs hydrophilicity [61-63, 124-126]. The effect of core composition will not be discussed here because the surface characteristics are more important than the bulk characteristics since the surface properties determine the protein corona and thereby possibly the biological impacts [127]. Experimental conditions (cell type, aggregation, opsonization) will be discussed with regard to studies on the effect of NP properties on cellular uptake. The major properties of NPs determining interaction with cells are depicted in Figure 2.2 and described consecutively. All values reported are taken directly from literature; therefore our results are also based on the assumptions of the researchers. Implications of assumptions such as no aggregation or no formation of surface layers are discussed in special sections under the effect of experimental conditions determining NP uptake.

Size. Spherical NPs up to 500 nm in size were taken up by non-phagocytic cells, whereas no particles with a diameter of 1000 nm were detected in these cells (Table 2.2). Previous research found a strong decrease in bead internalization and in the speed of the larger particles in comparison to 50 nm beads [73]. This is in good agreement with the results of He et al. [75], who found that several non-phagocytic cells favored the uptake of smaller particles. They also found a clear relation between the size and number of gold particles being stabilized with citric acid ligands in each HeLa cell. There was an uptake optimum for spherical NP of 50 nm [81]. In the resumption of the previously described work, the same size optimum was for transferrin-coated gold NPs, independent of cell line [82]. This size optimum of 50 nm has been confirmed for various NPs and cell types [74, 83-85]. The results of Rejman et al. [73] contradict the "maximum uptake size" assumption, stating that beads as large as 500 nm were taken up by caveolae. "Evidently, the actual size of single flask-shape caveolae is too small for accommodating particles as large as 500 nm. (…) Recruitment of an internalization machinery is needed to accommodate particles that extend beyond the actual size of a caveolae domain, which appears possible given internalization of bacteria and viruses along this pathway" [73]. This suggests that macropinocytosis can only be a minor mechanism for the internalization of NP, as was proven by the use of specific inhibitors.

Lévy et al. [129] doubted that there was a size optimum for uptake as observed in several studies [74, 81, 82]. They argued that the units in which the results were given had not been considered. An optimum based on the number of particles per cell does not necessarily lead to the same optimum in terms of mass [129]. Most of studies have reported the number of particles per cell, except Lu et al. [74]. Yue et al [130] expressed internalization of differently sized NPs by three different units (number of particles per cell, particle volume per cell and particle surface area per cell). They showed graphically that the size optimum varies depending on the unit. The surface area to volume ratio decreases with increasing volume. In addition, the sizes given usually refer to the pure NPs after synthesis, but changes might occur during the experiments due to aggregation or attachment of serum components might occur. This in turn may have altered the outcome of the experiments.

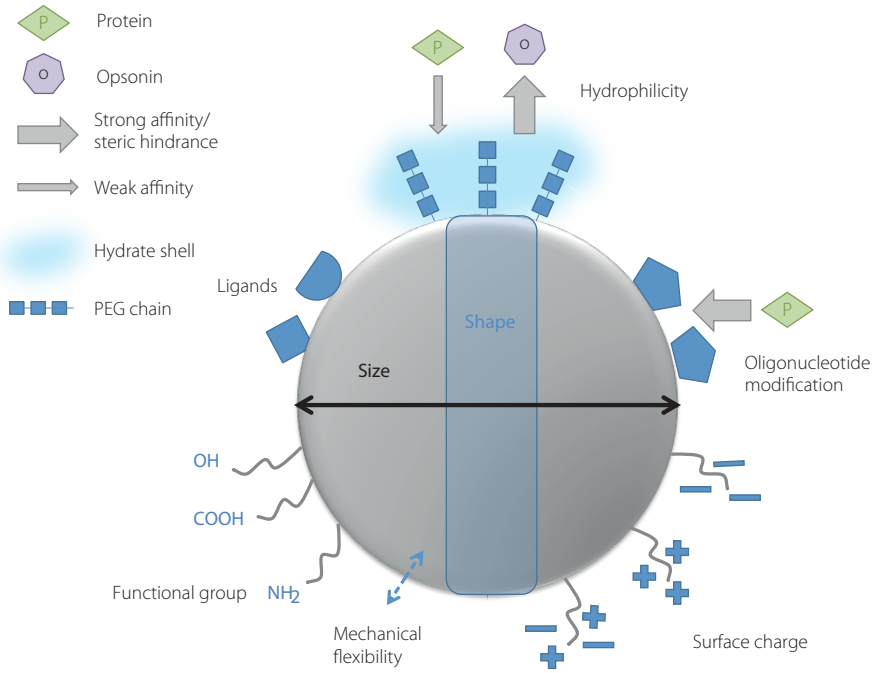

Figure 2.2 Determinants of nanoparticle (NP) interactions with cells as determined by experimental conditions (presence of protein and opsonins); shape (spheres, short-long rods, cubes and triangles with different aspect ratios), cell type, size, surface chemistry and addition of ligands. (modified after Chou et al. [128]). The state of aggregation outside the cell is not depicted here, which has been shown to play an important role in NP uptake [19].

The effect of NP size on the uptake into phagocytic cells is less well studied (Table 2.2). J774. A1 murine 'macrophage-like' cells readily took up both 20 nm and 200 nm COOH-modified coated polystyrene beads (PBs), but the smaller PBs were taken up relatively faster and more extensively [63]. This contradicts the observation that phagocytic cell lines favored the uptake of larger particles [75]. The highest attachment has been observed for particles with a longest dimension of 2-3 µm [131], which also represents the largest dimension of commonly found bacteria [110]. One possible explanation for those contradictions are "the difficulties in controlling the surface charge during the size control processes and the lack in surface functionality" [75]. Overall, particle uptake by non-phagocytic cells shows a clear trend: uptake increases with particle size to an optimum of about 50 nm and decreases for larger particles [73, 81-85]. For phagocytes, the uptake is not unequivocally related to particle size.

Shape and Geometry. The effect of the particle shape of cationic, monodisperse cross-linked poly ethylene glycol hydrogel particles on uptake has been studied in HeLa cells [87]. Pinocytosis, in parallel non-specific and receptor-mediated, was the determined uptake mechanism. The particles consisted of cylinders with different aspect ratios (AR) and a constant surface charge. Direct comparison of particles with the same AR showed that the ones with a smaller diameter were taken up to a lesser extent than the ones with a larger diameter and much larger volume ($2.4 \cdot 10^{-3}$ µm^3 versus $7.9 \cdot 10^{-3}$ µm^3) [87]. Particles with a diameter of 150 nm and a length of 450 nm were taken up four times faster by the cells than those with a diameter and a length of 200 nm, despite their similar volumes of $7.9 \cdot 10^{-3}$ µm^3 and $6.3 \cdot 10^{-3}$ µm^3, respectively. In agreement with this study, other found that cellular uptake by non-phagocytic A375 human melanoma cells increased in terms of numbers and speed with the aspect ratio of mesoporous silica NP (MSNP) spheres and rods of constant diameter [90]. The uptake of rod-shaped gold NPs with citric acid ligands and their spherical counterparts into HeLa cells has been compared by Chithrani et al. [81]. The same trend of a size optimum that was found for spherical particles was also seen for rod-shaped NPs. The larger rods with one dimension of more than 50 nm were taken up less than the smaller rods with a length of 40 nm [81]. In contrast to the study by Huang et al. [90], an increase in AR led to a decrease in uptake as shown by Chitrani et al. [81]. The larger contact area of rod-shaped NPs with the membrane led to a reduction in available binding sites [81]. In another study by Chithrani and co-workers, the same trend was found for Au NPs coated with transferrin [82]. Wrapping times increased with increasing surface area of the transferrin coated NPs [82]. The study by Gratton et al. underpins the dependence of internalization kinetics of NPs by HeLa cells on the absolute particle size rather than on the AR [87].

To be able to draw conclusions about the effect of particle shape on uptake despite experimental limitations and problems in the production processes of non-spherical NPs, modeling of the interplay of receptor-ligand binding and transport time across membranes has been performed for single particles and particle cluster [132]. In computer simulations,

the volume and ligand density of differently shaped NPs was kept constant. Particles were designed as spheres, long and short rods and disks. It was shown that endocytosis can be divided into two steps: Membrane invagination and particle wrapping [48]. During the first stage, NPs orientated towards the membrane in such a way that ligand-receptor binding became largest by maximizing the contact area. This caused the membrane to invaginate. The kinetics of the second stage, particle wrapping, were governed by the largest local mean curvature leading to a reorientation of shape anisotropic NPs (for example rods and disks). One requirement for successful internalization was the release of sufficient free energy by ligand-receptor binding to overcome the energy required for membrane bending during wrapping [48].

Clift et al. showed that the rate of uptake of MSNP in fibroblasts with deficient phagocytosis decreased with an increase in AR [89]. The uptake mechanism has not been determined in the same study as the rate of uptake, but in a previous study. There the same kind of particles were shown to be taken up into HeLa cells by clathrin-mediated endocytosis [133]. The effect of the cell line on NP uptake is discussed further under the section 'experimental conditions'. The rod shaped particles used by Clift et al. were much larger (L 400-1000 nm) than the dimensions of vesicles formed in clathrin-mediated endocytosis by fibroblasts. These vesicle sizes are not definitive, but are likely to be limited to confined cargo sizes [111]. Uptake curves determined by Clift et al. showed the same shape and saturation at the same time point for spherical and tubular MSNP by non-professional (sessile) phagocytic chinese hamster ovary cells [89]. At the same time, a tendency of tube like NPs to form larger aggregates with a wider size distribution of 955-1480 nm than the spherical particles, which had a sharp peak at 712 nm, was reported. This study confirms that the concept of primary particle size is not applicable under some experimental conditions (see further discussion under the section 'aggregation'). The same might be the case in the environment where ageing and aggregation possibly take place before the NPs reach an organism. Contradictory results have been reported for *in vivo* studies: a decrease in AR led to increased cellular uptake, measured as decreased circulation times in rodents. In agreement with this, spheres and short particles showed a higher uptake in human-derived macrophages *in vitro* [88].

The effect of shape on NP uptake using six different geometries (spheres, oblate ellipsoids, prolate ellipsoids elliptical disks, rectangular disks and UFOs) in alveolar macrophages has been studied by Champion and Mitragotri [134]. The shape was described by the angle of tangents of the particle as related to the membrane at the first point of contact. Shape rather than size determined the induction of the phagocytosis process. Phagocytosis was induced by the formation of a complex actin structure for angles smaller than 45 degrees, while spreading of the membrane took place for larger contact angles. Size determined whether internalization was successful. When the volume of the particle was larger than that of the cell, phagocytosis was not completed [134].

The AR alone does not offer enough information to draw conclusions about NP uptake, for example whether a certain size for vesicular uptake limit can be exceeded (Table 2.2). Particles with the same AR may have very different dimensions, such as length, diameter or volume, which affect the uptake and have to be considered. The above studies have been ambiguous regarding the effect of AR on non-phagocytic uptake. RME has been shown to increase with a smaller AR [81]. For macro-pinocytosis or an undefined non-phagocytic uptake mechanism, the higher AR led to increased uptake [87]. In phagocytosis, uptake increased for smaller AR or stayed the same, depending on the cell type [89]. However, it is not clear whether this can be attributed to a change in length or volume, or to both. Whether the length or the volume is dominant is difficult to assess, because studies where one factor is changed at a time are lacking. The reason appears to be the difficult production of spheres and rods with equal chemical composition [82].

Surface charge. Zero surface charges, either by neutral surface groups, e.g. hydroxyl groups, or by zwitterionic ligands, have been shown to lead to low cellular uptake compared to charged particles [75, 92, 93, 121, 122]. This can be explained by the low NP affinity towards the overall negatively charged cell membrane. Zero surface charges cause the hindrance of nonspecific protein adsorption [135, 136] and a strong hydration layer via electrostatic interaction may be formed [136].

A positive surface charge has been shown to increase particle uptake, both in phagocytes [75, 91, 97] and non-phagocytic cell lines [75, 97]. Positive surface charges (NH_2) increase cell surface affinity and uptake of NPs in both cell types. The uptake is determined by electrostatic attractions towards the slightly negatively charged cell membrane [137]. Increase of the NP uptake by macrophages has been observed for negative surface charges [75, 92]. For uptake of negatively charged NPs by RME, opposing results have been reported. On the one hand increase in cellular uptake was observed with increasing charge [93]. On the other hand decreasing uptake was reported by He et al. [75]. The possibility of changes in other surface properties during the charge control process, such as the hydrophobicity, has to be kept in mind. These might affect the uptake into cells as well. At a first glance, an increase of transport of more negatively charged NPs across the negatively charged cell membrane seems not logic due to repulsion. However, high charges prevent agglomeration and particles with low zeta-potential tend to aggregate lowering their uptake rate [19, 138]. Therefore, the uptake was possibly not determined by the lower zeta-potential but by the likely bigger size of the formed agglomerates. The issue of particle aggregation will be discussed under a separate section. When positive and negative surface charges were directly compared, keeping other properties the same, positively charged particles were shown to be taken up by non-phagocytes more favorably than negatively charged ones [75, 94]. The same finding was reported for phagocytes [75, 95].

In most studies an increase in positive or negative surface charge led to increased NP uptake in comparison to less or uncharged NPs. Only one study contradicted with these results [75]. In addition, positively charged particles seemed to be taken up more extensively compared to negatively charged NPs when the absolute zeta-potential was similar [75, 94].

Surface functional groups. Investigations on the effect of surface functional groups often include Poly Ethylene Glycol (PEG), which will be described in the next section on due to its high hydrophilicity, the negative carboxyl group (-COOH), neutral functional groups like hydroxyl groups (-OH) and the positive amine group ($-NH_2$). Increasing positive surface charge, by increasing amounts of amine groups, has been shown to increase uptake of NPs into cells for various cell lines, both non- and phagocytic, and various NPs [40, 96, 97, 123].

Carboxyl (-COOH) functional groups add a negative charge to the NPs and have been shown to increase NP uptake in both cell types. The uptake studies were conducted in a medium containing protein (fetal calf serum) [96]. This might have a great effect on particle uptake as will be described in a later chapter. On the other hand, carboxyl groups on dendrimers led to increased residence times *in vivo*. One possible explanation is the resistance to recognition by the immune system through protein adsorption [139]. These opposing results can be attributed to other NP properties, such as the hydrophilicity or differences in experimental conditions influencing NP uptake and vary widely between different studies (*in vitro* vs. *in vivo*).

Increasing uptake has been observed for hydroxyl (-OH) functional groups via a non-specific adsorptive uptake route in non-phagocytic cells [100]. Uptake is increased by the adsorption of serum proteins onto the negative surface by electrostatic and hydrophobic interactions. The negative surface of the NPs under investigation did not determine particle uptake, but the outer shell of serum protein [140]. In a similar manner ligands incorporated into the NP surface, such as mannosyl, immunoglobin, fibronectin lipoprotein, or galactosyl, have been found to increase particle uptake by interaction with phagocyte surface receptors [59].

Hydrophilicity and lipophilicity. Poly ethylene glycol (PEG) is a highly hydrophilic molecule. An increase in hydrophilicity led to decreased particle uptake by macrophages [61-63, 124], as well as in non-phagocytic HeLa cells [125]. This effect was explained by the surfactant properties of PEG [61, 124, 141]. The hydrate shell around the particle hinders the adhesion of large molecules. In addition, molecular mobile PEG chains present a steric hindrance for binding of opsonins to the particle. Without the binding of opsonins, uptake into phagocytes is prevented because the necessary recognition is suppressed. Amphipathic polymers showed a very similar effect as PEG. Their hydrophobic properties allowed adsorption on the NP's surface, while their hydrophilic part pointed toward the aqueous solution and hindered the adsorption of plasma proteins, leading to expanded longevity of the NPs [126]. Another particle property, namely flexibility**,** also decreased phagocytic uptake in comparison to rigid particles [64].

Experimental conditions determining NP uptake

The experimental conditions found to have the greatest effects on the uptake of NPs will be described subsequently. They might explain the observed differences in studies on the effect of NP properties on their uptake. The results of uptake or toxicity studies, described in the subsequent remaining sections, were retrieved from *in vitro* experiments using cell cultures or unicellular microalgae [142]. Kinetic and sorption studies are done without the use of cells [135, 136].

Cell types. Cell properties have been shown to affect NP uptake. As a result, uptake is related to differences between cell types, e.g. phagocytic vs. non-phagocytic, cancer vs. normal cells and monocytes vs. macrophages [143]. Cancer cells have been shown to express different amounts of receptors on their surface than normal cells. This may affect the available binding sites of cargos and their uptake [144, 145]. In addition, the metabolic activity of the cells used, may affect particle uptake as has been shown with contradictious results [146, 147]. Not surprisingly, small differences across species, in uptake kinetics and amount of NPs taken up, are observed [96]. Phagocytes and non-phagocytes have the same biological function across all species (see section 'Mechanisms for uptake of particles into cells'), therefore the observed differences between cells of the same endocytosis type are rather small and the trend in uptake is the same. Differences can be explained by small variations in the composition of the cell membrane, the available surface area and the cell volume/size.

Aggregation. Aggregation plays an important role in determining the mobility, fate, persistence and toxicity of NPs [148-151]. It depends on experimental conditions and NP properties. Zwitterionic ligands such as phosphoryl choline stabilize NPs, preventing aggregation under numerous conditions, such as the presence of negatively or positively charged proteins [136]. The absence of nonspecific interaction has also been demonstrated for zwitterionic disulfides; it led to increased colloid stability in the presence of salt, negatively and positively charged polyelectrolytes as well as positively and negatively charged proteins. The stabilization of citrate-capped and zwitterion-capped NPs was compared. Stabilization of zwitterions-capped NPs was observed under more experimental conditions (proteins and polyelectrolytes) than for citrate capped gold NP [135]. Aggregation can be prevented by sonication and shaking. Yet, aggregation may be caused by prolonged sonication itself [152]. Shaking of the NPs and cells in solution may increase particle uptake into cells due to a higher hitting frequency [142]. *Dispersants* may be used to prevent agglomeration, but their use may alter the bioavailability and uptake of NPs [142]. Changes in uptake are caused by increasing amounts of NPs delivered to the cell membrane inadvertently by the interaction of lipid-soluble dispersants with the membrane. Alternatively, coating of the NPs with the dispersants may alter the interaction between the cell surface and the NP. Aggregation is also influenced by the *ionic strength* of the medium and directly influences particle uptake. Compression of the electric double layer with increasing ionic strength takes place. The energy barrier of the electrostatic

repulsion of two particles of the same charge becomes smaller and the attachment probability in turn becomes larger [23].

Opsonization (marking for ingestion and destruction by a phagocyte [105]). Serum proteins can also become present on the surface of NPs when serum is used in the uptake experiments, similar to the addition of ligands in the preparation step of NPs. After addition of serum, particle uptake by phagocytes has been reported to be indifferent [103], to increase [101-103] or to decrease [103], depending on the kind of protein present (Table 2.1). These contradictory effects can be explained by the presence of different proteins in the medium, by a dynamic change of the protein corona composition over time due to protein abundance and affinity [127, 153, 154] and by possible particle opsonization. Lynch et al. [155] hypothesize that the subcellular localization of a NP is determined by the NP-protein corona, besides by size and shape. Lundqvist et al. found in their studies [127] that the corona composition depends on both size and surface properties of the NPs (plain polystyrene, carbocyl-modified, amine modified). It is proposed that such "surface modifications are able to entirely change the nature of the biological active proteins in the corona, and thereby possibly also the biological impacts" [127]. An increasing amount of serum present during incubation with non-phagocytic cells causes a decrease in cellular particle uptake. The degree of decrease depends on the particles' hydrophobicity. Increasing hydrophobicity increased the effect. The hydrophobicity of the particle controls the binding to hydrophobic pockets of bovine serum albumin (BSA). The anionic BSA shows greater avidity towards the more hydrophobic NPs and repulsive interaction with the negative cell membrane [104]. Serum shows different effects on particle uptake by phagocytes [101-103] and can be explained by the kind of proteins present in the medium, the protein corona composition and particle opsonization [156, 157]. In addition, the NP charge plays a dominant role because proteins can be positively (e.g., lysozymes) or negatively (e.g. bovine serum albumins) charged [136]. The differences in NP uptake by non-phagocytic cell lines can be explained by various properties of the cells such as different binding proteins present at their surface, the charge within and on the cell surface and the rate of receptor recycling [47, 144, 158].

Conclusions and recommendation

Our review showed that patterns, albeit sometimes uncertain, are gradually emerging. In general the following trends can be observed: Uptake of NPs in non-phagocytic shows an optimum at a particle size of around 50 nm, for phagocytes the results are inconclusive. Increased charge, either positive or negative favor the uptake in both cell types. When the absolute values are comparable, positive charged particles are taken up more extensively. Addition of amine- or carboxyl-groups leads to increased uptake as well. With increasing hydrophilicity, the uptake decreases. The presence of serum during incubation and

whether opsonization takes place have shown all possible effects on uptake. This can be attributed to the kind of proteins present. The effect of AR on NP uptake remains unsolved. The disparities might be caused by the difficulties in the production of NPs with one physical-chemical parameter changed at a time, e.g. changing the surface charge might affect the hydrophobicity as well. Therefore, to pin down the responsible property, either more exact studies only varying one parameter at a time are needed or a multivariate approach can be taken. In the latter case, all NP properties that might be changed have to be measured and published in the future to give a complete picture of causes and effects.

In general, several contradictions on data and conclusions from different studies were identified in the present study. The limited number of NP properties and widely varied experimental conditions tested lead to some uncertainty in the interpretation of the results. Information about NP properties determining accumulation is very limited compared to data from toxicological studies. Especially, the effect of NP shape on uptake remains unresolved. This is due to a lack of commercially available techniques to produce non-spherical NPs and limited procedures to obtain NPs with one property changed at a time only. The exact reciprocity of shape and the responsible determinant (length, volume or surface area) for NPs with constant surface chemistry still require experimental investigation. In most studies, it is assumed that particles are not aggregated. The particle size is often determined in the pure NP solution and their shelf life is detected. Effects of cell growth medium and biomolecules excreted by cells are not considered in those cases. Optical techniques like transmission electron microscopy (TEM) or microscopy can allow determining whether NPs are aggregated or not [82]. If NP uptake is determined by other techniques, aggregation might remain undetected and be reflected in contradictory results [159]. The test medium is an important factor determining aggregation. Nanoparticles might readily aggregate under high ionic strength [160] or in a nutrient-rich culture medium [161]. The occurrence of "agglomeration disqualifies the concept of primary particle size" [148]. Therefore, the aggregation state should always be determined under conditions as close to the experimental conditions as possible.

Future developments will benefit most from studies conducted according to standardized protocols, regarding cell type and experimental setups, to overcome incomparability between studies conducted in different laboratories and unveil more information about the underlying mechanism of particle uptake by cells. For detailed information about standardized protocols, the reader is directed to a critical review that suggests nano-specific modifications of test protocols [142]. Reference materials for NPs should be made available to avoid differences of the nominally same end product supplied by various manufacturers [26] or when produced by the researcher themselves. Particle properties such as size and charge should be measured wherever possible because interlaboratory deviations [162] and differences to the data from the supplier have been noticed [31, 163, 164]. Standardized test methods would possibly fill knowledge gaps and resolve apparent contradictions. On the other hand, standardized tests are

unlikely to completely cover the large and continuously growing number of engineered NPs. Consequently, extrapolation between different NPs and between different experimental conditions is needed. For that, modeling is indispensable.

Supplemental data

Table S 2.1 on cell type and NPs used in the reviewed studies.

Acknowledgement

This work is supported by NanoNextNL, a micro and nanotechnology consortium of the Government of the Netherlands and 130 partners. We would like to thank the anonymous reviewer for the detailed discussion and constructive suggestions that helped to greatly improve the final version of review.

Abbreviations

NP, nanoparticle; NM, nanomaterial; CME, clathrin-mediated endocytosis; RME, receptor-mediated endocytosis; SA, surface area; AR, aspect ratio; L, length; ø, diameter; BSA, bovine serum albumin; MSNP, mesoporous silica nanoparticle.

Cited Work

1. *Commission recommendation of 18 october 2011 on the definition of nanomaterial text with eea relevance.* 2011.
2. M.C. Garnett and P. Kallinteri, *Nanomedicines and nanotoxicology: Some physiological principles.* Occup. Med., **2006**. 56: p. 307-311.
3. S.F. Hansen, et al., *Categorization framework to aid hazard identification of nanomaterials.* Nanotoxicol., **2007**. 1 (3): p. 243-250.
4. B. Nowack and T.D. Bucheli, *Occurrence, behavior and effects of nanoparticles in the environment.* Environ Pollut, **2007**. 150: p. 5-22.
5. C. Hendren, et al., *Modeling approaches for characterizing and evaluating environmental exposure to engineered nanomaterials in support of risk-based decision making.* Environ. Sci. Technol., **2013**. 47: p. 1190-1205.
6. M.G. Lines, *Nanomaterials for practical functional uses.* Journal of Alloys and Compounds, **2008**. 449: p. 242-245.
7. A. Hinther, et al., *Nanometals induce stress and alter thyroid hormone action in amphibia at or below north american water quality guidelines.* Environ Sci Technol, **2010**. 44: p. 8314-8321.
8. F.R. Khan, et al., *Bioaccumulation dynamics and modeling in an estuarine invertebrate following aqueous exposure to nanosized and dilssolved silver.* Environ Sci Technol, **2012**. 46: p. 7621-7628.
9. N.L. Rosi, et al., *Oligonucleotide-modified gold nanoparticles for intracellular gene regulation.* Science, **2006**. 312: p. 1027-1030.
10. H. Vallhov, et al., *Mesoporous silica particles induce size dependent effects on human dendritic cells.* Nano Letters, **2007**. 7: p. 3576-3582.
11. T. Xia, et al., *Polyethyleneimine coating enhances the cellular uptake of mesoporous silica nanoparticles and allows safe delivery of sirna and DNA constructs.* ACS Nano, **2009**. 3 (10): p. 3273-3286.
12. M. Lewin, et al., *Tat peptide-derivatized magnetic nanoparticles allow in vivo tracking and recovery of progenitor cell.* Nat. Biotechnol., **2000**. 18: p. 410-414.
13. R. Weissleder, *Molecular imaging in cancer.* Science, **2006**. 312 (5777): p. 1168-1171.
14. P. Fortina, et al., *Applications of nanoparticles to diagnostics and therapeutics in colorectal cancer.* Trends Biotechnol., **2007**. 25 (4): p. 145-152.
15. K.K. Jain, *Applications of nanobiotechnology in clinical diagnostics.* Clinical Chemistry, **2007**. 53 (11): p. 2002-2009.
16. R. Wilson, *The use of gold nanoparticles in diagnostics and detection.* Chemical Society Reviews, **2008**. 37: p. 2028-2045.
17. A. Albanese, P.S. Tang, and W.C.W. Chan, *The effect of nanoparticle size, shape, and surface chemistry on biological systems.* Annual Review of Biomedical Engineering, **2012**. 14: p. 1-16.
18. R.A. Sperling, et al., *Biological applications of gold nanoparticles.* Chemical Society Reviews, **2008**. 37: p. 1896–1908.
19. C.-M. Zhao and W.-X. Wang, *Size-dependent uptake of silver nanoparticles in daphnia magna.* Environ Sci Technol, **2012**.
20. G. Oberdörster, V. Stone, and K. Donaldson, *Toxicology of nanoparticles: A historical perspective.* Nanotoxicol., **2007**. 1 (1): p. 2-25.
21. A. Shvedova, et al., *Exposure to carbon nanotube material: Assessment of nanotube cytotoxicity using human keratinocyte cells.* Journal of Toxicology and Environmental Health, **2003**. 66 (20): p. 1909-1926.
22. A. Kunzmann, et al., *Toxicology of engineered nanomaterials: Focus on biocompatibility, biodistribution and biodegradation.* Biochim. Biophys. Acta, **2011**. 1810: p. 361-373.
23. E. Navarro, et al., *Environmental behavior and ecotoxicity of engineered nanoparticles to algae, plants, and fungi.* Ecotoxicology, **2008**. 17: p. 372–386.
24. C.-M. Zhao and W.-X. Wang, *Biokinetic uptake and efflux of silver nanoparticles in daphnia magna.* Environ Sci Technol, **2010**. 44: p. 7699–7704.
25. J. Fabrega, et al., *Silver nanoparticle impact on bacterial growth: Effect of ph, concentration, and organic matter.* Environ Sci Technol, **2009**. 43: p. 7285-7290.
26. S.J. Klaine, et al., *Nanomaterials in the environment: Behavior, fate, bioavailability, and effects.* Environ. Toxicol. Chem., **2008**. 27 (9): p. 1825-1851.
27. N. Kumar, V. Shah, and V.K. Walker, *Influence of a nanoparticle mixture on an arctic soil community.* Environ. Toxicol. Chem., **2012**. 31 (1): p. 131-135.

28. M.J.C.V.D. Ploeg, et al., *Effects of c60 nanoparticle exposure on earthworms (lumbricus rubellus) and implications for population dynamics*. Environ. Pollut., **2011**. 159: p. 198-203.
29. B.P. Jackson, et al., *Bioavailability, toxicity, and bioaccumulation of quantum dot nanoparticles to the amphipod leptocheirus plumulosus*. Environ Sci Technol, **2012**. 46: p. 5550–5556.
30. J.D. Judy, J.M. Unrine, and P.M. Bertsch, *Evidence for biomagnification of gold nanoparticles within a terrestrial food chain*. Environ Sci Technol, **2011**. 45: p. 776–781.
31. C. Pang, et al., *Bioaccumulation, toxicokinetics, and effects of copper from sediment spiked with aqueous cu, nano-cuo, or micro-cuo in the deposit-feeding snail, potamopyrgus antipodarum*. Environ. Toxicol. Chem., **2013**. 32 (7): p. 1561-1573.
32. K. Tervonen, et al., *Analysis of fullerene-c_{60} and kinetic measurements for its accumulation and depuration in daphnia magna*. Environ. Toxicol. Chem., **2010**. 29 (5): p. 1072-1078.
33. A. Wegner, et al., *Effects of nanopolysytrene on the feeding behavior of the blue mussel (mytilus edulis l.)*. Environ. Toxicol. Chem., **2012**. 31 (11): p. 2490-2497.
34. J.L. Bouldin, et al., *Aquepus toxicity and food chain transer of quantum dots in freshwater algae and ceriodaphnia dubia*. Environ. Toxicol. Chem., **2008**. 27 (9): p. 1958-1963.
35. S.B. Lovern, J.R. Strickler, and R. Klaper, *Behavioral and physiological changes in daphnia magna when exposed to nanoparticle suspensions (titanium dioxide, nano-c_{60}, and c_{60}hxc_{70}hx)*. Environ Sci Technol, **2007**. 41: p. 4465-4470.
36. S.B. Lovern and R. Klaper, *Daphnia magna mortality when exposed to titanium dioxide and fulleren (c_{60}) nanoparticles*. Environ. Toxicol. Chem., **2006**. 25 (4): p. 1132-1137.
37. L. Mccarty, et al., *Advancing environmental toxicology through chemical dosimetry: External exposures versus tissue residues*. Integr Environ Assess Manag, **2010**. 7 (1): p. 7-27.
38. C. Brandenberger, et al., *Quantitative evaluation of cellular uptake and trafficking of plain and polyethylene glycol-coated gold nanoparticles*. **2010**.
39. C. Schweiger, et al., *Quantification of the internalization patterns of superparamagnetic iron oxide nanoparticles with opposite charge*. Journal of Nanobiotechnology, **2012**. 10 (28).
40. F. Alexis, et al., *Factors affecting the clearance and biodistribution of polymeric nanoparticles*. Molecular Pharmaceutics, **2008**. 5 (4): p. 505-515.
41. F. Ahsan, et al., *Targeting to macrophages: Role of physicochemical properties of particulate carriers- liposomes and micropheres- on the phagocytosis by macrophages*. J. Control. Release, **2002**. 79: p. 29-40.
42. P. Thevenot, W. Hu, and L. Tang, *Surface chemistry influence implant biocompatobility*. Current Topics in Medicinal Chemistry, **2008**. 8 (4): p. 270-280.
43. A. Verma and F. Stellacci, *Effect of surface properties on nanoparticle-cell interactions*. Small, **2010**. 1: p. 12-21.
44. B.D. Chithrani, *Intracellular uptake, transport, and processing of gold nanostructures*. Molecular Membrane Biology, **2010**. 27 (7): p. 299-311.
45. B.D. Chithrani, *Optimization of bio-nano interface using gold nanpstructures as a model nanoparticle system*. Inscience J., **2011**. 1 (3): p. 115-135.
46. S. Wua, et al., *A framework for using structural, reactivity, metabolic and physicochemical similarity to evaluate the suitability of analogs for sar-based toxicological assessments*. Regul Toxicol Pharmacol, **2010**. 56: p. 67-81.
47. A. Panariti, G. Miserocchi, and I. Rivolta, *The effect of nanoparticle uptake on cellular behavior: Disrupting or enabling functions?* Journal of Nanotechnology, Science and Applications, **2012**. 5: p. 87-100.
48. I. Canton and G. Battaglia, *Endocytosis at the nanoscale*. Chemical Society Reviews, **2012**. 41: p. 2718-2739.
49. B. Alberts, et al., *Molecular biology of the cell*. 4th ed. 2002, New York: Garland Science.
50. S.D. Conner and S.L. Schmid, *Regulated portals of entry into the cell*. Nature, **2003**. 422: p. 37-44.
51. H.T. Mcmahon and E. Boucrot, *Molecular mechanism and physiological functions of clathrin-mediated endocytosis*. Nature Reviews Molecular Cell Biology, **2011**. 12: p. 517-533.
52. P. Stahl and A.L. Schwartz, *Receptor-mediated endocytosis*. Journal of Clinical Investigation, **1986**. 77: p. 657-662.
53. C. Collinet, et al., *Systems survey of endocytosis by multiparametric image analysis*. Nature, **2010**. 464: p. 243-250.
54. S.C. Silverstein, R.M. Steinman, and Z.A. Cohn, *Endocytosis*. Annual Review of Biochemistry, **1977**. 46: p. 669-722.
55. M. Massignani, et al., *Controlling cellular uptake by surface chemistry, size, and surface topology at the nanoscale*. Small, **2009**. 5 (21): p. 2424–2432.
56. S. Balaz, *Modeling kinetics of subcellular disposition of chemicals*. Chemical Review, **2009**. 109: p. 1793-1899.

57. M.V.D. Ploeg, *Unravelling hazards of nanoparticles to earthworms, from gene to population*, in *Department of Toxicology*. 2012, Wagen University: Wageningen.
58. P. Biswas and C.-Y. Wu, *Nanoparticles and the environment*. J Air Waste Manage, **2005**. 55: p. 708-746.
59. Y. Kaneda, *Virosomes: Evolution of the liposome as a targeted drug delivery system*. Adv. Drug Deliver. Rev., **2000**. 43: p. 197-205.
60. F. Benyettou, et al., *Pegylated versus non-pegylated yfe2o3@alendronate nanoparticles*. Journal of bioanalysis & biomedicine, **2012**. 4 (3): p. 39-45.
61. A.S. Zahr, C.A. Davis, and M.V. Pishko, *Macrophage uptake of core-shell nanoparticles surface modified with poly(ethylene glycol)*. Langmuir, **2006**. 21 (19): p. 8178-8185.
62. Y. Tabata and Y. Ikada, *Phagocytosis of polymer microspheres by macrophages*. Adv. Polym.Sci, **1990**. 94: p. 107-141.
63. M.J.D. Clift, et al., *The impact of different nanoparticle surface chemistry and size on uptake and toxicity in a murine macrophage cell line*. Toxicol. Appl. Pharmacol, **2008**. 232: p. 418-427.
64. K.A. Beningo and Y.-L. Wang, *Fc-receptor-mediated phagocytosis is regulated by mechanical properties of the target*. Journal of Cell Science, **2002**. 115: p. 849-856.
65. M.M. Poranen, R. Daugelavičius, and D.H. Bamford, *Common principles in viral entry*. Annual Review of Microbiology, **2002**. 56: p. 521-538.
66. A.E. Smith and A. Helenius, *How viruses enter animal cells*. Science, **2004**. 304: p. 237-242.
67. J.R. Lead, ed. *Environmental and human health impacts of nanotechnology*. ed. E. Smith. 2009, Wiley-Blackwell: Chippenham, Great Britain.
68. B.Y. Moghadam, et al., *Role of nanoparticle surface functionality in the disruption of model cell membranes*. Langmuir, **2012**. 28: p. 16318–16326.
69. J. Mercer and A. Helenius, *Virus entry by macropinocytosis*. Nature Cell Biology, **2009**. 11 (5): p. 510-520.
70. J. Grove and M. Marsh, *The cell biology of receptor-mediated virus entry*. Journal of Cell Biology, **2011**. 195 (7): p. 1071–1082.
71. M. Marsh and A. Helenius, *Virus entry: Open sesame*. Cell, **2006**. 124: p. 729-740.
72. M. Geiser, et al., *Ultrafine particles cross cellular membranes by nonphagocytic mechanisms in lungs and in cultured cells*. Environ. Health Persp., **2005**. 113 (11): p. 1555-1560.
73. J. Rejman, et al., *Size-dependent internalization of particles via the pathways of clathrin- and caveolae-mediated endocytosis*. Biochemical Journal, **2004**. 377: p. 159-169.
74. F. Lu, et al., *Size effect on cell uptake in well-suspended, uniform mesoporous silica nanoparticles*. Small, **2009**. 10: p. 1-6.
75. C. He, et al., *Effects of particle size and surface charge on cellular uptake and biodistribution of polymeric nanoparticles*. Biomaterials, **2010**. 31: p. 3657-3666.
76. G.J. Doherty and H.T. Mcmahon, *Mechanisms of endocytosis*. Annual Review of Biochemistry, **2009**. 78: p. 857-902.
77. S.K. Basu, *Receptor-mediated endocytosis of hormones in cultured cells* Journal of Biosciences, **1984**. 6 (4): p. 535-542.
78. N. Doshi and S. Mitragotri, *Macrophages recognize size and shape of their targets*. PLoS one, **2010**. 5 (4).
79. I.H. Pastan and M.C. Willingham, *Receptor-mediated endocytosis of hormones in cultured cells*. Annual Review of Physiology, **1981**. 43: p. 239-250.
80. C. Watts and M. Marsh, *Endocytosis: What goes in and how?* Journal of Cell Science, **1992**. 103: p. 1-8.
81. B.D. Chithrani, A.A. Ghazani, and W.C.W. Chan, *Determining the size and shape dependence of gold nanoparticle uptake into mammalian cells*. Nano Letters, **2006**. 6 (4): p. 662-668.
82. B.D. Chithrani and W.C.W. Chan, *Elucidating the mechanism of cellular uptake and removal of protein-coated gold nanoparticles of different sizes and shapes*. NANO LETTERS, **2007**. 7 (6): p. 1542-1550.
83. W. Jiang, et al., *Nanoparticle-mediated cellular response is size-dependent*. Nat Nanotechnol., **2008**. 3: p. 145-150.
84. F. Osaki, et al., *A quantum dot conjugated sugar ball and its cellular uptake. On the size effects of endocytosis in the subviral region*. J am Chem Soc, **2004**. 126 (21): p. 6520–6521.
85. S.-H. Wang, et al., *Size-dependent endocytosis of gold nanoparticles studied by three-dimensional mapping of plasmonic scattering images*. Journal of Nanobiotechnology, **2010**. 8 (33).
86. M.J.D. Clift, et al., *The impact of different nanoparticle surface chemistry and size on uptake and toxicity in a murine macrophage cell line*. Toxicol. Appl. Pharm., **2008**. 232: p. 418-427.
87. S.E.A. Gratton, et al., *The effect of particle design on cellular internalization pathways*. Proc. Natl. Acad. Sci. USA, **2008**. 105 (33): p. 11613-11618.

88. Y. Geng, et al., *Shape effects of filaments versus spherical particles in flow and drug delivery.* Nat Nanotechnol., **2007**. 2: p. 249-255.
89. B.G. Trewyn, et al., *Biocompatible mesoporous silica nanoparticles with different morphologies for animal cell membrane penetration.* Chemical Engineering Journal, **2008**. 137: p. 23-29.
90. X. Huang, et al., *The effect of the shape of mesoporous silica nanoparticles on cellular uptake and cell function.* Biomaterials, **2010**. 31: p. 438–448.
91. R.A. Schwendener, P.A. Lagocki, and Y.E. Rahman, *The effects of charge and size on the internalization of unilamellar liposomes with macrophages*. Biochim. Biophys. Acta, **1984**. 772: p. 93-101.
92. T.M. Allen, et al., *Uptake of liposomes by cultured mouse bone marrow macrophages: Influence of liposome composition and size.* Biochimica et Biophysica Acta, **1991**. 1061: p. 56-64.
93. S. Patil, et al., *Protein adsorption and cellular uptake of cerium oxide nanoparticles as a function of zeta potential.* Biomaterials, **2007**. 28 (31): p. 4600-4607.
94. O. Harush-Frenkel, et al., *Targeting of nanoparticles to the clathrin-medaited endocytic pathway.* Biochemical and Biophysical Research Communications, **2007**. 353 (1): p. 26-32.
95. M. Roser, D. Fischer, and T. Kissel, *Surface-modified biodegradable albumin nano- and microspheres. Ii: Effect of surface charges on in vitro phagocytosis and biodistribution in rats*. Eur J Pharmaceut Biopharmaceut, **1998**. 46: p. 255-263.
96. V. Holzapfel, et al., *Synthesis and biomedical applications of functionalized fluorescent and magnetic dual reporter nanoparticles as obtained in the miniemulsion process.* Journal of Physics: Condensed Matter, **2006**. 18: p. 2581–2594.
97. M.R. Lorenz, et al., *Uptake of functionalized, fluorescent-labeled polymeric particles in different cell lines and stem cells.* Biomaterials, **2006**. 27: p. 2820–2828.
98. G. Orr, et al., *Submicrometer and nanoscale inorganic particles exploit the actinmachinery to be propelled along microvilli-like structures into alveolar cells.* American Chemical Society Nano, **2007**. 1 (5): p. 463–475.
99. P. Thevenot, W. Hu, and L. Tang, *Surface chemistry influence implant biocompatibility.* Current Topics in Medicinal Chemistry, **2008**. 8 (4): p. 270-280.
100. S. Kannan, et al., *Dynamics of cellular entry and drug delivery by dendritic polymers into human lung epithelial carcinoma cells.* Journal of Biomaterial Science, Polymer Edition, **2004**. 15 (3): p. 311-330.
101. S. Nagayama, et al., *Time-dependent changes in opsonin amount associated on nanoparticles alter their hepatic uptake characteristics.* International Journal of Pharmaceutics, **2007**. 342: p. 215-221.
102. A.J. Sbarra and M.L. Karnovsky, *The biochemical basis of phagocytosis*. Journal of Biological Chemistry, **1959**. 243 (6): p. 1355-1362.
103. Y. Ikada and Y. Tabata, *Phagocytosis of bioactive microspheres.* J. Bioact. Compat., **1986**. 1 (32): p. 32-46.
104. Z.-J. Zhu, et al., *The interplay of monolayer structure and serum protein interactions on the cellular uptake of gold nanoparticles.* Small, **2012**.
105. H. Rus, C. Cudrici, and F. Niculescu, *The role of the complement system in innate immunity.* Immunologic Research, **2005**. 33 (2): p. 103-112.
106. P. Cosson and T. Soldati, *Eat, kill or die: When amoeba meets bacteria.* Current Opinion in Microbiology, **2008**. 11: p. 271-276.
107. C. Rosales, ed. *Molecular mechanisms of phagocytosis*. 2005, Springer: New York.
108. A. Aderem and D.M. Underhill, *Mechanisms of phagocytosis in macrophages.* Annual Review of Immunology, **1999**. 17: p. 593–623.
109. S.K. Basu, *Receptor-mediated endocytosis of hormones in cultured cells.* Journal of Biosciences, **1984**. 6 (4): p. 535-542.
110. K. Hirota and H. Terada, *Endocytosis of particle formulations by macrophages and its application to clinical treatment*, in *Molecular regulation of endocytosis*, B. Ceresa, Editor. 2012, InTech: Rijeka, Croatia.
111. L.N. Patel, J.L. Zaro, and W.-C. Shen, *Cell penetrating peptides: Intracellular pathways and pharmaceutical perspectives.* Pharmaceut Res, **2007**. 24 (11): p. 1977-1992.
112. Y. Xu, T.S. Tillman, and P. Tang, eds. *Pharmacology: Principles and practice.* 1 ed., ed. M. Hacker, W. Messer, and K. Bachmann. 2009, Academic Press: Burlington, USA.
113. J.L. Goldstein, et al., *Receptor-mediated endocytosis: Concepts emerging from the ldl receptor system.* Annual Review of Cell Biology, **1985**. 1: p. 1-39.
114. H. Gao, W. Shi, and L.B. Freund, *Mechanics of receptor-mediated endocytosis.* Proc. Natl. Acad. Sci., **2005**. 102: p. 9469-9474.

115. H. Yuan and S. Zhanga, *Effects of particle size and ligand density on the kinetics of receptor-mediated endocytosis of nanoparticles*. Applied Physics Letters, **2010**. 96.
116. J.A. Arnot, et al., *Molecular size cutoff criteria for screening bioaccumulation potential: Fact or fiction?* Integrated Environmental Assessment and Management, **2010**. 6: p. 210-224.
117. D. Christensen, ed. *Introduction to biomedical engineering: Biomechanics and bioelectricity*. ed. J.D. Enderle. 2009, Morgan and Claypool: San Rafael, Calif., USA.
118. H.P. Erickson, *Size and shape of protein molecules at the nanometer level determined by sedimentation, gel filtration, and electron microscopy*. Biological Procedures Online, **2009**. 11 (1): p. 32-51.
119. P. Demchick and A.L. Koch, *The permeability of the wall fabric of escherichia coli and bacillus subtilis*. J. Bacteriol., **1996**. 178 (3).
120. I. Fraunhofer, *Effects of molecular size and lipid solubility on bioaccumulation potential*. 2007, Fraunhofer IME.
121. A. Raz, et al., *Biochemical, morphological, and ultrastructural studies on the uptake of liposomes by murine macrophages*. Cancer Res, **1981**. 41: p. 487-494.
122. T.D. Heath, N.G. Lopez, and D. Papahadjopoulos, *The effects of liposome size and surface charge on liposome-mediated delivery of methotrexate-ψ–aspartate to cells in vitro*. Biochim. Biophys. Acta, **1985**. 820: p. 74-84.
123. G. Orr, et al., *Submicrometer and nanoscale inorganic particles exploit the actin machinery to be propelled along microvilli-like structures into alveolar cells*. ACS Nano, **2007**. 1 (5): p. 463–475.
124. F. Benyettou, et al., *Pegylated versus non-pegylated yfe2o3@alendronate nanoparticles*. Journal of Bioanalysis and Biomedicine, **2012**. 4 (3): p. 39-45.
125. P. Nativo, I.A. Prior, and M. Brust, *Uptake and intracellular fate of surface-modified gold nanoparticles*. ACS Nano, **2008**. 2 (8): p. 1639-1644.
126. T. Blunk, et al., *Differential adsorption: Effect of plasma protein adsorption patterns on organ distribution of colloidal drug carriers*. Proc. 20th Int. Symp. Control. Release Bioact. Mater, **1993**: p. 256-257.
127. M. Lundqvist, et al., *Nanoparticle size and surface properties determine the protein corona with possible implications for biological impacts*. Proc. Natl. Acad. Sci., **2008**. 105 (38): p. 14265-14270.
128. L.Y.T. Chou, K. Ming, and W.C.W. Chan, *Strategies for the intracellular delivery of nanoparticles*. Chemical Society Reviews, **2011**. 40: p. 233–245.
129. R. Lévy, et al., *Gold nanoparticles delivery in mammalian live cells: A critical review*. Nano Reviews, **2010**. 1 (4889).
130. H. Yue, et al., *Particle size affects the cellular response in macrophages*. European Journal of Pharmaceutical Sciences, **2010**. 41: p. 650-657.
131. T.D. Santos, et al., *Quantitative assessment of the comparative nanoparticle-uptake efficiency of a range of cell lines*. Small, **2011**. 7 (23): p. 3341-3349.
132. J. Meng, et al., *Lhrh-functionalized superparamagnetic iron oxide nanoparticles for breast cancer targeting and contrast enhancement in mri*. Materials Science and Engineering, **2009**. 29: p. 1467-1479.
133. I. Slowing, B.G. Trewyn, and V.S.-Y. Lin, *Effect of surface functionalization of mcm-41-type mesoporous silica nanoparticles on the endocytosis by human cancer cells*. J am Chem Soc, **2006**. 128: p. 14792-14793.
134. J.A. Champion and S. Mitragotri, *Role of target geometry in phagocytosis*. Proceedings of the National Academy of Science, **2006**. 103 (12): p. 4930-4934.
135. L.L. Rouhana, J.A. Jaber, and J.B. Schlenoff, *Aggregation-resistant water-soluble gold nanoparticles*. Langmuir, **2007**. 23: p. 12799-12801.
136. Q. Jin, et al., *Zwitterionic phosphorylcholine as a better ligand for stabilizing large biocompatible gold nanoparticles*. Chemical Communications, **2008**: p. 3058–3060.
137. H. Jin, et al., *Size-dependent cellular uptake and expulsion of single-walled carbon nanotubes: Single particle tracking and a generic uptake model for nanoparticles*. ACS Nano, **2009**. 3: p. 149-158.
138. D. Hanaor, et al., *The effects of carboxylic acids on the aqueous dispersion and electrophoretic deposition of* zro_2. Journal of the European Ceramic Society, **2012**. 32: p. 235–244.
139. T.F. Vandamme and L. Brobeck, *Poly(amidoamine) dendrimers as ophthalmic vehicles for ocular delivery of pilocarpine nitrate and tropicamide*. J Control Release, **2005**. 102: p. 23-38.
140. D.A. Giljohann, et al., *Oligonucleotide loading determines cellular uptake of DNA-modified gold nanoparticles*. Nano Letters, **2007**. 7 (12): p. 3818-3821.
141. N. Privitera, et al., *Phagocytic uptake by mouse peritoneal macrophages of microspheres coated with phospho-choline or polyethylene glycol phosphate-derived perfluoroalkylated surfactants*. Int. J. Pharm., **1995**. 120: p. 73-82.

142. R. Handy, et al., *Ecotoxicity test methods for engineered nanomaterials: Practical experiences and recommendations from the bench*. Environ. Toxicol. Chem., **2011**. 31 (1): p. 15–31.
143. K. Unfried, et al., *Cellular responses to nanoparticles: Target structures and mechanisms*. Nanotoxicol., **2007**. 1 (1): p. 52-71.
144. I.H. El-Sayed, X. Huang, and M.A. El-Sayed, *Surface plasmon resonance scattering and absorption of anti-egfr antibody conjugated gold nanoparticles in cancer diagnostics: Applications in oral cancer.* Nano Letters, **2005**. 5 (5): p. 829-834.
145. E. Ruoslahti, S.N. Bhatia, and M.J. Sailor, *Targeting of drugs and nanoparticles to tumors.* Journal of Cell Biology, **2010**. 188 (6): p. 759–768.
146. T.J. Brunner, et al., *In vitro cytotoxicity of oxide nanoparticles: Comparison to asbestos, silica, and the effect of particle solubility.* Environ Sci Technol, **2006**. 40: p. 4374-4381.
147. S.a.M. Murphy, K.A. Bérubé, and R.J. Richards, *Bioreactivity of carbon black and diesel exhaust particles to primary clara and type ii epithelial cell cultures*. Occupational and Environmental Medicine, **1999**. 56: p. 813-819.
148. L.K. Limbach, et al., *Oxide nanoparticle uptake in human lung fibroblasts: Effects of particle size, agglomeration, and diffusion at low concentrations*. Environ Sci Technol, **2005**. 39: p. 9370-9376.
149. K.L. Chen and M. Elimilech, *Aggregation and deposition kinetics of fulleren (c_{60}) nanoparticles*. Langmuir, **2006**. 22: p. 10994-11001.
150. N.B. Saleh, L.D. Pfefferle, and M. Elimelech, *Aggregation kinetics of multiwalled carbon nanotubes in aquatic systems: Measurements and environmental implications*. Environ. Sci. Technol., **2008**. 42: p. 7963-7969.
151. N.B. Saleh, L.D. Pfefferle, and M. Elimelech, *Influence of biomacromolecules and humic acid on the aggregation kinetics of single-walled carbon nanotubes*. Environ. Sci. Technol., **2010**. 44: p. 2412-2418.
152. A. Delgado and E. Matijevié, *Particle size distribution of inorganic colloidal dispersions: A comparison of different techniques*. Part Part Syst Char, **2004**. 8: p. 128-135.
153. I. Lynch and K.A. Dawson, *Protein-nanoparticle interactions.* nanotoday, **2008**. 3: p. 40-47.
154. M. Lundqvist, et al., *The evolution of the protein corona around nanoparticles: A test study.* ACS Nano, **2011**. 5 (9): p. 7503–7509.
155. I. Lynch, K.A. Dawson, and S. Linse, *Detecting cryptic epitopes created by nanoparticles*. Sci. STKE, **2006**. 327.
156. A. Lesniak, et al., *Serum heat inactivation affects protein corona composition and nanoparticle uptake*. Biomaterials, **2010**. 31: p. 9511-9518.
157. A.E. Nel, et al., *Understanding biophysicochemical interactions at the nano-bio interface.* Nat. Mater., **2009**. 8: p. 543-557.
158. F.R. Maxfield and T.E. Mcgraw, *Endocytic recycling*. Nature Reviews Molecular Cell Biology, **2004**. 5: p. 121-132.
159. Z.-J. Zhu, et al., *Effect of surface charge on the uptake and distribution of gold nanoparticles in four plant species*. Environ Sci Technol, **2012**. 46: p. 12391–12398.
160. H.H. Liu, et al., *Analysis of nanoparticle agglomeration in aqueous suspensions via constant-number monte carlo simulation*. Environ Sci Technol, **2011**. 45: p. 9284–9292.
161. X. Jin, et al., *High-throughput screening of silver nanoparticle stability and bacterial inactivation in aquatic media: Influence of specific ions*. Environ Sci Technol, **2010**. 44: p. 7321–7328.
162. G. Roebben, et al., *Interlaboratory comparison of size and surface charge measurements on nanoparticles prior to biological impact assessment.* J. Nanopart. Res, **2011**. 13: p. 2675-2687.
163. R.F. Domingos, et al., *Characterizing manufactured nanoparticles in the environment: Multimethod determination of particle sizes*. Environ. Sci. Technol., **2009**. 43: p. 7277-7284.
164. H. Park and V.H. Grassian, *Commercially manufactured engineered nanomaterials for environmental and health studies: Important insights provided by independent characterization.* Environ. Toxicol. Chem., **2010**. 29 (3): p. 515-721.

Appendix

Table S 2.1 Information on cell lines, nanoparticle type and serum use of the studies reviewed

Cell line	NP type & surface coating	Use of serum	Reference
Blood-drawn human neutrophils, human macrophage THP1, A549	Block copolymers of EOm-EEn, EOm-CLn	yes	[88]
HeLa	Cross-linked poly(ethylene glycol) hydrogels	yes	[87]
L02, HEK 293, 786-O, HFL-I, A549, SMMC-7721, H-22	RhB-CMCNP, RhB-CHNP	FCS	[75]
CL1-0, HeLa	AuNPs with ssDNA	FBS	[85]
HeLa	"Glycovirus" - Quantum Dot Conjugated Sugar Ball	no	[84]
B 16-F10 mouse melanoma	Fluorescent latex beads	no	[73]
J774.A1 macrophage-like	Polystyrene beads	FCS	[63]
HeLa	AuNPs stabilized by citric acid ligands	yes	[81]
HeLa, SNB19, STO cells	Transferrin-coated gold NPs	yes	[82]
SK-BR-3	Gold and silver NP coated with antibodies	BSA	[83]
CHO, human fibroblasts	Fluorescein isothiocyanate-doped MSNs	no	[89]
A375	Fluorescent labeled MSNs	no	[90]
A549	Microemulsion ceria and Hydrothermal ceria	FBS	[93]
HeLa	PLA and mPEG-PLA	no	[94]
HeLa, MSCs, Jurkat, KG1a	magnetic polystyrene particles encapsulating magnetite nanoparticles in a hydrophobic poly(styrene-*co*-acrylic acid) shell	FCS	[96]
HeLa, MSCs, Jurkat, KG1a	Fluorescent-labeled polymeric particles	FCS	[97]
C10	Amorphous silica particles modified with amine groups	no	[98]
A549	PAMAM-NH_2, PAMAM-OH, Polyol-OH	FCS	[100]
Kupffer	Lecithin-coated polystyrene nanospheres	Rat serum, IgG, complement C3	[101]

Table S 2.1 Continued

Cell line	NP type & surface coating	Use of serum	Reference
Leucocytes	Polystyrene latex	Dialyzed protein fraction of human plasma	[102]
HeLa	AuNPs, quaternary amine and various head groups	FBS	[104]
C-166, HeLa, A549	AuNP with monolayer of polyanionic DNA	yes	[140]
HUVEC, MDA-MB-231	Iron oxide NPs coated with alendronate or alendronate-PEG	no	[124]
Suspension macrophages	Sulfate modified fluorescent polystyrene beads with multilayers of PLL, CHI and HS, modified with PEG	BSA	[61]
DC2.4	AuNPs coated with: MUS, MUS and OT, MUS and br-OT	both	[43]
Bone-marrow-derived macrophages from mice	BSA covalently coupled to polyacrylamide beads	---	[64]
HeLa	FITC-MSNs	no	[74]

3

Exploring the effect of silver nanoparticle size and medium composition on uptake into pulmonary epithelial 16HBE14o-cells

Published in
Journal of Nanoparticle Research, 2016. Vol. 18, No. 182

Katja Kettler[a], Petra Krystek[b,c], Christina Giannakoud[e], A. Jan Hendriks[a], and Wim H. de Jong[d]

[a] Department of Environmental Science, Institute for Water and Wetland Research, Radboud University, Nijmegen, The Netherlands
[b] Institute for Environmental Studies (IVM), VU University, Amsterdam, The Netherlands
[c] Philips Innovation Services, Eindhoven, The Netherlands
[d] National Institute for Public Health and the Environment (RIVM), Bilthoven, The Netherlands
[e] Department of Toxicogenomics, Maastricht University, Maastricht, The Netherlands

Abstract

The increasing number of nanotechnology products on the market poses increasing human health risks by particle exposures. Adverse effects of silver nanoparticles (AgNPs) in various cell lines have been measured based on exposure dose after a fixed time point but NP uptake kinetics and the time-dependent internal cellular concentration are often not considered. Even though knowledge about relevant time-scales for NP uptake is essential, e.g. for time- and cost-effective risk assessment through modelling, insufficient data is available. Therefore, the authors examined uptake rates for three different AgNP sizes (20, 50 and 75 nm) and two tissue culture medium compositions (with and without fetal calf serum, FCS) under realistic exposure concentrations in pulmonary epithelial 16HBE14o-cells. The quantification of Ag in cells was carried out by High Resolution Inductively Coupled Plasma Mass Spectrometry. We show for the first time that uptake kinetics of AgNPs into 16HBE14o-cells was highly influenced by medium composition. Uptake into cells was higher in medium without FCS, reaching approximately twice the concentration after 24 hours than in medium supplemented with FCS, showing highest uptake for 50 nm AgNPs when expressed on a mass basis. This optimum shifts to 20 nm on a number basis, stressing the importance of the measurand in which results are presented. The importance of our research identifies that not just the uptake after a certain time point should be considered as dose but that also the process of uptake (timing) might need to be considered when studying the mechanism of toxicity of nanoparticles.

Keywords

Nanoparticle, uptake kinetics, size dependence, internal cellular concentration, serum proteins, health and safety effects, biomedicine

Introduction

Nanoparticles (NPs) are used in increasing amounts and number of applications [1, 2] due to their unique physical and chemical properties. Consumer products with NPs include toothpaste, wound dressings, antibacterial towels and sportswear, as well as in deodorants and in sprays for textiles and shoes [3-6]. Of special interest for consumer products, medical applications and industry are silver nanoparticles (AgNPs), attributable, besides others, to their antimicrobial properties. Several *in vitro* studies showed that AgNPs affect various cell lines, including phagocytosing cell like THP-1-derived macrophages, and serious concerns about toxicological and environmental effects have been raised [7-10].

So, it can be concluded that adverse effects can occur after contact with NPs. Exposure routes include dermal, intestinal and inhalation uptake, whereas injection may be used for nano-medical products. Inhalation of AgNPs (aerosols) is possible by consumers during product use (e.g. spray applications) or by workers during the production and processing of NPs [11]. Also for AgNPs respiratory toxicity was reported in various animals' studies [12-16]. On the long term, the product containing the NPs may end up in the environment through wash off, posing a potential risk to human health and biota [17]. Unfortunately, effects are often measured after a single fixed time point based on exposure dose, neglecting uptake kinetics and the therefore time-dependent internal cellular concentration. NP properties, such as size, influence uptake as shown for various cell lines *in vitro*. Unfortunately uptake was detected only after a fixed time point [18-22].

Small NPs can enter cells after contact via one of the four exposure routes through a fundamental biological process called endocytosis as previously summarized [23]. Particulate matter, such as proteins and other nutrients, are taken up into eukaryotic cells via enclosure by the cell membrane [24]. Endocytosis and is a form of active transport. Endocytosis is usually employed by non-phagocytic cells like 16HBE to take up biomolecules from the environment. The cell membrane forms itself around the molecules/particle to be taken up, the size of the resulting vesicles depends on the presence of ligands and the protein involved in vesicle formation [25]. Macropinocytosis is a non-specific mechanism by which the cell surrounding fluid and its content are taken up in a concentration as present with vesicles from 100 nm to 5 µm in size [26]. The other pathways are receptor-mediated, uptake occurs after binding of a ligand to specific receptors in the cell surface, which results in uptake of the ligand in higher concentration then in the medium. These pathways are further distinguished by the protein involved in vesicle formation. Vesicles in receptor-mediated endocytosis reach sizes up to roughly 80 nm in diameter (i.d.) (caveolae-mediated) [27] or 120 nm i.d. (clathrin-mediated) [24, 27]. Internalized NPs may cause the production of reactive oxygen species due to their effects on mitochondrial respiration [28] and antioxidant species might be depleted in the cell [29]. Metals in the form of NPs may employ this mechanism and metal ions then may enter cells by a so called Trojan horse effect. Especially in the case of soluble metal particles this

can result in high levels of the metal in various ionic species inside the cell resulting in further reactions [30, 31]. By this mechanism, AgNPs can enter cells and release toxic Ag ions inside the cell "bypassing its barriers to "normal"-sized Ag, and then releasing Ag ions that damage cell machinery" [32], thereby increasing the intracellular bioavailability of Ag. It was shown that AgNPs can induce a higher toxic damage than Ag ions [10, 32]. As summarized previously, several experimental conditions may influence NP uptake [23]. Especially the presence or absence of serum proteins has been shown to have great effects through the formation of a so called protein corona on the NPs surface. Uptake can be increased, decreased or remain the same, depending on the type of protein present [33-36]. In this study, we aim to determine rates of uptake for different AgNP sizes and cell culture medium with and without serum proteins, therefore exposing 16HBE14o-cells to NP for different periods of time over 24 hours. We apply NP concentrations of 0.01 µg Ag/mL that represent realistic concentrations for short term exposures [37]. This concentration is much lower, namely by a factor of up to 10 000, than in some of the existing literature where uptake rates have been determined [38, 39]. These data will deliver new insights into the effect of NP size on their uptake rate and are required to model and predict NP uptake rates based on easily measurable NP properties. Combining of empirical data and modelling will be an indispensable tool for time- and cost-effective risk assessment of NPs.

Material and Methods

Nanomaterials

For non-phagocytic cells like 16HBE14o a maximum vesicle size of 80-120 nm has been found [24, 27], therefore three differently sized AgNPs were investigated in this study: 20 nm Citrate BioPure™ Silver, 50 nm Citrate BioPure™ Silver and 75 nm Citrate BioPure™ Silver were purchased from NanoComposix Inc (San Diego, CA) in the form of stock dispersion with concentrations of 1 mg/mL in aqueous 2 mM citrate buffer. The supplier provided detailed information about the NPs characteristics as summarized in Table 3.1. The diameter was detected by the manufacturer NanoComposix Inc using transmission electron microscopy (TEM) (JEOL 1010 Transmission Electron Microscope), the hydrodynamic diameter trough dynamic light scattering (DLS) (Malvern Zetasizer Nano ZS). The material for TEM imaging is prepared by drying nanoparticles on a copper grid; samples for DSL measurements are undiluted in case of 20 nm AgNPs, and diluted with water by a factor of 10 and a factor of 20 for 50 nm and 75 nm AgNPs, respectively. According to the supplied information, the NPs are stable for at least one year, however, prolonged exposure to light may the change the material size. Accordingly, the NPs were always kept out of light as much as possible, but light exposure could not be completely prevented during handling.

Table 3.1 AgNP characteristics as provided by the manufacturer NanoComposix Inc

AgNP product [nm]	Average Diameter [nm]	Coefficient of variation [%]	SD [nm]	Average Hydrodynamic diameter [nm]	Zeta Potential [mV]	Mass concentration [mg Ag/ml]
20 nm	19.6	8.1	1.6	24.0	-30.4	1.09
50 nm	53.5	8.3	4.4	56.0	-53.6	0.95
75 nm	74.8	5.8	4.3	78.5	-37.6	0.99

Preparation of AgNPs dispersions

Due to the significant effects serum proteins present in tissue culture growth medium may have on uptake, these uptake studies were conducted with two types of medium, with fetal calf serum (+FCS) and without (w/o) the addition of FCS [34, 35, 40]. The dilutions of AgNPs dispersions were performed in complete tissue culture medium (see below), either without or with FCS, prior to exposure. Final exposure concentrations of 0.01 µg Ag/mL were obtained in several steps and pre-dilutions: Per 1 mL medium 10 µL of the NP dispersion were added for the first pre-dilution and mixed thoroughly. This pre-dilution was further diluted in in three steps to reach the exposure concentration of 0.01 µg Ag/mL. 200 µL of the final dilution were added to each well. We used concentrations of 0.01 µg/mL at which no change in metabolic toxicity has been shown in 16HBE14o-cells for NPs of the same type, from the same manufacturer and same sizes (20 and 50 nm) in absence of FCS in order to study uptake in uncompromised cells [41].

Cells and cell culture conditions

The human pulmonary epithelial cell line 16HBE14o (kindly provided by Dr. Gruenert, USA) was used in this study. 16HBE14o cells were cultured in Dulbecco's Modified Eagle Medium/Nutrient Mixture F-12 + GlutaMAX (DMEM/F-12, Gibco, the Netherlands), supplemented with antibiotics (1% Penicillin-Streptomycin (Pen/Strep), Gibco, the Netherlands) and 5% Fetal calf serum (FCS, Gibco, the Netherlands) designated complete medium. When the cells reached an 80-100% confluent monolayer they were subcultured, usually 1:5 once a week in new 75 mL tissue culture flasks (CellStar®, Greiner Bio-one, the Netherlands). 16HBE14o-cells were harvested enzymatically using Trypsin solution (Trypsin-EDTA (0.05%), phenol red, Gibco, the Netherlands), counted, diluted and seeded into 96 well plates at cell densities of 60 000-65 000 cells/well 24 hours before exposure to allow them to rest and to reach 80-90% confluence the day of exposure. Cells were constantly incubated at 37°C and 5% CO_2 atmosphere.

Cellular uptake of AgNPs

Cells were seeded in 96 well tissue culture plates as described in the "cell and cell culture conditions"-section and exposed to 200 µl of 0.01 µg/mL AgNP dispersions. The total

exposure times were 0, 2, 4, 8, 12 and 24 hours. At the end of exposure, cells were thoroughly washed with Dulbecco's Phosphate-Buffered Saline (DPBS, Without Calcium, Magnesium, Phenol Red, Gibco, the Netherlands) twice to remove loosely attached Ag ions and/or NPs from the cell membrane. 200 µL trypsin solution was added to detach the cells from the bottom of the well. Through pipetting it was made sure that all cells were detached, and successful detachment was confirmed by optical inspection with a light microscope (magnification 50x). Subsequently the sample was transferred to 15 mL polystyrene centrifuge tubes (Corning Life Sciences, the Netherlands) to be stored at 4°C until their measurement of tightly attached and internalized NPs. The samples were treated with 2 mL aqua regia (nitric acid, ultrapure and hydrochloric acid, ultrapure 1:3, both from Merck, Germany) and further diluted with ultra-pure water to a final volume of 10 mL prior to the determination of the total Ag concentration (particle-associated as well as ionic Ag) by HR-ICP-MS type ELEMENT XR, ThermoFisher Scientific, Bremen, Germany. The sample introduction systems consisted of a concentric nebulizer, a cyclone spray chamber and nickel cones (all from the instrument supplier). For the quantification, external calibration with internal standard correction (Rhodium as $^{103}Rh^{+}$) was applied. Sample pre-treatment and analysis were carried out in a cleanroom facility class 10 000. Each experiment was conducted independently two times for 50 and 75 nm AgNPs, and once for 20 nm AgNPs.

Statistical evaluation and calculations

For the determination of uptake rate constants c and elimination rate constants k, experimental results were evaluated with Microsoft Excel 2010 and the corresponding application "Solver" according to the one compartment model using Equation 3.1. Solver is a tool that determines the optimal value for variables, here c and k, within given limits in order to minimize differences between experimental and model data.

Equation 3.1

$$c(t) = \frac{c}{k} \cdot (1 - e^{-kt})$$

Where t is the time of exposure in hours; c is the uptake rate constant in ng Ag·well^{-1}·d^{-1}; and k is the elimination rate constant in ng Ag·well^{-1}·d^{-1}. Values for k were set to a minimum of 10^{-8} in order to avoid divisions by zero during the calculations, no other limits are set. Ag concentrations were standardized to a starting concentration of zero by subtracting the initial concentration in the cells from the concentrations in the cells at the later time point. To convert the amount of Ag/well as detected by HR-ICP-MS to assumed spherical NP numbers/well (NP No/well), the formulas according to [42] were used.

Results

The original result of each sample point as well as the model uptake curves are given in Figure 3.1. Uptake did not clearly level off during the time course for all samples. For the 50 and 75 nm samples without FCS the slope of the uptake curve clearly became less steep with time; the curve of the 75 nm samples with FCS levelled off slightly. In our set-up the uptake of 50 AgNPs was higher for medium without FCS than in medium supplemented with FCS, reaching approximately twice the maximum concentration after 24 hours of exposure. Uptake was also faster, as represented by the significantly different 95% confidence interval of the uptake rate constant c of $1.1 \cdot 10^{-1}$-$1.2 \cdot 10^{-1}$ and $6.9 \cdot 10^{-3}$-$5.2 \cdot 10^{-2}$ ng Ag·well^{-1}·d^{-1} without and with FCS, respectively. For 20 nm and 75 nm AgNPs, the same trend was observed but not as pronounced, the difference in uptake rates is statistically not significant.

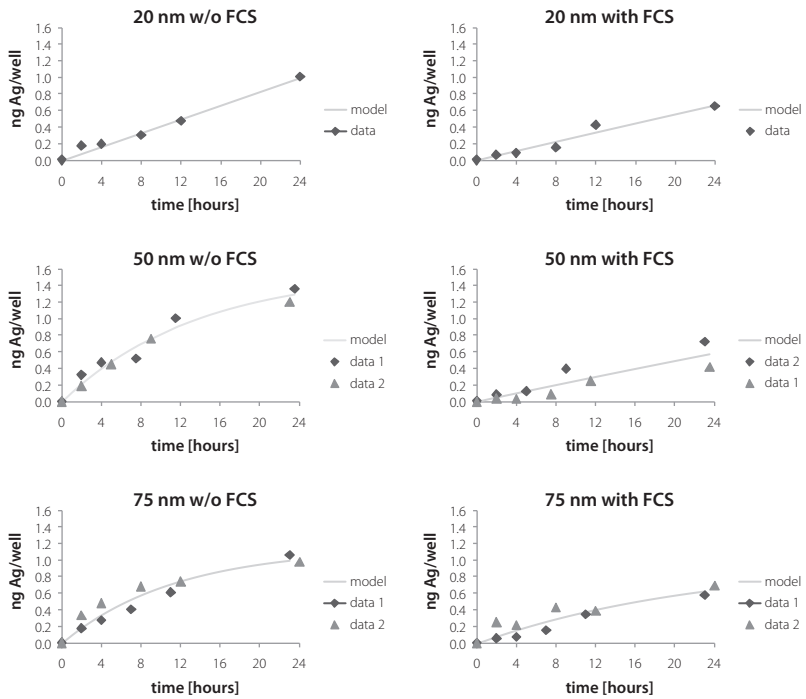

Figure 3.1 Ag amount in cells on mass basis with the fitted line for three NP sizes and medium without and with the addition of fetal calf serum based on one and two independent experiments for 20, and 50 and 75 nm particles, respectively. Note: Due to logistic aspects, the time points at which the samples have been obtained are slightly shifted sometimes (maximum 1 hour).

No differences in uptake, expressed as ng Ag per well, for the three NP sizes could be observed in the presence of FCS (Table 3.2), their uptake rate constants were not significantly different. The mean of all three AgNP sizes fell within the same narrow range.

Uptake in medium without FCS was faster and a size effect regarding the concentration at the latest time point could be seen (Figure 3.1, Figure S 3.1), although there is large variation between replicates. Uptake expressed as mass was highest for AgNPs with a size of 50 nm, reaching internal cell concentrations of approximately 65 % of the nominal concentration, followed by AgNPs of 75 nm and of 20 nm, each with roughly 50 % Ag uptake. For the latter AgNP size, only a single experiment was conducted, yet it did not fall into the confidence interval of the 50 nm samples. The uptake and elimination rates have been determined as presented in Table 3.2 and Table S 3.2, respectively. For medium supplemented with FCS, no difference in uptake rates could be detected (range: 0.03 to 0.05 ng Ag·well^{-1}·d^{-1}). The observed trend of highest uptake for 50 nm AgNPs was not reflected in the uptake rate, as the confidence intervals overlap for 50 and 75 nm AgNPs.

Table 3.2 Overview of the uptake curves based on mass [ng] Ag. Average uptake rate constants c, their standard deviation (Std. dev) and 95 % confidence Interval (CI) based on NP mass, all given in ng Ag·well^{-1}·d^{-1}.

NP size [nm], medium type	c	Std. dev. of c	95% CI of c
20 w/o FCS	$4.2 \cdot 10^{-2}$	n.a.	n.a.
50 w/o FCS	$1.1 \cdot 10^{-1}$	$4.0 \cdot 10^{-3}$	$1.1 \cdot 10^{-1}$-$1.2 \cdot 10^{-1}$
75 w/o FCS	$1.1 \cdot 10^{-1}$	$6.10 \cdot 10^{-2}$	$2.7 \cdot 10^{-2}$-$2.0 \cdot 10^{-1}$
20+FCS	$2.8 \cdot 10^{-2}$	n.a.	n.a.
50+FCS	$2.9 \cdot 10^{-2}$	$1.6 \cdot 10^{-2}$	$6.9 \cdot 10^{-3}$-$5.2 \cdot 10^{-2}$
75+FCS	$4.8 \cdot 10^{-2}$	$2.9 \cdot 10^{-2}$	$7.5 \cdot 10^{-3}$-$8.8 \cdot 10^{-2}$

n.a. not analyzed

A size optimum based on particle numbers does not necessarily lead to the same uptake optimum regarding NP mass [43]. To test whether this was the case here as well, the values were converted to particle numbers and their uptake rates compared. In this case, a clear difference, represented by the slope, was observed (Figure 3.2). The uptake rate, expressed as particle numbers per well per day, differed significantly for 20 nm AgNPs from the rate of 50 and 75 nm AgNPs, both in the absence and presence of FCS (Table 3.3). No difference in the uptake rate in presence of FCS could be observed for 50 and 75 nm AgNPs, while the rate was higher for 50 nm AgNPs than 75 nm AgNPs in the absence of FCS.

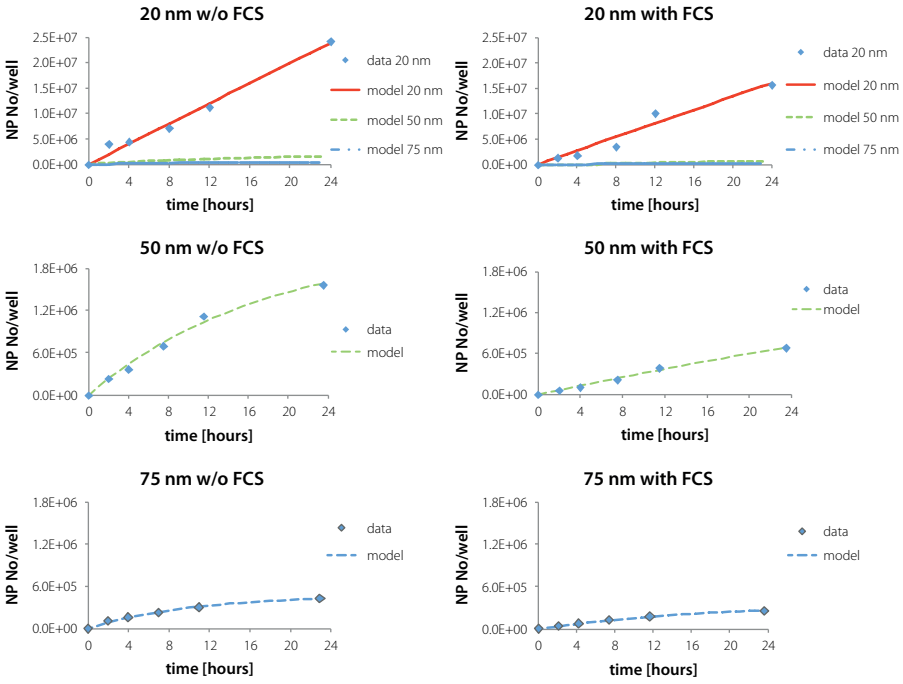

Figure 3.2 Average Ag content in cells on a NP number basis calculated from the independent mass based values for three NP sizes and medium without and with fetal calf serum as shown in figure 3.1. The two top graphs show model data for all three NP sizes for easy comparison and calculated average NP numbers for 20 nm AgNPs. The four graphs on the bottom show the average Ag content and the corresponding model data for 50 nm and 75 nm AgNPs in more detail. Note: Due to logistic aspects, the time points at which the samples have been obtained are slightly shifted sometimes (maximum 1 hour); different scaling on the y-axes.

Table 3.3 Overview of the uptake curves based on NP numbers [NP No]. Average uptake rate constants c, their standard deviation (Std. dev) and 95 % confidence Interval (CI) based on NP number, all given in NP number·well^{-1}·d^{-1}.

NP size [nm], medium type	C	Std. dev. of c	95% CI of c
20 w/o FCS	$1.0 \cdot 10^6$	n.a.	n.a.
50 w/o FCS	$1.4 \cdot 10^5$	$4.7 \cdot 10^3$	$1.3 \cdot 10^5$-$1.4 \cdot 10^5$
75 w/o FCS	$4.8 \cdot 10^4$	$2.6 \cdot 10^4$	$1.2 \cdot 10^4$-$8.4 \cdot 10^4$
20+FCS	$6.8 \cdot 10^5$	n.a.	n.a.
50+FCS	$3.5 \cdot 10^4$	$1.9 \cdot 10^4$	$8.2 \cdot 10^3$-$6.1 \cdot 10^4$
75+FCS	$2.1 \cdot 10^4$	$1.3 \cdot 10^4$	$3.2 \cdot 10^3$-$3.8 \cdot 10^4$

n.a.: not analyzed

Discussion

Our results show that the tissue culture medium composition in terms of presence or absence of fetal calf serum, effects NP uptake significantly, as confirmed by literature [34, 35, 40]. When no FCS is present final concentrations after 24 hours expressed on a mass basis are higher for 50 nm AgNPs than for 20 and 75 nm AgNPs. Internal cellular concentrations, expressed as a percentage of the nominal added concentrations, reached roughly 50% (20, 75 nm NPs) and 65 % (50 nm NPs). FCS decreases the amount of silver taken up on a mass basis by roughly 25 %, 54 % and 40 % for 20 nm, 50 nm and 75 nm AgNPs, respectively. A possible explanation is the formation of a protein corona around the AgNPs in the medium with FCS that reduces their uptake. Anionic bovine serum albumin for example showed repulsive interaction with the negatively charged cell membrane [44]. Recently it was reported that also for the uptake of fluorescent silica NPs an increase in serum concentration in the tissue culture medium resulted in a decrease in cellular uptake in human mesenchymal stem cells (hMSC) [45]. We show the importance to consider various medium compositions in toxicity studies, yet further confirmation for NPs of different charge and various types of serum proteins is needed. The higher uptake of 50 nm particles on mass basis in absence of FCS might be partially attributed to the more negative Zeta Potential of these AgNPs. At first, a higher uptake of more negatively charged NPs across the overall negatively charged cell membrane seems illogical due to repulsion. Yet, an early study already reports that positively charged patches on the cell surface exist [46]. The positively charged residues "seem to be accumulated in coated pits" [47] and could, therefore, be responsible for the binding and uptake of negatively charged NPs. An increase in the absolute Zeta Potential usually leads to increased NP uptake in comparison with less charged NPs of the same size [23]. Whether size or charge has the greater influence on uptake remains unknown up to today due to a limited number of

uptake kinetics studies and a lack in availability of NPs with proper characteristics to study these phenomena. This stresses the need for commercially available NPs with only one property changed at a time or, ideally, that reference materials were made available.

In contrast to the uptake studies by Chithrani et al. over 10 hours, uptake did not always clearly level off in time in our setup (Figure 3.1) [42]. This might be attributed to the different elemental NP composition (gold versus Ag) [48] and different cell lines (HeLa versus 16HBE14o) as summarized by us previously [23]; uptake of NPs also shows a concentration-dependency [30, 42, 49, 50]. Giljohann et al. showed that uptake does not necessarily relate to exposure concentrations in a linear fashion [45, 49]. Catalano et al. observed a levelling-off of the NP uptake in hMSC in the presence of serum whereas such a levelling-off was not present in the testing conditions without serum over a time course of only 6 hours, what makes a comparison with our results difficult [45]. Yet, our results show the opposite trend also for such short incubation times. Overall, our results show that uptake kinetics differ per NP and should be taken into account in toxicity studies.

Although generally mass is used as dosing parameter (it is also highly practical and convenient) for nanoparticles the unit that reacts with a cell is the whole particle. When mass is used as a dose for a soluble chemical this translates to a number of molecules reacting with a cell or cell receptors. Although nanoparticles also are composed of molecules and these molecules can react with cell receptors, due to its form (e.g. spherical, cube or tube-like) not all individual molecules can react with a cell or cell receptor. It is the whole particle that can be composed of a few but also many molecules depending on the size (and size distribution) of the investigated nanoparticle. So, a dose in mass, for nanoparticles, cannot be translated in a dose of molecules interacting with a cell or cell receptor. The dose in nanotoxicology is still under debate and can be dependent on the toxic parameter investigated. For example for lung inflammation the total surface area was found to be a better dose description than mass [14]. Also, it is debated whether for *in vitro* cytotoxicity experiments the dose in the medium should be used (in concentration of mass, surface area or particle number) or the dose as what the cells see or take up [51, 52].

It is also clearly shown that the measurand, in which results are presented, plays a very important role in the interpretation of the results. While in most cases no significant difference in uptake rate can be detected on a mass basis, there is a very clear effect of particle size on the uptake rate of 20 nm AgNPs when the results are presented on a number of particle basis (Figure 3.2). Uptake of smaller particles is faster than of larger particles independent of the culture medium composition, except for 50 and 75 nm AgNPs^{+} FCS where no significant difference was observed, but the total mass is equally fast, except for 20 and 50 nm AgNPs w/o FCS. The size optimum, which relates to the highest uptake rate, of 50 nm is only in good agreement with other studies when expressed on a mass basis, while it is not when expressed as particle number [39, 42]. In contrast to us, those studies found the highest uptake rate at 50 nm based on a particle number basis in various cell lines. Few other studies exist where uptake rates have been

determined, yet they are difficult to compare to our studies. The reasons for this is the difference in the used NP sizes. The following results are all converted to and reported on NP number basis. Uptake rates are found to be highest for 44 nm, followed by 114 nm and 33 nm [53]. The other researchers find 32 nm to show highest uptake rates, followed by 70 nm, 102 nm, and 118 nm respectively [38]. They originally report their results on mass basis, then the order is as follows: 102 nm, 70 nm, 118 nm, 32 nm. No clear pattern can be observed on mass basis. Only one of the few studies that also determine uptake rates is in agreement with our results. Expressed on NP number basis, uptake rates are also highest for 20 nm particles, followed by 40 nm and lowest for 100 nm [54]. Therefore, no conclusions about uptake optima based on particle number basis can be directly drawn even though all studied cell lines can utilize the mechanism of endocytosis just as 16HBE cells. The exact uptake mechanism for AgNPs into 16HBE cells used in our experiments is unknown because the determination of the exact uptake mechanism is very complex. It requires the determination of the exact concentration and incubation time for various inhibitors and has to be adjusted for each cell line separately [55]. Pinocytosis can be excluded as the uptake mechanism because it is a non-saturable process and saturation is clearly observed [56].

The non-uniform way of presenting results may lead to misinterpretation and false conclusions about agreement between studies, as criticized by [43]. They showed that an optimum based on the number of particles per cell does not necessarily lead to the same optimum in terms of mass. This was also nicely shown by Yue et al., who graphically showed that the size optimum depends on the measurand (number of particles per cell, particle volume per cell, and particle surface area per cell) [57].

We therefore recommend to pay close attention to the measurand given in various studies and would find it helpful if the optimum was given also in different measurands in one study for comparability between studies. Often important data for such conversions are not directly accessible in publications, e.g. it might be difficult to calculate the number of atoms per particle because only the total diameter is known but not the thickness of a coating.

Conclusion

The present study shows that the medium composition (absence or presence of FCS), has a large effect on the speed of uptake and therefore the maximum concentration after 24 hours of exposure. This should be taken into consideration in (toxicity-) studies, where uptake and internal concentration play a crucial role in understanding the mechanism of the observed effects. Uptake in medium without FCS shows a trend towards higher uptake for 50 nm AgNPs than 75 and 20 nm AgNPs on a mass basis. This uptake optimum shifts to 20 nm AgNPs when expressed on AgNP number basis in contrast to other results

reported in literature. For comparability between studies, direct conversion of uptake expressed as NP number and mass in one publication is advantageous; sometimes the necessary information to do so oneself is not directly available in the publication. Future developments will greatly benefit from the use of reference materials. Since the large and continuously growing number of engineered NPs cannot all be covered experimentally, comparability between studies would possibly help to close knowledge gaps and allow for extrapolation regarding uptake between different NPs by modelling. Modelling will be an indispensable tool to cover the large and continuously growing number of engineered NPs and to predict the uptake of untested NPs.

Supplementary material

Figure S 3.1 Ag amount on bass basis with 95% confidence intervals; Table S 3.2 Overview of the elimination rates based on mass [ng] Ag; Table S 3.3 Overview of the elimination rates based on NP numbers [NP No].

Acknowledgement

We would like to thank Henny Verharen and Eric Gremmer (both from RIVM) for their technical assistance.

Cited Work

1. B. Nowack and T.D. Bucheli, *Occurrence, behavior and effects of nanoparticles in the environment.* Environ. Pollut., **2007**. 150: p. 5-22.
2. C. Hendren, et al., *Modeling approaches for characterizing and evaluating environmental exposure to engineered nanomaterials in support of risk-based decision making.* Environ Sci Technol, **2013**. 47: p. 1190-1205.
3. S. Wijnhoven, et al., *Nanomaterials in consumer products: Update of products on the european market in 2010.* 2011, RIVM. p. 78.
4. A. Oomen, et al., *Nanomaterial in consumer products: Detection, characterisation and interpretation.* 2011, RIVM. p. 96.
5. T. Kuiken, et al. *The project on emerging nanotechnologies*. Consumer Products Inventory 2014 [cited 2014 July 28th]; Available from: http://www.nanotechproject.org/cpi/.
6. M.E. Vance, et al., *Nanotechnology in the real world: Redeveloping the nanomaterial comsumer products inventory.* Beilstein Journal of Nanotechnology, **2015**. 6: p. 1769-1780.
7. R. Foldbjerg, et al., *Pvp-coated silver np and silver ions induce ros, apoptosis and necrosis in thp-1 monocytes*. Toxicol Lett, **2009**. 190 (2): p. 156-163.
8. A. Haase, et al., *Toxicity of silver nanoparticles in human macrophages: Uptake, intracellular distribution and cellular responses* in *Journal of Physics: Conference Series*. 2011.
9. R.P. Singh and P. Ramarao, *Cellular uptake, intracellular trafficking and cytotoxicity of silver nanoparticles.* Toxicol Lett, **2012**. 213: p. 249-259.
10. M.V.D.Z. Park, et al., *The effect of particle size on the cytotoxicity, inflammation, developmental toxicity and genotoxicity of silver nanoparticles.* Biomaterials, **2011**. 32 (36): p. 9810-9817.
11. A. Maynard and E. Kuempel, *Airborne nanostructured particles and occupational health.* J Nanopart Res, **2005**. 7: p. 587–614.
12. R. Silva, et al., *Pulmonary effects of silver nanoparticle size, coating, and dose over time upon intratracheal instillation.* Toxicol Sci, **2015**. 144: p. 151-162.
13. F. Herzog, et al., *Exposure of silver-nanoparticles and silver-ions to lung cells in vitro at the air-liquid interface.* Part Fibre Toxicol, **2013**. 10 (11).
14. H. Braakhuis, et al., *Identification of the appropriate dose metric for pulmonary inflammation of silver nanoparticles in an inhalation toxicity study.* Nanotoxicol., **2016**. 10: p. 63-73.
15. J. Seiffert, et al. *Pulmonary toxicity of instilled silver nanoparticles: Influence of size, coating and rat strain.* PloS One, **2015**. DOI: 10.1371/journal.pone.0119726.
16. J. Ji, et al., *Twenty-eight-day inhalation toxicity study of silver nanoparticles in sprague–dawley rats*. Inhalaton Toxicology, **2007**. 19: p. 857–871.
17. F. Christensen, et al., *Nano-silver - feasibility and challenges for human health risk assessment based on open literature.* Nanotoxicology, **2010**. 4 (3): p. 284-95.
18. W. Jiang, et al., *Nanoparticle-mediated cellular response is size-dependent.* Nat Nanotechnol., **2008**. 3: p. 145-150.
19. C. He, et al., *Effects of particle size and surface charge on cellular uptake and biodistribution of polymeric nanoparticles*. Biomaterials, **2010**. 31: p. 3657-3666.
20. J. Rejman, et al., *Size-dependent internalization of particles via the pathways of clathrin- and caveolae-mediated endocytosis*. Biochemical Journal, **2004**. 377: p. 159-169.
21. S.-H. Wang, et al., *Size-dependent endocytosis of gold nanoparticles studied by three-dimensional mapping of plasmonic scattering images.* Journal of Nanobiotechnology, **2010**. 8 (33).
22. F. Lu, et al., *Size effect on cell uptake in well-suspended, uniform mesoporous silica nanoparticles.* Small, **2009**. 5 (12): p. 1408–1413.
23. K. Kettler, et al., *Cellular uptake of nanoparticles as determined by particle properties, experimental conditions, and cell type.* Environ. Toxicol. Chem., **2014**. 33 (3): p. 481-492.
24. S.D. Conner and S.L. Schmid, *Regulated portals of entry into the cell.* Nature, **2003**. 422: p. 37-44.
25. G.J. Doherty and H.T. Mcmahon, *Mechanisms of endocytosis.* Annual Review of Biochemistry, **2009**. 78: p. 857-902.
26. S.K. Basu, *Receptor-mediated endocytosis of hormones in cultured cells.* Journal of Biosciences, **1984**. 6 (4): p. 535-542.
27. K. Hirota and H. Terada, *Endocytosis of particle formulations by macrophages and its application to clinical treatment*, in *Molecular regulation of endocytosis*, B. Ceresa, Editor. 2012, InTech: Rijeka, Croatia.

28. T. Xia, et al., *Cationic polystyrene nanosphere toxicity depends on cell-specific endocytic and mitochondrial injury pathways.* ACS Nano, **2008**. 2 (1): p. 85-96.
29. E.J. Park, et al., *Oxidative stress and apoptosis induced by titanium dioxide nanoparticles in cultured beas-2b cells.* Toxicol Lett, **2008**. 180 (3): p. 222-229.
30. L. Limbach, et al., *Exposure of engineered nanoparticles to human lung epithelial cells: Influence of chemical composition and catalytic activity on oxidative stress.* Environ Sci Technol, **2007**. 41: p. 4158–4163.
31. S.N. Luoma, *Silver nanotechnologies and the environment: Old problems or new challenges?* 2008, The Pew Charitable Trusts.
32. N. Lubick, *Nanosilver toxicity: Ions, nanoparticles–or both?* Environ Sci Technol, **2008**. 42: p. 8617.
33. Y. Ikada and Y. Tabata, *Phagocytosis of bipactive microspheres.* Journal of Bioactive and Compatible Polymers, **1986**. 1: p. 32-46.
34. A.J. Sbarra and M.L. Karnovsky, *The biochemical basis of phagocytosis.* Journal of Biological Chemistry, **1959**. 243 (6): p. 1355-1362.
35. S. Nagayama, et al., *Time-dependent changes in opsonin amount associated on nanoparticles alter their hepatic uptake characteristics.* International Journal of Pharmaceutics, **2007**. 342: p. 215-221.
36. P. Krystek, et al., *Exploring influences on the cellular uptake of medium-sized silver nanoparticles into thp-1 cells.* Microchemical Journal, **2015**. 120: p. 45-50.
37. S. Gangwal, et al., *Informing selection of nanomaterial concentrations for toxcast in vitro testing based on occupational exposure potential.* Environ. Health Persp., **2011**. 119 (11): p. 1539-1546.
38. X. Huang, et al., *The effect of the shape of mesoporous silica nanoparticles on cellular uptake and cell function.* Biomaterials, **2010**. 31: p. 438–448.
39. K. Shapero, et al., *Time and space resolved uptake study of silica nanoparticles by human cells.* Mol Biosyst, **2010**. 7 (3): p. 371-378.
40. Y. Ikada and Y. Tabata, *Phagocytosis of bioactive microspheres.* Journal of Bioactive and Compatible Polymers, **1986**. 1: p. 32-46.
41. H. Braakhuis, et al., *Simple in vitro models can predict pulmonary toxicity of silver nanoparticles.* Nanotoxicol., **2016**. 10 (6): p. 770-779.
42. B.D. Chithrani, A.A. Ghazani, and W.C.W. Chan, *Determining the size and shape dependence of gold nanoparticle uptake into mammalian cells.* Nano Letters, **2006**. 6 (4): p. 662-668.
43. R. Lévy, et al. *Gold nanoparticles delivery in mammalian live cells: A critical review.* Nano Reviews, **2010**. 1, DOI: 10.3402/nano.v1i0.4889.
44. Z.-J. Zhu, et al., *The interplay of monolayer structure and serum protein interactions on the cellular uptake of gold nanoparticles.* Small, **2012**.
45. F. Catalano, et al., *Factors ruling the uptake of silica nanoparticles by mesenchymal stem cells: Agglomeration versus dispersions, absence versus presence of serum proteins.* small, **2015**. 11 (24): p. 2919-2928.
46. N. Ghinea and N. Simionescu, *Anionized and cationized heme undecapeptides as probes for cell surface charge and permeability studies: Differentiated labeling of endothelial plasmalem.* Journal of Cell Biology, **1986**. 100: p. 606-612.
47. L. Ghitescu and A. Fixman, *Surface charge distribution on the endothelial cell of liver sinusoids.* Journal of Cell Biology, **1984**. 99 (2): p. 639-647.
48. F. Ahsan, et al., *Targeting to macrophages: Role of physicochemical properties of particulate carriers- liposomes and micropheres- on the phagocytosis by macrophages.* J. Control. Release, **2002**. 79: p. 29-40.
49. D.A. Giljohann, et al., *Oligonucleotide loading determines cellular uptake of DNA-modified gold nanoparticles.* Nano Letters, **2007**. 7 (12): p. 3818-3821.
50. P.V. Asharani, M. Prakash Hande, and S. Valiyaveettil, *Anti-proliferative activity of silver nanoparticles.* BMC Cell Biology, **2009**. 10 (65).
51. G. Deloid, et al. *Advanced computational modeling for in vitro nanomaterial dosimetry.* Part Fibre Toxicol, **2015**. 12, DOI: 10.1186/s12989-015-0109-1.
52. J.G. Teeguarden, et al., *Particokinetics in vitro: Dosimetry considerations for in vitro nanoparticle tocixity assessments.* Toxicol Sci, **2007**. 95 (2): p. 300-312.
53. J.A. Varela, et al. *Quantifying size-dependent interactions between fluorescently labeled polystyrene nanoparticles and mammalian cells.* Journal of Nanobiotechnology, **2012**. 10, DOI: 10.1186/1477-3155-10-39.

54. Z. Wang, et al., *Size and dynamics of caveolae studied using nanoparticles in living endothelial cells.* ACS Nano, **2009**. 3 (12): p. 4110–4116.
55. D.A. Kuhn, et al., *Different endocytotic uptake mechanisms for nanoparticles in epithelial cells and macrophages.* Beilstein J. Nanotechnol., **2014**. 5: p. 1625-1636.
56. E. Fröhlich, *The role of surface charge in cellular uptake and cytotoxicity of medical nanoparticles.* Int. J. Nanomed, **2012**. 7: p. 5577–5591.
57. H. Yue, et al., *Particle size affects the cellular response in macrophages.* European Journal of Pharmaceutical Sciences, **2010**. 41: p. 650-657.

Appendix

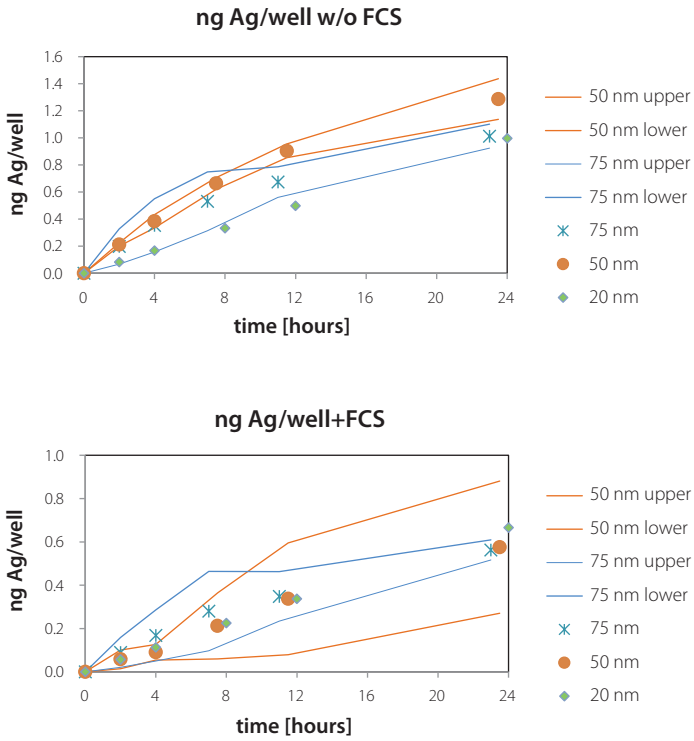

Figure S 3.1 Ag amount on bass basis with 95% confidence intervals.

Table S 3.1 Overview of the elimination rates based on mass [ng] Ag. Average elimination rate constants k, their standard deviation (Std. dev) and 95 % confidence Interval (CI) based on NP mass, all given in ng Ag·well^{-1}·d^{-1}.

NP size [nm], medium type	k	Std. dev. of k	95% CI of k
20 w/o FCS	$1.0 \cdot 10^{-7}$	n.a.	n.a.
50 w/o FCS	$7.3 \cdot 10^{-2}$	$5.3 \cdot 10^{-3}$	$6.5 \cdot 10^{-2}$-$8.0 \cdot 10^{-2}$
75 w/o FCS	$9.9 \cdot 10^{-2}$	$8.9 \cdot 10^{-2}$	$-2.4 \cdot 10^{-2}$-$2.2 \cdot 10^{-1}$
20+FCS	$1.9 \cdot 10^{-3}$	n.a.	n.a.
50+FCS	$1.1 \cdot 10^{-2}$	$1.6 \cdot 10^{-2}$	$-1.1 \cdot 10^{-2}$-$3.3 \cdot 10^{-2}$
75+FCS	$4.9 \cdot 10^{-2}$	$6.2 \cdot 10^{-2}$	$-3.6 \cdot 10^{-2}$-$1.3 \cdot 10^{-1}$

n.a.: not analyzed

Table S 3.2 Overview of the elimination rates based on NP numbers [NP No]. Average elimination rate constants k, their standard deviation (Std. dev) and 95 % confidence Interval (CI) based on NP number, all given in NP number·well^{-1}·d^{-1}.

NP size [nm], medium type	k	Std. dev. of k	95 % CI of k
20 w/o FCS	$1 \cdot 10^{-8}$	n.a.	n.a.
50 w/o FCS	$7.3 \cdot 10^{-2}$	$5.3 \cdot 10^{-3}$	$6.5 \cdot 10^{-2}$-$8.0 \cdot 10^{-2}$
75 w/o FCS	$1.0 \cdot 10^{-1}$	$8.9 \cdot 10^{-2}$	$-2.4 \cdot 10^{-2}$-$2.2 \cdot 10^{-1}$
20+FCS	$1.9 \cdot 10^{-3}$	n.a.	n.a.
50+FCS	$1.1 \cdot 10^{-2}$	$1.6 \cdot 10^{-2}$	$-1.1 \cdot 10^{-2}$-$3.3 \cdot 10^{-2}$
75+FCS	$4.9 \cdot 10^{-2}$	$6.2 \cdot 10^{-2}$	$-3.6 \cdot 10^{-2}$-$1.4 \cdot 10^{-1}$

n.a.: not analyzed

4

Uptake of silver nanoparticles by monocytic THP-1 cells depends on particle size and presence of serum protein

Published in
Journal of Nanoparticle research, 2016. Vol. 18, No. 286

Katja Kettler[a], Christina Giannakou[b,c], Wim H. de Jong[b], A. Jan Hendriks[a], and Petra Krystek[d,e]

[a] Department of Environmental Science, Institute for Water and Wetland Research, Radboud University, Nijmegen, The Netherlands
[b] National Institute for Public Health and the Environment (RIVM), Bilthoven, The Netherlands
[c] Department of Toxicogenomics, Maastricht University, Maastricht, The Netherlands
[d] Institute for Environmental Studies (IVM), VU University, Amsterdam, The Netherlands
[e] Philips Innovation Services, Eindhoven, The Netherlands

Abstract

Human health risks by silver nanoparticle (AgNP) exposure are likely to increase due to the increasing number of NP containing products and demonstrated adverse effects in various cell lines. Unfortunately, results from (toxicity-) studies are often based on exposure dose and are often measured only at a fixed time point. NP uptake kinetics and the time-dependent internal cellular concentration are often not considered. Macrophages are the first line of defense against invading foreign agents including NPs. How macrophages deal with the particles is essential for potential toxicity of the NPs. However, there is a considerable lack of uptake studies of particles in the nanometer range and macrophage-like cells. Therefore, uptake rates were determined over 24 hours for three different AgNPs sizes (20, 50 and 75 nm) in medium with and without fetal calf serum. Non-toxic concentrations of 10 ng Ag/mL for monocytic THP-1 cells, representing realistic exposure concentration for short term exposures, were chosen. The uptake of Ag was higher in medium without fetal calf serum and showed increasing uptake for decreasing NP sizes, both on NP mass and number basis. Internal cellular concentrations reached roughly 32%/ 10%, 25%/ 18%, and 21%/ 15% of the nominal concentration in absence of fetal calf serum/with fetal calf serum for 20, 50 and 75 nm NPs, respectively. Our research shows that uptake kinetics in macrophages differ for various NP sizes. To increase the understanding of the mechanism of NP toxicity in cells, the process of uptake (timing) should be considered.

Introduction

Nanoparticles (NPs) have dimensions from 1 nm up to 100 nm by common consensus [1]. Their unique physical and chemical properties arouse high interest by industry regarding their use for consumer products and medical applications as previously described in more detail [2]. The same properties that make them interesting for industrial applications, especially their small size and high reactivity, raise serious concerns regarding a potential risk to human health and biota on the long term [3] through exposure via one of the four exposure routes: injection, dermal and intestinal uptake, and inhalation; the latest being considered the most important especially during NP production and processing [4]. Exposure to NPs and subsequent uptake has been shown to affect various cell lines, including phagocytosing cells like THP-1-derived macrophages [5-8]. Unfortunately, uptake kinetics and time-dependent internal cellular concentrations are often neglected in experiments with measurements after a single fixed point in time and toxicity is related to exposure dose instead. Uptake is known to be influenced by NP properties such as size, as shown for various cell lines *in vitro*. Unfortunately, uptake has only been detected after a fixed time point in many studies [9-13].

Uptake of NPs into cells, after contact via one of the four exposure routes, occurs through two fundamental biological processes namely pinocytosis and phagocytosis, both tailor fit for their biological function. These fundamental biological mechanisms are responsible for the uptake of molecules from the environment. NPs have been shown to be able to enter cells via these two mechanisms as summarized by [14]. Pinocytosis, a mechanism usually employed by eukaryotic cells, such as 16HBE14o cells, to take up small essential nutrients [15], is described in more details elsewhere [2]. The vesicles reach sizes of up to 80 nm in diameter (i.d.) for caveolae-mediated endocytosis or 120 nm i.d. for clathrin-mediated endocytosis. Phagocytosis on the other hand is a more specialized mechanism that can be found in unicellular organisms as well as in complex multicellular animals [16, 17]. Phagocytosis as part of the immune defense in animals, is special in the way that it is restricted to a few types of cells, such as monocytes, neutrophils, and macrophages, to which THP-1 cells belong. Phagocytosis is a ligand-induced process, so especially the presence or absence of serum proteins have great effects on NP uptake as summarized previously [14]; the formed vesicles reach sizes between 0.5 µm to 10 µm [18]. In presence of proteins a so called protein corona on the NPs surface may be formed, leading to uptake that can be increased, decreased or remain the same, depending on the surface composition of the NPs, the type of cell and proteins and/or other biomolecules present on the NP surface [19-21].

Very few efforts have been made to study the size-dependent uptake of NPs with diameters smaller than 100 nm into phagocytising cells. Uptake rates over time where determined in two studies only [22, 23], while the majority only reports uptake at one single point in time [11, 24-26]. In addition, these studies are also inconclusive about the

effect of size on uptake into phagocytising cells. To overcome this lack in data, we determine uptake rates for different AgNPs sizes in cell culture medium with and without FCS in this study. Previously it was shown that similar AgNPs induced cellular toxicity for the murine macrophage cell line RAW264.7 at concentrations of approximately 10 µg/mL and higher [8]. In this study low nontoxic concentrations of 0.01 µg/mL were used to study cell uptake without inducing toxicity. Cells were, therefore, exposed to NPs for different periods of time over 24 hours under realistic concentrations for short term exposures. These data will deliver new insights into the effect of NP size on their uptake rate and are required to model and predict NP uptake rates based on easily measurable NP properties. The number of applications and produced quantities of NPs are increasing [27-29] and especially the combination of empirical data like ours and modelling will allow for time- and cost-effective risk assessment of the ever increasing number of NPs.

Material and Methods

A detailed description of the material and methods can be found elsewhere [2], so here only a brief description is given.

Nanoparticles

Keeping the possible vesicles size of up to 80 nm in diameter (i.d.) for caveolae-mediated endocytosis in mind and to avoid an overlap in the size distribution of NPs, we chose NPs with diameter of 20, 50 and 75 nm. The following AgNPs were purchased from NanoComposix Inc (San Diego, CA): 20 nm Citrate BioPure™ Silver, 50 nm Citrate BioPure™ Silver and 75 nm Citrate BioPure™ Silver. The supplier provided detailed information about the NPs characteristics [2].

Preparation of AgNPs dispersions

Due to the significant effects serum proteins present in cell culture growth medium may have on uptake, these uptake studies were conducted with media with fetal calf serum (+FCS) and without (w/o) [19-21]. The dilutions of AgNPs dispersions were performed in complete cell culture medium (see below), either without or with FCS, prior to exposure. Final exposure concentrations of 0.01 µg Ag/mL were obtained in several steps of pre-dilutions. We used very low concentrations of 0.01 µg/mL at which we do not expect cellular cytotoxicity. Similar AgNPs (20 nm and 80 nm) of the same supplier induced cellular toxicity for the murine macrophage cell line RAW264.7 at concentrations of approximately 10 µg/mL and higher (Park et al., 2011). Also for .THP-1-cells at low concentrations no cytotoxicity was noted for similar (20 and 50 nm) AgNPs of the same manufacturer (H.M. Braakhuis, personal communication). In addition, these concentrations represent realistic concentrations for short term occupational alveolar lung exposures [30].

Cells and cell culture conditions

The human monocytic cell line (THP-1, ATCC) was used in this study. THP-1 cells were cultured in Roswell Park Memorial Institute (RPMI) 1640 cell culture growth medium, supplemented with 10% Fetal calf serum, and antibiotics (1% Penicillin-Streptomycin (Pen/Strep), all obtained from Gibco, The Netherlands). This is designated complete medium. Cells were subcultured usually twice a week not to exceed a concentration of $1{\cdot}10^6$ viable cells/mL. Subcultures where started with a cell density of $2{\cdot}10^5$ to $4{\cdot}10^5$ viable cells/mL. Cells were constantly incubated at 37°C and 5% CO_2 atmosphere. Seven days prior to exposure to AgNPs, THP-1 were differentiated to macrophages according to the following procedure: THP-1 were diluted to a concentration of $5{\cdot}10^5$ viable cells/mL to which phorbol myristate acetate (PMA, Sigma, The Netherlands) was added to reach a final concentration of 30 ng PMA/mL. Afterwards, $1{\cdot}10^5$ viable cells were added per well of a 96 flat button cell culture plate to differentiate and become adherent. On day 5, medium was replaced by fresh medium; on day 7 the cells were exposed to AgNPs as described in section 'cellular uptake of AgNPs'.

Cellular uptake of AgNPs

Cells were seeded in 96 well cell culture plates as described in the "cell and cell culture conditions"-section and exposed to 200 µl of 0.01 µg/mL AgNP dispersions. The total exposure times were 0, 2, 4, 8, 12 and 24 hours. Note: Due to logistic aspects, the time points at which the samples have been obtained are slightly shifted sometimes (maximum 2 hours). At the end of exposure, cells were thoroughly washed with Dulbecco's Phosphate-Buffered Saline (DPBS, Without Calcium, Magnesium, Phenol Red, Gibco, the Netherlands) twice to remove loosely attached Ag ions and/or NPs from the cell membrane. 200 µL trypsin solution (Gibco, The Netherlands) was added to detach the cells from the bottom of the well. Through pipetting it was made sure that all cells were detached, and successful detachment was confirmed by optical inspection with a light microscope (magnification 50x). Each experiment was conducted independently two times for 20 nm AgNPs, and three times for 50 and 75 nm AgNPs.

Statistical evaluation and calculations

For the determination of uptake rate constants c and elimination rate constants k, experimental results were evaluated with Microsoft Excel 2010 and the corresponding application "Solver" according to the one compartment model using Equation 4.1. Solver is a tool that determines the optimal value for variables, here c and k, within given limits in order to minimize differences between experimental and model data.

Equation 4.1

$$c(t) = \frac{c}{k} \cdot (1 - e^{-kt})$$

Where t is the time of exposure in hours; c is the uptake rate constant in ng Ag·well^{-1}·day^{-1}; and k is the elimination rate constant in ng Ag·well^{-1}·day^{-1}. Values for k were set to a minimum of 10^{-8} in order to avoid divisions by zero during the calculations, no other limits are set. Ag concentrations were standardized to a starting concentration of zero by subtracting the initial concentration in the cells from the concentrations in the cells at the later time point.

Results

The results for each replicate, as well as the according model uptake curves, for the three NP sizes are given in Figure 4.1. The data points displayed in light grey belonging to data set 3 of the 50 nm samples w/o and +FCS were evaluated as outliers, likely due to insufficient washing, and were not considered in the calculations for the model curve. Uptake clearly levelled off during the time course for all samples except for the 50 nm +FCS where the rate of uptake stayed constant over 24 hours. In our set-up, the average uptake in absence of FCS was higher than in the presence of FCS for 20 and 50 nm particles, reaching highest intra cellular concentrations after 24 hours. This effect was most pronounced for 20 nm particles reaching an approximately three fold higher maximum concentration after 24 hours of exposure in the absence of FCS than in presence of it. Average internal cellular concentrations after 24 hours decreased with increasing particle size in absence of FCS, reaching approximately 32%, 25% and 21% of the nominal concentration for 20, 50 and 75 nm particles, respectively.

The uptake and elimination rates on mass basis are given in Table 4.1 and Table S 4.1. The uptake rate constants are significantly different between media composition for 20 and 50 nm particles. In absence of FCS, uptake was also faster for the smallest particles compared to 50 nm particles as represented by the significantly different 95% confidence interval of the uptake rate constant c. No significant difference in uptake rate was found between the other NP sizes due to the large difference in uptake rates between replicates of 75 nm particles.

The measurand in which results are presented (mass versus number of NP) is crucial because a size optimum based on mass does not necessarily lead to the same uptake optimum regarding NP numbers [31]. In our case, where uptake on mass basis is highest for the smallest NP size, the same will hold true on NP basis. Yet, when expressed on NP number basis, the difference might become significant. To test whether this is the case, and for comparison with other studies, NP numbers were calculated. The results without FCS change in so far, that the uptake rate of 20 nm AgNPs differs significantly from those of 50 nm and 75 nm AgNPs.

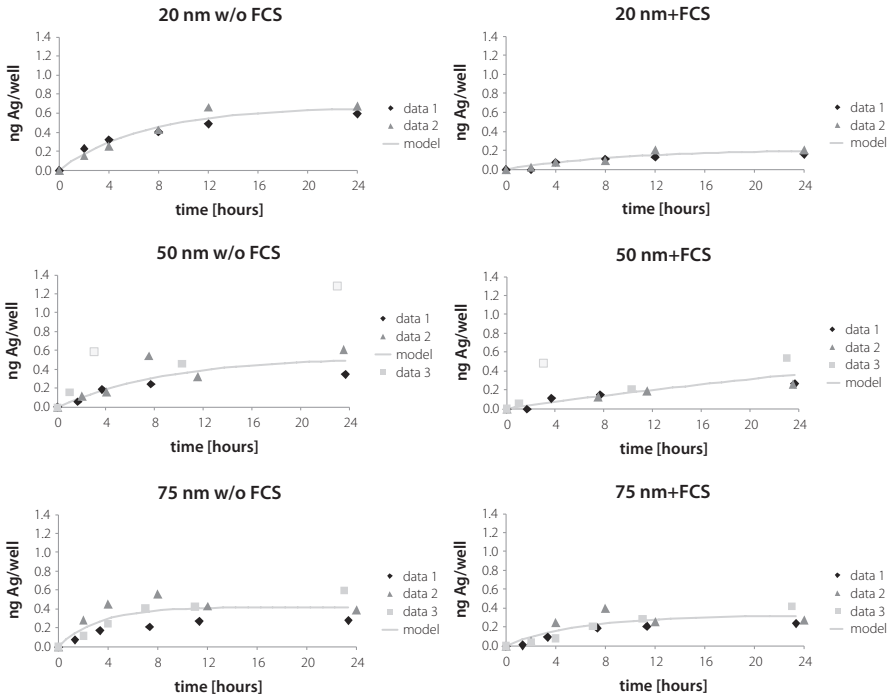

Figure 4.1 Ag amount in cells on mass basis with the fitted line for three NP sizes and medium without and with fetal calf serum based on at least two independent experiments (data 1 to data 3). The *light gray* data points belonging to data set 3 are indicated as outliers and were not considered in the determination of the fitted line. *Note* Due to logistic aspects, the time points at which the samples have been obtained are slightly shifted sometimes.

Table 4.1 Overview of the uptake rates based on mass [ng] Ag

NP size [nm], medium type	c	Std. dev. of c	95% CI of c
20 w/o FCS	$1.0 \cdot 10^{-1}$	$1.5 \cdot 10^{-2}$	$8.0 \cdot 10^{-2}$-$1.2 \cdot 10^{-1}$
50 w/o FCS	$5.6 \cdot 10^{-2}$	$2.0 \cdot 10^{-2}$	$3.3 \cdot 10^{-2}$-$7.8 \cdot 10^{-2}$
75 w/o FCS	$1.4 \cdot 10^{-1}$	$1.2 \cdot 10^{-1}$	$9.5 \cdot 10^{-3}$-$2.7 \cdot 10^{-1}$
20+FCS	$2.1 \cdot 10^{-2}$	$1.1 \cdot 10^{-3}$	$1.9 \cdot 10^{-2}$-$2.3 \cdot 10^{-2}$
50+FCS	$2.2 \cdot 10^{-2}$	$5.8 \cdot 10^{-3}$	$1.6 \cdot 10^{-2}$-$2.9 \cdot 10^{-2}$
75+FCS	$5.6 \cdot 10^{-2}$	$3.5 \cdot 10^{-2}$	$1.6 \cdot 10^{-2}$-$9.6 \cdot 10^{-2}$

Average uptake rate constants *c* and elimination rate constants *k*, their standard deviation (Std. dev) and 95 % confidence Interval (CI) based on mass, all given in ng Ag·well^{-1}·day^{-1}.

The uptake rates are not significantly different for 50 and 75 nm AgNPs in absence of FCS. THP-1 cells favor the uptake of smaller AgNPs on NP number basis in absence of FCS. This is depicted in Figure 4.2.

Discussion

Our results show that the cell culture medium composition in terms of presence or absence of FCS, affected the AgNP uptake in the macrophages considerably for 20 nm AgNPs (3 times higher uptake) and 50 nm AgNPs, as confirmed by literature [19-21]. In medium with FCS, a so called "protein corona" around the AgNPs might be formed reducing uptake.

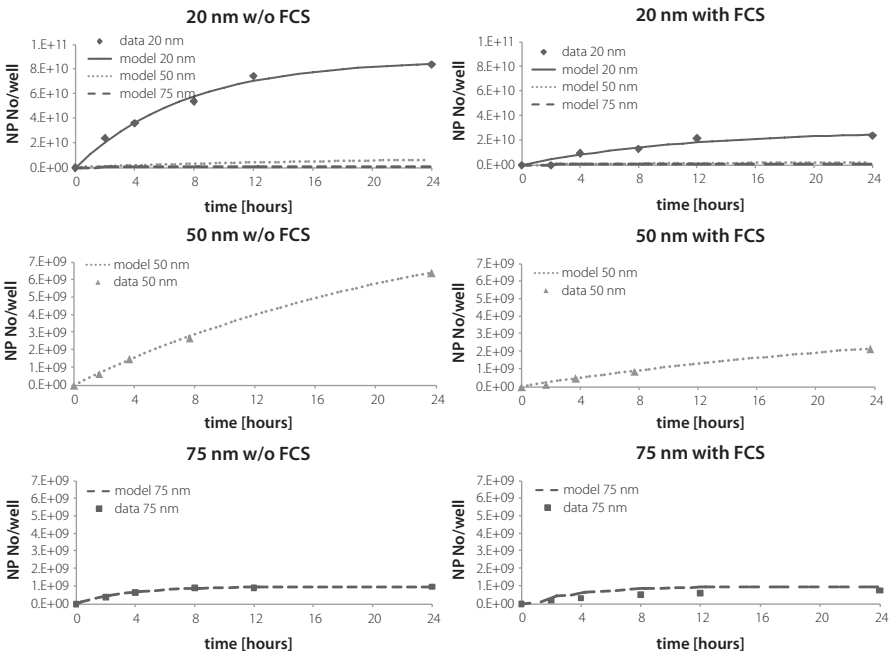

Figure 4.2 Average Ag content in cells on a NP number basis calculated from the independent mass based values for three NP sizes and medium without and with fetal calf serum as shown in Figure 4.1. The two top graphs show model data for all three NP sizes for easy comparison and calculated average NP numbers for 20 nm AgNPs. The four graphs on the bottom show the average Ag content and the corresponding model data for 50 nm and 75 nm AgnPs in more detail. *Note* Due to logistic aspects, the time points at which the samples have been obtained are slightly shifted sometimes; different scaling on the y-axes.

The protein corona can lead to repulsive interaction with the negatively charged cell membrane as shown for anionic bovine serum albumin [32]. Yet, further confirmation for NPs of different charge and various types of serum proteins and other biomolecules that might be part of the protein corona is needed. When no FCS was present, final concentrations after 24 hours were found to be higher for the smaller NPs. Uptake changes over time and levels off after approximately 12 hours. Overall, our results show that uptake kinetics may differ per NP and therefore should be taken into account in toxicity studies (Table 4.2).

Table 4.2 Overview of the uptake rates based on AgNP numbers

NP size [nm], medium type	c	Std. dev. of c	95% CI of c
20 w/o FCS	$1.2{\cdot}10^{10}$	$1.6{\cdot}10^{9}$	$1.0{\cdot}10^{10}$-$1.5{\cdot}10^{10}$
50 w/o FCS	$4.5{\cdot}10^{8}$	$1.1{\cdot}10^{8}$	$3.4{\cdot}10^{8}$-$5.7{\cdot}10^{8}$
75 w/o FCS	$3.1{\cdot}10^{8}$	$2.6{\cdot}10^{8}$	$1.8{\cdot}10^{7}$-$6.0{\cdot}10^{8}$
20+FCS	$2.5{\cdot}10^{9}$	$1.4{\cdot}10^{8}$	$2.3{\cdot}10^{9}$-$2.7{\cdot}10^{9}$
50+FCS	$1.3{\cdot}10^{8}$	$3.4{\cdot}10^{7}$	$9.5{\cdot}10^{7}$-$1.7{\cdot}10^{8}$
75+FCS	$1.2{\cdot}10^{8}$	$8.0{\cdot}10^{7}$	$3.3{\cdot}10^{7}$-$2.1{\cdot}10^{8}$

Average uptake rate constants *c* and elimination rate constants *k*, their standard deviation (Std. dev) and 95 % confidence Interval (CI) based on AgNP numbers, all given in AgNPs·well^{-1}·day^{-1}.

After inhalation lung macrophages are the most important cells for removal of the inhaled NPs from the lung. However, studies determining uptake by phagocytosing cells for particles in the nano-range and considering uptake over time are scarce and up to now inconclusive. Our results show that the amount taken up was in the order 20>50=75 nm without FCS, and 50=75>20 nm in the presence of FCS on mass basis. In contrast to our findings that uptake is highest for smallest NPs, uptake by macrophages based on mass is less effective for smaller PEGylated NPs than their larger counterparts [22]. Uptake efficiency increases from 30 nm NPs, over 40 nm NPs, to 100 nm NPs. HeLa cells on the other hand favor the intermediate size with uptake in the following order: 50>30>74>14>100 on NP number basis [23]. It would be interesting to see whether and how these trends changes when expressed on mass basis.

We therefore recommend that the optimum uptake is presented in both measurands to allow for comparability between studies. Alternatively, data that allow for such conversions might be given. Such a conversion is difficult if, e.g. the total diameter is known but not the thickness of a coating. Levy et al. also showed that an optimum based on the number of NPs per cell does not necessarily lead to the same optimum in terms of mass [31]. Yue et al. graphically visualized the dependence of the size optimum on the measurand (number of particles per cell, particle volume per cell, and particle surface area per cell) [33].

Different trends in the optimal particle size for uptake can be attributed to the numerous experimental factors that differ between studies, for example different NP materials and the use of FCS during incubation and whether opsonisation takes place, as summarized previously by us [14]. Surface charge also effects NP uptake, an increase in the absolute Zeta Potential usually leads to increased NP uptake in comparison with less charged NPs [14]. For the 50 nm AgNPs used in this study, charge might to some extend also determine uptake in comparison to the other AgNPs because their Zeta Potential differs from that of the 20 and 75 nm AgNPs from the same manufacturer. This stresses the need for commercially available NPs with only one property changed at a time or, ideally, that reference materials we made available.

Other factors that influence uptake are the use of various cell lines, different possible uptake mechanisms, and exposure concentration. While phagocytosis is usually considered to take place for materials with sizes larger than 0.5 µm, Kuhn et al. showed that polystyrene NPs with sizes of 28 nm were taken up by J774A.1 macrophages via micropinocytosis and phagocytosis, as well as clathrin-mediated endocytosis [34]. The exact uptake mechanism for AgNPs into THP-1 cells used in our experiments is unknown. The uptake mechanism can vary between differentiated and undifferentiated THP-1 cells [35]. In addition, the determination of the exact concentration and incubation time for the various inhibitors is very complex and have to be adjusted for each cell line separately [34]. Saturation of uptake is observed, therefore pinocytosis, a non-saturable process, as the uptake mechanism can be excluded [36].

Conclusions

Our study clearly shows that the presence of FCS reduces cellular uptake for AgNPs of different sizes in the macrophage cell line THP-1 and that uptake should be reported both as NP number and mass based uptake. Our results show that reporting both in every study is important as the order of uptake in relation to NP size might change with the measurand and would be advantageous for easy comparison of results. Studies that determine uptake kinetics of particles with sizes below 100 nm by phagocytosing cells are scarce, stressing the need for further experimental investigation similar to the presented work. Therefore, patterns for the effect of particle size on uptake rate into phagocytosing cells are uncertain. Future developments will benefit most from studies where either the same NPs are tested in various phagocytosing cell lines known for their different endocytic uptake mechanisms (e.g. clathrin- versus caveolae-mediated endocytosis) or NPs of different chemical composition that are tested in the same cell line in order to fill knowledge gaps and resolve apparent contradictions. Once patterns emerge, extrapolation between different NPs and between different experimental conditions will be possible. Modelling will be an indispensable tool to cover the large and continuously growing number of engineered NPs and to predict the uptake of untested NPs.

Supplementary material

Table S 4.1 Overview of the elimination rates based on mass [ng] Ag. Table S 4.2 Overview of the elimination rates based on AgNP numbers.

Acknowledgement

We would like to thank Henny Verharen and Eric Gremmer (both from RIVM) for their technical assistance. The present study was supported by NanoNextNL, a micro and nanotechnology consortium of the Government of the Netherlands and 130 partners.

Cited Work

1. European Commission, *Commission recommendation of 18 october 2011 on the definition of nanomaterial (text with eea relevance).* 2011: Brussels, Belgium.
2. K. Kettler, et al., *Exploring the effect of silver nanoparticle size and medium composition on uptake into pulmonary epithelial 16hbe14o-cells*, in *J Nanopart Res*. 2016.
3. F. Christensen, et al., *Nano-silver - feasibility and challenges for human health risk assessment based on open literature.* Nanotoxicology, **2010**. 4 (3): p. 284-95.
4. A. Maynard and E. Kuempel, *Airborne nanostructured particles and occupational health.* J Nanopart Res, **2005**. 7: p. 587–614.
5. R. Foldbjerg, et al., *Pvp-coated silver np and silver ions induce ros, apoptosis and necrosis in thp-1 monocytes.* Toxicol Lett, **2009**. 190 (2): p. 156-163.
6. A. Haase, et al., *Toxicity of silver nanoparticles in human macrophages: Uptake, intracellular distribution and cellular responses* in *Journal of Physics: Conference Series*. 2011.
7. R.P. Singh and P. Ramarao, *Cellular uptake, intracellular trafficking and cytotoxicity of silver nanoparticles.* Toxicol Lett, **2012**. 213: p. 249-259.
8. M.V.D.Z. Park, et al., *The effect of particle size on the cytotoxicity, inflammation, developmental toxicity and genotoxicity of silver nanoparticles.* Biomaterials, **2011**. 32 (36): p. 9810-9817.
9. C. He, et al., *Effects of particle size and surface charge on cellular uptake and biodistribution of polymeric nanoparticles.* Biomaterials, **2010**. 31: p. 3657-3666.
10. W. Jiang, et al., *Nanoparticle-mediated cellular response is size-dependent.* Nat Nanotechnol., **2008**. 3: p. 145-150.
11. F. Lu, et al., *Size effect on cell uptake in well-suspended, uniform mesoporous silica nanoparticles.* Small, **2009**. 5 (12): p. 1408–1413.
12. J. Rejman, et al., *Size-dependent internalization of particles via the pathways of clathrin- and caveolae-mediated endocytosis.* Biochemical Journal, **2004**. 377: p. 159-169.
13. S.-H. Wang, et al., *Size-dependent endocytosis of gold nanoparticles studied by three-dimensional mapping of plasmonic scattering images.* Journal of Nanobiotechnology, **2010**. 8 (33).
14. K. Kettler, et al., *Cellular uptake of nanoparticles as determined by particle properties, experimental conditions, and cell type.* Environ. Toxicol. Chem., **2014**. 33 (3): p. 481-492.
15. S.D. Conner and S.L. Schmid, *Regulated portals of entry into the cell.* Nature, **2003**. 422: p. 37-44.
16. P. Cosson and T. Soldati, *Eat, kill or die: When amoba meets bacteria.* Current Opinion in Microbiology, **2008**. 11: p. 271-276.
17. C. Rosales, *Mechanisms of phagocytosis.* 2005, New York, NY, USA: Springer.
18. C. Watts and M. Marsh, *Endocytosis: What goes in and how?* Journal of Cell Science, **1992**. 103: p. 1-8.
19. Y. Ikada and Y. Tabata, *Phagocytosis of bioactive microspheres.* Journal of Bioactive and Compatible Polymers, **1986**. 1: p. 32-46.
20. A.J. Sbarra and M.L. Karnovsky, *The biochemical basis of phagocytosis.* Journal of Biological Chemistry, **1959**. 243 (6): p. 1355-1362.
21. S. Nagayama, et al., *Time-dependent changes in opsonin amount associated on nanoparticles alter their hepatic uptake characteristics.* International Journal of Pharmaceutics, **2007**. 342: p. 215-221.
22. S. Yu, et al., *Size- and charge-dependent non-specific uptake of pegylated nanoparticles by macrophages.* Int. J. Nanomed, **2012**. 7: p. 799-813.
23. B.D. Chithrani, A.A. Ghazani, and W.C.W. Chan, *Determining the size and shape dependence of gold nanoparticle uptake into mammalian cells.* Nano Letters, **2006**. 6 (4): p. 662-668.
24. C.D. Walkey, et al., *Nanoparticle size and surface chemistry determine serum protein adsorption and macrophage uptake.* J. Am. Chem. Soc., **2011**. 134: p. 2139-2147.
25. A. Vonarbourg, et al., *Evaluation of pegylated lipid nanocapsules versus complement system activation and macrophage uptake.* Journal of Biomedical Materials Research, **2006**. 78: p. 620–628.
26. C. Tsai, et al., *Size-dependent attenuation of tlr9 signaling by gold nanoparticles in macrophages.* Journal of Immunology, **2012**. 188 (1): p. 68-76.
27. B. Nowack and T.D. Bucheli, *Occurrence, behavior and effects of nanoparticles in the environment.* Environ. Pollut., **2007**. 150: p. 5-22.

28. C. Hendren, et al., *Modeling approaches for characterizing and evaluating environmental exposure to engineered nanomaterials in support of risk-based decision making.* Environ Sci Technol, **2013**. 47: p. 1190-1205.
29. M.E. Vance, et al., *Nanotechnology in the real world: Redeveloping the nanomaterial comsumer products inventory.* Beilstein Journal of Nanotechnology, **2015**. 6: p. 1769-1780.
30. S. Gangwal, et al., *Informing selection of nanomaterial concentrations for toxcast in vitro testing based on occupational exposure potential.* Environ. Health Persp., **2011**. 119 (11): p. 1539-1546.
31. R. Lévy, et al. *Gold nanoparticles delivery in mammalian live cells: A critical review.* Nano Reviews, **2010**. 1, DOI: 10.3402/nano.v1i0.4889.
32. Z.-J. Zhu, et al. *The interplay of monolayer structure and serum protein interactions on the cellular uptake of gold nanoparticles.* Small, **2012**. DOI: 10.1002/smll.201200794.
33. H. Yue, et al., *Particle size affects the cellular response in macrophages.* European Journal of Pharmaceutical Sciences, **2010**. 41: p. 650-657.
34. D.A. Kuhn, et al., *Different endocytotic uptake mechanisms for nanoparticles in epithelial cells and macrophages.* Beilstein J. Nanotechnol., **2014**. 5: p. 1625-1636.
35. O. Lunov, et al., *Differential uptake of functionalized polystyrene nanoparticles by human macrophages and a monocytic cell line.* ACS Nano, **2011**. 5 (3): p. 1657–1669.
36. E. Fröhlich, *The role of surface charge in cellular uptake and cytotoxicity of medical nanoparticles.* Int. J. Nanomed, **2012**. 7: p. 5577–5591.

Appendix

Table S 4.1 Overview of the elimination rates based on mass [ng] Ag.

NP size [nm], medium type	k	Std. dev. of k	95% CI of k
20 w/o FCS	$1.6 \cdot 10^{-1}$	$5.3 \cdot 10^{-2}$	$8.3 \cdot 10^{-2}$-$2.3 \cdot 10^{-1}$
50 w/o FCS	$9.4 \cdot 10^{-2}$	$8.5 \cdot 10^{-2}$	$-1.9 \cdot 10^{-3}$-$1.9 \cdot 10^{-1}$
75 w/o FCS	$3.2 \cdot 10^{-1}$	$2.4 \cdot 10^{-1}$	$4.8 \cdot 10^{-2}$-$5.9 \cdot 10^{-1}$
20+FCS	$1.0 \cdot 10^{-1}$	$1.9 \cdot 10^{-2}$	$7.3 \cdot 10^{-2}$-$1.3 \cdot 10^{-1}$
50+FCS	$4.2 \cdot 10^{-2}$	$4.7 \cdot 10^{-2}$	$-1.2 \cdot 10^{-2}$-$9.5 \cdot 10^{-2}$
75+FCS	$1.7 \cdot 10^{-1}$	$1.3 \cdot 10^{-1}$	$2.7 \cdot 10^{-2}$-$3.2 \cdot 10^{-1}$

Average elimination rate constants *k*, their standard deviation (Std. dev) and 95 % confidence Interval (CI) based on mass, all given in ng Ag·well^{-1}·day^{-1}.

Table S 4.2 Overview of the uptake and elimination rates based on AgNP numbers.

NP size [nm], medium type	k	Std. dev. of k	95% CI of k
20 w/o FCS	$1.4 \cdot 10^{-1}$	$4.3 \cdot 10^{-2}$	$8.4 \cdot 10^{-2}$-$2.0 \cdot 10^{-1}$
50 w/o FCS	$8.6 \cdot 10^{-2}$	$7.6 \cdot 10^{-2}$	$4.2 \cdot 10^{-4}$-$1.7 \cdot 10^{-1}$
75 w/o FCS	$3.0 \cdot 10^{-1}$	$2.3 \cdot 10^{-1}$	$3.44 \cdot 10^{-2}$-$5.6 \cdot 10^{-1}$
20+FCS	$9.1 \cdot 10^{-2}$	$1.5 \cdot 10^{-2}$	$7.0 \cdot 10^{-2}$-$1.1 \cdot 10^{-1}$
50+FCS	$3.7 \cdot 10^{-2}$	$4.1 \cdot 10^{-2}$	$-9.3 \cdot 10^{-3}$-$8.4 \cdot 10^{-2}$
75+FCS	$1.6 \cdot 10^{-1}$	$1.2 \cdot 10^{-1}$	$2.3 \cdot 10^{-2}$-$3.0 \cdot 10^{-1}$

Average elimination rate constants *k*, their standard deviation (Std. dev) and 95 % confidence Interval (CI) based on AgNP numbers, all given in AgNPs·well^{-1}·day^{-1}.

5

Exploring influences on the cellular uptake of medium-sized silver nanoparticles into THP-1 cells

Published in
Microchemical Journal, 2015. Vol. 120, pp. 45-50

Petra Krystek[1,2*], Katja Kettler[3,4], Bas van der Wagt[5], Wim H. de Jong[3]

[1] Institute for Environmental Studies (IVM), VU University, Amsterdam, The Netherlands
[2] Philips Innovation Services, Eindhoven, The Netherlands
[3] National Institute for Public Health and the Environment (RIVM), Bilthoven, The Netherlands
[4] Department of Environmental Science, Institute for Water and Wetland Research, Radboud University, Nijmegen, The Netherlands
[5] Faculty of Earth & Life Sciences, VU University, Amsterdam, The Netherlands

*Corresponding author: petra.krystek@philips.com

Abstract

The evaluation of the uptake of nanomaterials by cells *in vitro* tests is of great relevance to understand potential toxicity mechanisms of nanomaterials. As an example, the uptake of medium-sized nanosilver (size range of 50 and 75 nm) was studied closely for a relevant human lung cell line (THP-1). Time dependent uptake was studied in relation to different cell culture media with or without the addition of fetal calf serum (FCS). After cell isolation, washing, acid digestion and quantification of silver (Ag) by inductively coupled plasma mass spectrometry (ICPMS) were applied to study the general uptake. It is demonstrated that the uptake of Ag (from 75 nm Ag nanoparticles) is a factor of 5 higher in a medium without FCS in comparison to the medium with FCS. In addition, the stability and the abundance of Ag nanoparticles in the supernatant after cell exposure were studied in relation to different timings. By means of asymmetric flow field flow fractionation (AF4) for the size dependent particle separation and an on-line hyphenation to the sensitive elemental detection by ICPMS, different Ag particles were separated and further identified. By combining results from the total uptake of Ag by cells with results obtained from the analysis of the supernatant, total recoveries of 98 to 104% were determined in relation to the exposed concentration of Ag. Finally, the influence of the medium composition (with or without FCS) on the stability of 50 nm Ag nanoparticles was studied directly after spiking. A method by AF4-ICPMS was applied and the obtained fractograms confirm a clear influence of the different composed media composition and particle size on cellular uptake. The developed and applied ICPMS methods were found to be suitable approaches to evaluate the potential uptake of inorganic nanoparticles by cells.

Keywords
Silver nanoparticles, cell medium, macrophages THP-1 cell line, asymmetric flow field flow fractionation, inductively coupled plasma mass spectrometry

Introduction

Engineered nanomaterials (ENMs) and nanoparticles (ENPs) are used in a rapidly increasing number of modern products. It is crucial to understand and effectively manage potential human health and environmental risks of these materials [1-5]. Human exposure may occur via the release of ENMs and ENPs from the material during the use of consumer products and/or indirectly at the end of the product life cycle and possible release in the environment.

Silver (Ag) and Ag ENPs have an inherent antimicrobial activity which has led to their use in consumer products such as spray application with disinfectants, deodorants, antimicrobial sprays and powders [6]. Exposure to nanosilver can occur through ingestion or dermal contact but inhalation is considered as the most relevant route of exposure for potential hazardous effects [7, 8]. The capacity of ENPs to pass (or not) barriers and subsequently become systemically bioavailable is of great interest. Various parameters, like particle size/size distribution, shape, elemental composition, agglomeration/ aggregation state, surface composition, purity, surface area, surface chemistry and surface charge, must be taken into account [5]. *In vivo* inhalation studies with nanosilver show diverse outcomes up to now. Some studies showed no induction of adverse effects [9, 10], while other studies reported adverse effects varying from a minimal inflammatory response to the presence of inflammatory lesions in the lungs [11].

In vitro experiments represent a relevant and fast approach to screen ENPs on their cytotoxicity, inflammation, genotoxicity and develop- mental toxicity [12] and *in vitro* assays may also be used to mimic inhalatory routes of exposure by a so-called air liquid interface model. The solubility under physiological conditions and translocation of ENPs can be studied by systematic variations of experimental conditions. A large range of human cell lines is available for *in vitro* testing. Human liver cells like HepG2 and colon Caco2 cells are well studied cell lines in relation to nanosilver [13, 14]. As ENPs tend to end up in phagocytizing cells, a human acute monocytic leukemia cell line (THP-1) can be used for exposure testing. Since their establishment thirty years ago, THP-1 cells have become one of most widely used cell lines to investigate the function and regulation of monocytes and macrophages in the cardiovascular system [15]. So far, there are no detailed studies published about the exposure and the uptake of Ag ENPs by THP-1 cells.

It is crucial for the interpretation of *in vitro* uptake studies that sufficient information on the particle stability of the chosen ENPs under the given experimental circumstances is available. The concept of primary particle size must be confirmed under the given experimental conditions. The development of new methods for the analytical characterization of ENPs in complex matrices will be extended to guarantee sufficient reliability of the analytical results. From an analytical point of view, inductively coupled plasma mass spectrometry (ICPMS) offers an ideal platform to study possible effects.

An analytical tool platform needs to be established to obtain more details about the Ag ENPs stability in *in vitro* experiments with cells lines. After cell isolation, washing and acid dissolution, the total content of Ag taken up by cells is determined by ICPMS. Determination in hyphenation to on-line size dependent particle separation by asymmetric flow field flow fractionation (AF4) represents a new challenge. Recently, methods for the identification and quantification of ENPs were developed. Asymmetric flow field flow fractionation (AF4)-inductively coupled plasma mass spectrometry (ICPMS) is applied for quantification of metallic ENPs [16-18]. Commonly, Ag ENPs in less complex matrices like aqueous matrices can be separated by AF4 [19, 20]. To the best of our knowledge, only one publication is dealing about the analytical method of nanosilver in relation to cell line; in this case smaller (15 nm) ENPs and Ag(I) were studied with HepG2 cells by AF4-ICPMS [14].

Within this study, three experimental scenarios with medium-sized (range 50 and 75 nm) Ag ENPs are investigated in relation to human lung cells (THP-1) and variable tissue culture media compositions in which the presence or absence of the most widely used serum- supplement fetal calf serum (FCS) is of great importance.

Material and methods

Chemicals

Two sizes of Ag NPs were used for studying their stability in different Complex *in vitro* media:

1. Ag nanospheres of 75 nm with citrate capping agent: 1 mg/mL Ag;
2. Ag nanospheres of 50 nm with citrate capping agent: 1 mg/mL Ag.

For the identification of derivatives, also Ag nanospheres of 20 nm with citrate capping agent: 1 mg/mL Ag, were used.

The related particle sizes refer to the specification sheets provided by the manufacturer. All NPs were from the product line BioPure and supplied by NanoComposix, San Diego, USA. In addition, the suspensions of NPs were stored and handled according to the supplier's instructions which were given on the related specification sheets.

Ultrapure water (H_2O) with a resistivity of > 18 M Ω cm was obtained from a Milli-Q Plus system (Millipore, Amsterdam, the Netherlands). Hydrochloric acid (HCl), 30%, ultrapur and nitric acid (HNO_3), 65%, ultrapur, were purchased from Merck, Darmstadt, Germany. Sodiumdodecylsulfate (SDS), > 99%, was purchased from Sigma Aldrich, Zwijndrecht, the Netherlands. The calibration standard solution of Ag and the internal standard related to the ICPMS measurement (chosen element: rhodium (Rh)) were made of single element stock solutions with a concentration of 1 mg/mL from Inorganic Ventures, Christiansburg, USA.

Cell line and media

The human macrophage THP-1 cell line was obtained from ATCC (LGC Standards, Wesel, Germany). The cells were seeded in CELLSTAR® 96 well plates, supplied by Greiner Bio-One B.V., Alphen a/d Rijn, The Netherlands, at a density of 100,000 cells/well. RPMI 1640 medium supplemented with 10 vol. % fetal calf serum (FCS; Gibco 16010-159), 1 vol. % penicillin–streptomycin solution (10,000 U/mL/10,000 lg/mL, Gibco 15040) was used. The medium RPMI 1640 is composed of 42 components; the detailed composition is given on [21]. All cell media were supplied by Life Technologies Europe BV, Bleiswijk, The Netherlands. Phorbol myristate acetate (PMA; from Sigma Aldrich, Zwijndrecht, The Netherlands) was added to the medium with a final concentration of 30 ng/mL in order to stimulate differentiation from the monocytic phenotype to macrophages until day five. The medium was refreshed and the cells were left to rest for two more days. The cells were constantly grown at 37 °C with 5% CO_2.

Instrumentation

For the total quantification of Ag in cell pellets, a high resolution (HR)-ICPMS type ELEMENT XR, Thermo Fisher Scientific, Bremen, Germany, was utilized. The used sample introduction systems consist of a concentric nebulizer, a cyclone spray chamber and nickel cones (all from the instrument supplier). The operating conditions as well as the method and measuring parameters of the HR-ICPMS are summarized in Table 5.2. Sample pretreatment and analysis were carried out in a cleanroom facility class 10,000.

All samples containing cell media, were analyzed with a Postnova AF1000 system (Postnova Analytics GmbH, Landsberg, Germany) consisting of an Asymmetric Flow-Field-Flow Fractionation (AF4) module for particle size separation coupled serially to an ICPMS. The instrumental settings of the AF4 and the developed method are given in Table 5.2. F or the elemental detection and quantification, the out flow of the AF4 system was further coupled to the nebulizer of an ICPMS type XSeries II (Thermo Fisher Scientific, Breda, the Netherlands). The sample introduction system (all from the instrument supplier) and the instrumental operating conditions of ICPMS as well as the method and measuring parameters of ICPMS are summarized in Table 5.3. During separation processes, there is the possibility of analyte loss due to strong and potentially irreversible interactions; e.g. with the ultra-filtration membrane [20]. A calibration strategy by standard addition of the original nanoparticles to the matrix of interest was carried out. In addition, internal standard correction by continuous on-line addition of Rh solution directly after the fractionation and prior to the entry of the nebulizer is applied [22] for correcting variations in the instrument response (e.g. drift) and for calculating the analyte concentrations in combination with the standards.

For several experiments, an UV/VIS detector S3206 (Sykam, Fuerstenfeldbruck, Germany) was additionally connected directly after the outlet of the AF4. The absorbance was monitored at a wavelength of 254 nm, which is typically used for the identification of abundant organic compounds.

Table 5.1 Operating and measurement conditions of HR-ICPMS

Parameter	Setting
RF power [W]	1250
Cool gas flow [L/min Ar]	16
Nebuliser gas flow [L/min Ar]	1.04
Auxiliary gas flow [L/min Ar]	0.8
Isotopes	$^{107}Ag^+$ (quantification), $^{109}Ag^+$ (control), $^{103}Rh^+$ (internal standard: on-line addition: 1:1)
Method	Acquisition mode: E-scan Mass window: 150% Search window: 150% Integration window: 80% Sample time: 50 ms Samples per peak: 10 Detection mode: triple
Number of replicates	9

Experiments

Three series of experiments were carried out:

a) Total quantification of Ag by HR-ICPMS for the identification of the cellular uptake of 75 nm Ag ENPs.
   The THP-1 cells were grown in RPMI 1640 medium supplemented with FCS. The cells were exposed to 10 µg/mL Ag of 75 nm Ag ENPs. The time- and medium composition dependent uptake was studied during a period of 0 to 14 h. Dilutions of the Ag ENPs stock solution were made with RMPI 1640 medium without and with FCS supplement. After the selected period of time, the cells were isolated and washed. All other details of the cell experiments and more variations in particle sizes and timings are described in [23]. The obtained cell pellets were digested with 2 mL aqua regia conc. (HNO_3: HCl; 1:3) and further diluted prior to the total quantification of Ag by HR-ICPMS.
b) Identification of Ag fractions in supernatants of cell exposure experiments by AF4-ICPMS
   After carrying out the cell exposure experiments with 10 µg/mL Ag of 75 nm Ag ENPs (see a)), the supernatant above the cells was collected at selected timings (after 4 and 14 h) and the particle presence was investigated by AF4-ICPMS. The quantification is based on two calibration curves obtained from 20 and 75 nm Ag NPs.
c) Stability testing of Ag NPs in different cell media without cells
   The possible interaction of the cell media, this means pure media without cells, with Ag NPs was studied with 50 nm Ag NPs at the concentration level of 10 µg/mL Ag of 50 nm Ag NPs. Both cell media (RPMI 1640 without and with FCS) were investigated. All samples and spikes were freshly prepared within 1 h prior to qualitative analysis by AF4-ICPMS.

Table 5.2 Instrumental configuration as well as method and measuring parameters of AF4

Parameter	Setting
Ultra filtration membrane	Regenerated cellulose (RC), cutoff 10 kDa
Spacer / channel: height	350 µm
Eluent	0.01% SDS in ultrapure water
Injection volume	100 µL
Channel out flow	1 mL/min
1.Rinsing	
Injection flow	0.5 mL/min
Focus flow	1.5 mL/min
Rinse time	60 s
2.Injection and focusing	
Injection flow	0.1 mL/min
Focus time	700 s
3.Fractionation	
Cross flow	0.5 mL/min
Time	30 s
Cross flow	0.8 mL/min
Time	72 min

Table 5.3 Sample introduction system, instrumental operating conditions and measuring parameters of ICPMS

Sample introduction system	
Operation mode	On-line mixing of eluent (0.01% SDS in ultrapure water) and acidified internal standard (20 µg/L Rh in 2% HNO_3), 1:1
Nebulizer	Concentric nebulizer; pumped mode
Spray chamber	Stable sample introduction system (cyclone - double pass spray chamber)
Cones	Nickel
Instrumental operating conditions	
RF power	1000 W
Cool gas flow	13 L/min Ar
Auxiliary gas flow	0.7 L/min Ar
Nebuliser gas flow	0.75 L/min Ar
Measuring mode	No collision cell technique (CCT) applied
Isotope (internal standard)	$^{107}Ag^+$ ($^{103}Rh^+$)
Measuring mode	Time resolved analysis (TRA)
Dwell time	300 ms
Resolution	Standard
Run time	85 min (and longer)

Results and Discussion

For the interpretation of *in vitro* uptake studies, it is crucial that sufficient information on the particle stability of the chosen ENPs under the given experimental circumstances is available. Therefore, three complementary, experimental series (a) to c)) by HR-ICPMS and AF4-ICPMS were setup for the understanding of matrix effects and uptake processes in relation to medium-sized Ag NPs and human cell line THP-1 as well as cell media with or without FCS supplement.
For each experimental series, the results are presented and discussed in detail.

a) Time dependent cellular uptake of 75 nm Ag NPs by total quantification with HR-ICPMS
The analytical method applied for the total quantification of Ag in cells was developed based on own experience of the quantification of noble metal nanoparticles in biological matrices [24]. The use of aqua regia as digestion media for nanosilver is more advantageous in comparison to nitric acid since in biological matrices also silver chloride (AgCl) is formed which is not dissoluble in nitric acid but which will be dissolved in aqua regia by forming a complex of silver di chloride $(AgCl_2)^-$ [25]. The measurement method was optimized and the settings are given in Table 5.1. Due to the absence of poly-atomic interference, the measurements were carried out in low resolution mode of the HR-ICPMS which leads to the highest sensitivity.
The time dependent uptake of 75 nm Ag ENPs by exposed THP-1 cells in cell culture media was monitored at five time points (0, 2, 4, 8, and 14 h) with regards to two different cell culture media. The related uptake curves are given in Figure 5.1. Both curves show a first increase of Ag concentration already after 2 h and uptake stability is achieved after 8 h. However, the related concentrations are significantly different. While the THP-1 cells in cell culture medium without FCS show an uptake of around 50% of the exposed Ag amount, the uptake of Ag by the same cells in the FCS rich medium is drastically lower with only around 15%. Already, these first experiments show that the composition of culture media is of great influence on the uptake of the selected medium-sized Ag ENPs. Within this study, the abundance of ionic Ag in the original nanoparticle suspensions or in mixed culture media was not further studied. It is known that especially for bio-available Ag ENPs and if these ENPs are additionally of smaller sizes (< 20 nm), this might be of influence [14].

b) Identification of Ag fractions in supernatants of cell exposure experiments by AF4-ICPMS and balance of *in vitro* experiments
Next to the total quantification of Ag in cells (see a)), the remaining supernatant of the spiked cell media after THP-1 cell exposure was identified, integrated and quantified for the abundances of containing Ag particles. For this approach, supernatants of 75 nm Ag ENPs from two timings (after 4 h and 14 h of exposure) were selected and

analyzed by AF4-ICPMS. During the method development by AF4-ICPMS, the most relevant aspect for method optimization deals with the study and the handling of matrix effects from various *in vitro* relevant matrices. Details about the optimized conditions are described under Material and methods. Obtained fractograms showed one resp. two fractions. The particle identification and the quantification of the smaller particle size fraction (range: < 20 nm) were done in relation to 20 nm Ag ENPs while the larger fraction was matched with 75 nm Ag ENPs. Both calibrations were carried out as two-point-calibration of Ag ENPs diluted with eluent matrix (SDS). The on-line addition of an internal standard was used to control the general stability of the system; in this case no specific internal standard correction was applied. The results for both timings and both cell media are given in Figure 5.2.

After both timings (4 h and 14 h) different composed supernatants were identified for both cell culture media. In the cell culture medium without FCS (see Figure 5.2, left), already after 4 h no 75 nm Ag ENP fraction could be identified. However, a significant concentration of around 10 µg Ag/mL supernatant was determined in the particle fraction up to 20 nm, while this concentration further decreased to 4 µg Ag/mL supernatant after 14 h.

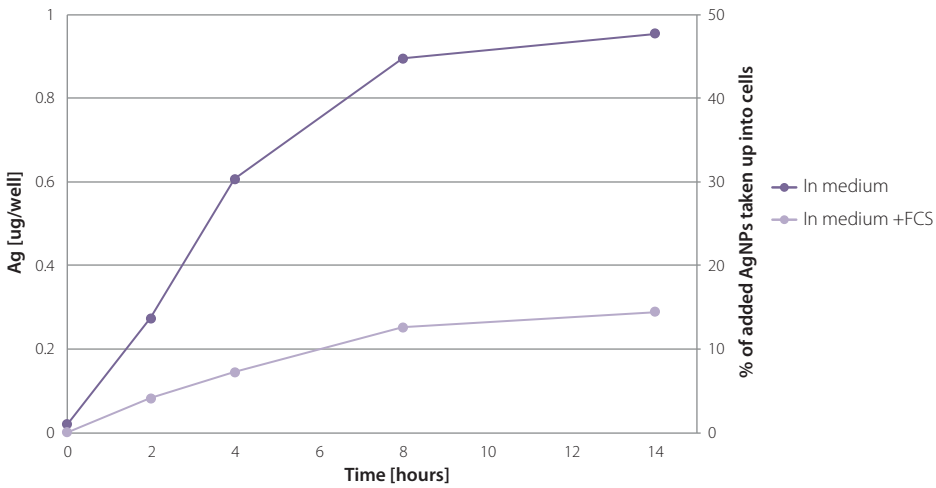

Figure 5.1 Time dependent uptake of 75 nm Ag by exposed macrophages THP-1 cells in cell culture media of different compositions.

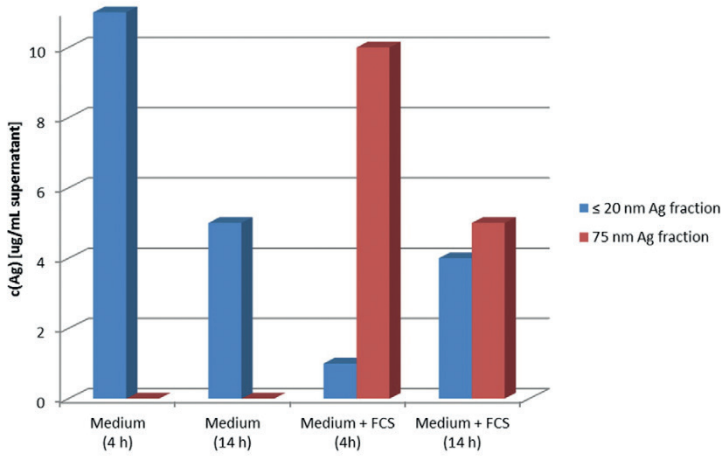

Figure 5.2 Ag concentrations from spiked 75 nm Ag ENPs in supernatants of cell media with different compositions; after 4 resp. 14 hours of cellular contact. Quantification of two fractions in relation to known concentrations of 20 nm Ag ENPs resp. 75 nm Ag ENPs in eluent matrix.

Table 5.4 Balance between cellular included Ag and Ag fractions in supernatants after 14 h exposure of 75 nm Ag ENPs (10 µg/mL Ag) in THP-1 cells with different media

Sample	Uptake of total Ag by cells; (Experiment a) [µg/mL Ag]	Supernatant: First fraction (Experiment b) [µg/mL Ag]	Supernatant: Second fraction (Experiment b) [µg/mL Ag]	Total recovery [%]
Medium	4.75	5	< 0.5	98
Medium + FCS	1.35	4	5	104

With FCS supplemented medium (see Figure 5.2, right), two fractions of particles were identified at both timings (4 h and 14 h). In this case, also particles of the originally spiked 75 nm Ag ENPs fraction are still abundant. While after 4 h, the 75 nm Ag is strongly abundant also a low concentration of smaller particles (< 20nm) is measured. After14h, the concentration of 75 nm AgENPs is decreased, but comparable concentrations of b 20 nm and 75 nm Ag ENPs are still abundant. Altogether, it is shown that 75 nm Ag ENPs are instable in the "normal" cell culture medium in comparison to the cell culture medium with FCS. The presence of serum plays an important role and the story is further

complicated by the capacity of ENPs to interact with, and potentially disturb the functioning of biomolecules such as proteins, enzymes and DNA as well as to generate reactive oxygen species [26].

After 14 h, a steady-state situation is reached (see Figure 5.1) and the balance between cellular included Ag and Ag fractions in supernatants was made by combining results from the total quantification of Ag in cells (see a) and the obtained concentrations of Ag in fractions of supernatant. These results are given in Table 5.4. While estimated, expanded measurement uncertainties from both procedure (a) and b)) of 15 to 20 % must be taken into account, the total recovery of Ag for both experiments (with and without FCS in cell culture medium) are comparable and in the range of 98 to 104 %.

c) Stability testing of Ag NPs in different cell media without cells

As shown with the experimental series b), the medium composition is of great importance on the uptake process and the particle stability. By excluding the presence of THP-1 cells, it is possible to study direct, possible interactions of Ag ENPs with cell culture medium which was used without or with FCS. The analysis was also carried out by AF4-ICPMS and 50 nm Ag ENPs were used for these test. All obtained fractograms are shown in Figure 5.3. The black fractogram obtained from "pure" 50 nm Ag ENPs in eluent shows a maximum fraction at a retention time of 35 min and a void peak of smallest, not separated Ag ENPs. After spiking the same 50 nm Ag ENPs to cell culture medium, a broader fraction of Ag ENPs becomes abundant and the recovery of Ag ENPs in the presence of the medium is lower (see green fractogram).

Using the cell culture medium supplemented with FCS, effects in the elution profile are observed and in principle three fractions can be identified (see blue fractogram). Next to the fraction of 50 nm Ag ENPs at 35 min and the void peak, a third, significant fraction of Ag species of lower size with a retention time of 23 min is identified between both known fractions. The experiment of 50 nm Ag ENPs in cell culture medium supplemented by FCS was measured by AF4-ICPMS but also an intermediate UV/VIS detection at 254 nm; see text in Figure 5.3. Only the first fraction with a retention time of 11 to 15 min could be confirmed by UV/VIS and the fractogram showed the same curve progression. As long as 254 nm is a typical absorbance wavelength for the detection of separated proteins and/or dissolved organic compounds [27]; therefore it can be assumed that Ag^+ protein complexes are formed and/or that especially the smallest Ag ENPs or Ag^+ are surrounded by the so called protein corona (PC) [28]. ENMs readily associate proteins that form a PC on their surface, while this PC influences the ENMs surface characteristics and may impact their interaction with cells. The identification and quantification are possible by label-free liquid chromatography double mass spectrometry (LC-MS/MS). Already studied Ag ENPs (20 and 110 nm with citrate coating), which agree with the materials used in this study, are associated with a common subset of eleven proteins including albumin, apolipoproteins, keratins, and other serum proteins [28].

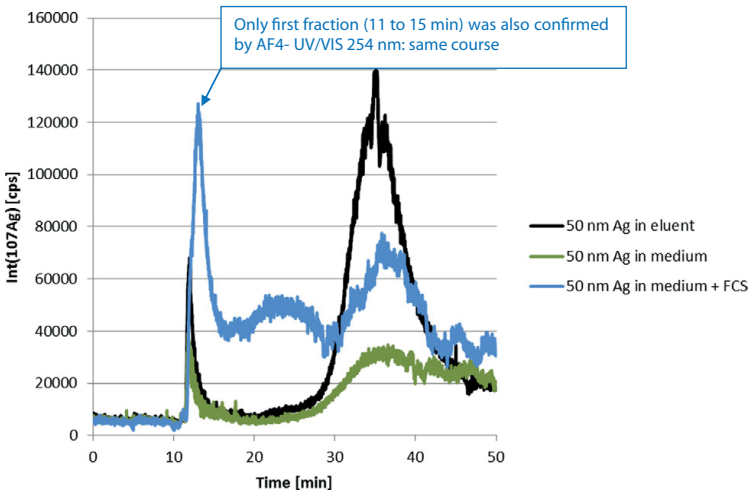

Figure 5.3 Fractograms by AF4-ICPMS obtained of identical concentrations (0.5 µg/mL Ag) of 50 nm Ag ENPs spiked to two different cell media *versus* the reference fractogram of "pure" 50 nm Ag ENPs in eluent.

Conclusions

With the investigations carried out in this study, a relevant method to determine the stability of medium-sized nanosilver in cell media by AF4-ICPMS is developed. Relevant insight in the stability and the interpretation of uptake scenarios of Ag ENPs by different complex cell media of the macrophage THP-1 cell line are obtained which explains different uptake results. The great influence of (fetal calf) serum on the stability of nanosilver was confirmed, which can be associated with a protein corona effect or by Ag^+ complexes with proteins. Applying only the "classical" approach of acid dissolution followed by the total quantification by ICPMS might otherwise lead to incomplete or wrong conclusions in nanotoxicity studies by *in vitro* experiments.

It is shown that the nature of the matrix appears to affect the stability of Ag ENPs strongly. It is shown that transformations occur within a few minutes after the addition of the Ag ENPs to the medium. This effect was also observed in other aqueous matrices like domestic waste water [20].

The time dependent presence of various sized and composed particles has been also confirmed. By the presence of cells further particle change processes take place.
The identification of AgNPs associated with cells can also help to better understand the mechanisms of toxicity of the NPs. However, due to the larger particles sizes, also other

field flow fractionation approaches, e.g. by sedimentation (SdFFF) should be studied more closely and might be more advantageous [29].

Regarding all analytical results in this study, it can be concluded that a promising platform by HR-ICPMS and AF4-ICPMS is developed for obtaining insights into the stability of nanosilver and the cellular uptake in *in vitro* systems. This tool will enable a better control and monitoring of Ag ENPs in *in vitro* tissue culture media, and *in vitro* assay systems.

Acknowledgement

This work is funded by NanoNext.nl, a micro- and nanotechnology consortium of the Dutch Government and 130 partners. Dr. Ingrid Snijkers-Hendrickx (Philips Innovation Services) and Prof. Jan Hendriks (Radboud University Nijmegen) are acknowledged for support on the project realization. John Visser (Faculty of Earth & Life Sciences, VU University) is acknowledged for general technical support in the analytical laboratory. Hedwig Braakhuis and Henny Verharen (both from the National Institute for Public Health and the Environment (RIVM)) are acknowledged for instructions and support of *in vitro* tests.

Cited Work

1. H.M. Braakhuis, et al., *Particle size dependent deposition and pulmonary inflammation after short-term inhalation of silver nanoparticles.* Part Fibre Toxicol, **2014**. 11.
2. G. Oberdorster, et al., *Principles for characterizing the potential human health effects from exposure to nanomaterials: Elements of a screening strategy.* Part Fibre Toxicol, **2005**. 2: p. 8-43.
3. M. Scheringer, *Nanoecotoxicology: Environmental risks of nanomaterial.* Nature Nanotechnology, **2008**. 3: p. 322-323.
4. S.W.P. Wijnhoven, et al., *Nano-silver — a review of available data and knowledge gaps in human and environmental risk assessment.* Nanotoxicology, **2009**. 3: p. 109–138.
5. P. Krystek, et al., *Application of plasmaspectrometry for the analysis of engineered nanoparticles in suspensions and products.* Journal of Analytical Atomic Spectrometry, **2011**. 26: p. 1701– 1721.
6. K. Park, et al., *Bioavailability and toxicokinetics of citrate-coated silver nanoparticles in rats.* Archives of Pharmacal Research, **2011**. 34: p. 153– 158.
7. H.M. Braakhuis, et al., *Particle size dependent deposition and pulmonary inflammation after short-term inhalation of silver nanoparticles.* Part Fibre Toxicol, **2014**.
8. F.M. Christensen, et al., *Nano-silver— feasibility and challenges for human health risk assessment based on open literature.* Nanotoxicology, **2010**. 4: p. 284– 295.
9. J.H. Sung, et al., *Acute inhalation toxicity of silver nanoparticles.* Toxicology and Industrial Health, **2011**. 27: p. 149- 154.
10. J. Ji, et al., *Twenty-eight-day inhalation toxicity study of silver nanoparticles in sprague–dawley rats.* Inhalaton Toxicology, **2007**. 19: p. 857–871.
11. L. Stebounova, et al., *Nanosilver induces minimal lung toxicity or inflammation in a subacute murine inhalation model.* Part Fibre Toxicol, **2011**. 8 (5).
12. M.V.D.Z. Park, et al., *The effect of particle size on the cytotoxicity, inflammation, developmental toxicity and genotoxicity of silver nanoparticles.* Biomaterials, **2011**. 32 (36): p. 9810-9817.
13. S.C. Sahu, et al., *Comparative genotoxicity of nanosilver in human liver hepg2 and colon caco2 cells evaluated by fluorescent microscopy of cytochalasin b-blocked micronucleus formation.* Journal of Applied Toxicology, **2014**. 34: p. 1200- 1208.
14. E. Bolea, et al., *Detection and characterization of silver nanoparticles and dissolved species of silver in culture medium and cells by asflfff-uv-vis-icpms: Application to nanotoxicity tests.* Analyst, **2014**. 139: p. 914-922.
15. Z. Qin, *The use of thp-1 cells as a model for mimicking the function and regulation of monocytes and macrophages in the vasculature.* Atherosclerosis, **2012**. 221: p. 2-11.
16. E. Bolea, et al., *Size characterization and quantification of silver nanoparticles by asymmetric flow field-flow fractionation coupled with inductively coupled plasma mass spectrometry.* Analytical and Bioanalytical Chemistry, **2011**. 401: p. 2723– 2732.
17. K. Loeschner, et al., *Optimization and evaluation of asymmetric flow field flow fractionation of silver nanoparticles.* Journal of Chromatography A, **2013**. 1272: p. 116-125.
18. H. Hagendorfer, et al., *Application of an asymmetric flow field flow fractionation multi-detector approach for metallic engineered nanoparticle characterization — prospects and limitations demonstrated on au nanoparticles.* Analytica Chimica Acta, **2011**. 706: p. 367-378.
19. O. Geiss, et al., *Size and mass determination of silver nanoparticles in an aqueous matrix using asymmetric flow field flow fractionation coupled to inductively coupled plasma mass spectrometer and ultraviolet-visible detector.* Journal of Chromatography A, **2013**. 1321: p. 100-108.
20. P. Krystek, P.S. Bäuerlein, and P.J.F. Kooij, *Analytical assessment about the simultaneous quantification of releasable pharmaceutical relevant inorganic nanoparticles in tap water and domestic waste water.* Journal of Pharmaceutical and Biomedical Analysis, **2014**: p. 7031-7085.
21. T. Scientific. *Rpmi 1640 (atcc modification), a10491.* 2014; Available from: http://www.lifetechnologies.com/nl/en/home/technical-resources/media-formulation.244.html.
22. D.P.K. Lankveld, et al., *The kinetics of the tissue distribution of silver nanoparticles of different sizes.* Biomaterials, **2010**. 31: p. 8350– 8361.

23. K. Kettler, et al., *Uptake of silver nanoparticles by monocytic thp-1 cells depends on particle size and presence of serum proteins.* J Nanopart Res, **2016**. 18 (286).
24. P. Krystek, *A review on approaches to bio distribution studies about gold and silver engineered nanoparticles by inductively coupled plasma mass spectrometry,.* Microchemical Journal, **2012**. 105: p. 39-43.
25. C. Bianco, et al., *Pilot study on the identification of silver in skin layers and urine after dermal exposure to a functionalized textile.* Talanta, **2015**. 136: p. 23-28.
26. B. Reidy, et al., *Mechanisms of silver nanoparticle release, transformation and toxicity: A critical review of current knowledge and recommendations for future studies and applications.* Materials, **2013**. 6: p. 2295– 2350.
27. C.N. Ferrarello, et al., *Multi-elemental speciation studies of trace elements associated with metallothionein-like proteins in mussels by liquid chromatography with inductively coupled plasma time-of-flight mass spectrometric detection.* Journal of Analytical Atomic Spectrometry, **2000**. 15: p. 1558– 1563.
28. J.H. Shannahan, et al., *Silver nanoparticle protein corona composition in cell culture media.* PLoS ONE, **2013**.
29. C. Mélin, et al., *Sedimentation field flow fractionation monitoring of in vitro enrichment in cancer stem cells by specific serum-free culture medium.* Journal of chromatography. B, Analytical technologies in the biomedical and life sciences, **2014**. 963: p. 40-46.

6

Exploring the possibility of read-across on the extent of nanoparticle uptake into living cells

Under review
Beilstein Journal of Nanotechnology

Katja Kettler, Dik van de Meent, and A. Jan Hendriks

Department of Environmental Science, Institute for Water and Wetland Research,
Radboud University, Nijmegen, the Netherlands

Abstract

The ever increasing number of nanoparticles cannot all be tested separately for their (cellular) uptake and possible subsequent toxicity. The prediction of the extent to which spherical nanoparticles are taken up by living cells is highly desirable for risk assessment. We tested the hypothesis that cellular nanoparticle uptake follows (quasi) first-order kinetics. Furthermore, we determined whether the values of the parameters of first-order kinetics are correlated to easily measurable NP properties such as size or charge to derive QSARs. Nanoparticle uptake often follows first-order kinetics for different nanoparticles, cell lines and experimental conditions. Neither nanoparticle size nor charge appear to be correlated with the parameters of first-order kinetics. Other factors than size and charge influence uptake kinetics more strongly.

Keywords
cellular uptake; first-order kinetics; modelling; nanoparticle; QSARs

Introduction

Engineered nanoparticles are used in increasing amounts and numbers of applications due to the often occurring change in properties with decreasing size in comparison to the bulk material of the same chemical composition [1-3].They are widely applied in the field of electronics and as industrial catalysts and they are part of numerous consumer products such as sportswear and personal hygiene products. In addition, they are also used in the medical field as drug delivery systems and diagnostic tools [4-8]. The widespread application of NPs may lead to unwanted exposure of humans, during production, use and disposal of NP containing products.

The same properties that render NPs interesting for the new fields of application mentioned (their small size and high reactive surface area), may lead to unintended biological impacts due to their ability to access the cellular machinery. In contrast to many traditional chemicals that diffuse freely in or out of a cell, NPs enter the cell by energy-dependent pathways as do proteins and other biomolecules. Once humans or biota come into contact with NPs via one of the four exposure routes (inhalation, dermal or intestinal uptake, injection for medical use), uptake into cells via a fundamental biological process called receptor-mediated endocytosis (RME) becomes possible [9, 10]. RME is an active uptake mechanism employed by nearly all eukaryotic cells to take up small molecules and nutrients from the surrounding medium via enclosure by the cell membrane. The resulting vesicles reach sizes up to 120 nm in diameter [11, 12]. The cargo size determines the vesicle size to some extent, yet the maximum vesicle size is species and cell type dependent [13, 14]. Therefore, these vesicle sizes are not rigid, but their size is most likely limited to allow only cargos of defined sizes to enter cells [15]. Specialized mammalian cells can employ an additional uptake mechanism called phagocytosis. It is a ligand-induced process by which particulate matter with sizes of 0.5 to 10 µm is taken up. This mechanism is usually employed by cells of the immune system in order to clear the body from cell debris and foreign cells [16]. NPs can enter cells via this mechanism [10].

Uptake kinetics describe the ability of NPs to cross natural barriers, influencing their ability to cause toxicity. Many toxicity studies have been conducted and negative health impacts have been found (to a larger extent than for the same element in ionic form) [17], for example through the formation of reactive oxygen species or depletion of the amount of antioxidant species in the cell [18, 19]. Therefore, the extent to which NPs are taken up into cells over time is a factor to be considered in toxicity assessment. Cellular uptake is listed as one toxicological endpoint to be addressed for the risk assessment of nanomaterials under REACH (Registration, Evaluation, Authorization and Restriction of Chemicals) [20]. Prolonged exposure times lead to increased internalized NP concentrations. The present paper focuses on predictive quantification of the extent of uptake of NPs by living cells. The increasing risk related to NP exposure in combination with the ever-increasing amount of different NPs (core material, surface coating, size, charge…), raises the

question whether it is possible to relate NP uptake kinetics to easily measurable NP properties. This would allow to overcome the obstacle that not every type of NP can be tested for uptake and toxicity. The NP properties determining NP uptake kinetics are currently of growing interest for safe implementation of nanotechnology [6, 21, 22] and medical applications such as drug delivery [23, 24]. Correlating uptake to easily measurable NP properties such as size facilitates prioritization for toxicity and bioaccumulation potential.

Several studies report NP uptake in dependence of NP size [13, 25-29]. Unfortunately, uptake is often determined after a fixed time point and does not represent uptake over time. Blechinger et al. demonstrate the importance to compare uptake efficiencies (between cell lines) also over time [30]. The number of NPs taken up by HeLa cells within the first 4 hours was lower than for HUVEC cells. The opposite was the case at longer exposure times due to increased uptake kinetics. Such studies lead to increased understanding of uptake mechanisms and enhance the accuracy of risk assessment. Studying uptake and elimination over time is often assessed to determine accumulation of traditional chemicals. Some studies determine uptake of NPs over time [31-33]. Yet, these studies are usually limited either to different particles in only one cell type or vice versa. In addition, the effect of NP concentration, NP properties (size and charge), cell line and serum on uptake is rarely addressed. It is, therefore, of practical importance to explore options for modelling.

In this study, we have tested whether uptake can be described by first-order kinetics and derive the adjacent parameters' value. We have also attempted to derive QSARs that describe the parameters of first-order uptake as a function of NP properties.

Material and Methods

Data collection

As only a few sources published data from parameters of (first-order) uptake kinetics, we collected data from studies that determine NP uptake in dependence of NP properties or experimental conditions. A literature search was conducted via Web of Science and Google Scholar, using the following key words in various combinations: nanoparticles, (cellular) uptake, (receptor-mediated) endocytosis, time-dependent, kinetics. The studies had to fulfil the following prerequisites. Cellular concentrations of NPs over time had to be reported and particle sizes were limited to a maximum of 120 nm in diameter according to the ubiquitous uptake mechanism. Besides these prerequisites, no further restrictions have been placed on the selected publications to allow for sufficient data to be collected. Due to their different uptake mechanisms non-phagocytic and specialized phagocytosing cell lines were analyzed separately.

The data collection resulted in 21 studies that meet the mentioned criteria. Seven of these studies tested cell lines known to be phagocytes (e.g. THP-1, RAW 264.7, HUVEC). This resulted in 54 data for non-phagocytes and 38 for phagocytes. The number of data obtained for various size classes are given Table 6.1. These data cover a broad range of NP types (e.g. gold, silica oxide, polystyrene), surface modifications (e.g., citrate, poly(allyamine hydrochloride), poly(vinyl alcohol)) and cell lines (e.g., HeLa, HBE, A549). The cell lines were first grouped according to their origin, i.e. from animals or humans. The particle sizes reported here are those measured in the exposure medium whenever possible. If this information was lacking due to the detection method (e.g. transmission electron microscopy TEM), the core size excluding a protein corona is used here. If no measurement of aggregation was conducted, the concept of primary particle size was assumed to be valid.

Table 6.1 Number of published data points for various NP size classes, distinguished for non-phagocytes and phagocytosing cells.

NP size [nm]	No of data non-phagocytes	No of data phagocytes
0< NP ≤ 10	2	2
10< NP ≤ 20	8	1
20< NP ≤ 30	2	2
30< NP ≤ 40	3	1
40< NP ≤ 50	6	-
50< NP ≤ 60	1	-
60< NP ≤ 70	2	4
70< NP ≤ 80	7	-
80< NP ≤ 90	8	1
90< NP ≤ 100	11	1
100< NP ≤ 110	1	1
110< NP ≤ 120	3	25

Data treatment

Data sources reported uptake data obtained with various detection techniques, e.g. flow cytometry, confocal scanning microscopy, fluorescence-activated cell sorting, ICP-MS. We extracted uptake data from the published figures by means of the software package 'Digitize it' (http://www.digitizeit.de). Conversion to NP numbers or fluorescence intensity was necessary to allow for comparison between uptake data from different studies. Uptake data given in units other than fluorescence intensity or NP numbers, were

converted to NP numbers according to Chithrani et al. [31]. If no conversion was possible, data were discarded. Amounts of NPs (i.e. numbers of particles) were expressed as dimensionless ratios to the theoretical maximum NP number accumulated at steady state. Observed particle numbers taken up at time t were scaled to the expected value at infinite time per study, so that all relative amounts taken up would range between zero (at t=0) and 1 (t=∞), regardless of the original units of measurement. The theoretical maximum concentration of NPs was calculated for the NP with the highest observed concentration per study. This allows easier fitting and interpretation of the rate parameters from the reported amount-time series.

Model

The normalized (dimensionless) uptake amounts were then fitted to a first-order one-compartment model [34]. Such a model takes the uptake rate u (in dimensionless relative uptake units per hour) and the first order elimination rate constant k_e [hour^{-1}] into account as shown in Equation 6.1. Uptake has been observed in the numerous studies described here. Elimination, also called exocytosis, describes the reduction of the concentration in an organism or cell after refreshment of the medium without a chemical; it has been occasionally observed [32, 35, 36]. In our model, we express the relative NP uptake rate per hour:

Equation 6.1

$$\frac{N_c(t)}{N_c(\infty)} = \frac{N_m}{N_c(\infty)} \cdot \frac{k_u}{k_e} \cdot (1 - e^{-k_e t}) = \frac{u}{k_e} \cdot (1 - e^{-k_e t})$$

where $N_c(t)$ is the amount of nanomaterial [unit] taken up by cells after exposure of t hours to a medium containing N_m particles [unit], $N_c(\infty)$ is the amount of nanomaterial from the medium, u ($=k_u \cdot N_m/N_c(\infty)$) is the relative uptake rate [hour^{-1}], k_e is the first-order rate constant of removal of nanomaterial from the cell per hour, and t [hours] is the time of exposure. The units of measurement are either number of nanoparticles or fluorescence intensity. The quotient u/k_e represents the relative amount taken up at infinitive time. For simplicity, the relative NP uptake rate will be called 'NP uptake rate' here after.

We tested the hypothesis that NP uptake follows first-order kinetics, as proposed before [37-39]. The results were evaluated with Microsoft Excel 2010 and the corresponding application 'Solver'. Solver is a tool that determines the optimal values for variables, here u and k_e, to minimize differences between experimental and model data.

To provide a measure of the goodness of fit between observed and model data, the squared Pearson product-moment correlation coefficient r^2, as calculated with the "RSQ" function in Excel based on fractions, was reported.

Next, we wanted to relate uptake parameters to NP properties by so called QSAR-models. The Excel 2010 add in 'Analysis ToolPak' was used to derive regressions with the

variables 'diameter', 'zeta potential', 'surface area', 'volume' and a multivariate regression using the two variables 'diameter' and 'zeta potential' at the same time to detect whether they are good descriptors of uptake. The confidence interval was set to 95%. This add in also automatically provides a measure of the goodness of fit of the regressions, called r^2. In addition, the Excel add in 'Solver' was used to determine whether the fitted model parameters u and k_e are normally distributed or whether they can be fitted through a linear or parabolic regression. As an additional, absolute error measure, the root-mean-square error (RMSE) was calculated according to the following equation:

Equation 6.2

$$RSME = \sqrt{\frac{1}{n} \times \sum_{i=1}^{n} (0i - Pi)^2}$$

where n is the number of data points, O_i the observed value, and P_i the predicted value. Calculating the average difference between the measured values and predicted ones, takes into account both systematic bias and random error [40].

Results

We have used the one-compartment model described by Equation 6.1 to test whether uptake of nanoparticles in cells obeys first-order kinetics. Results for phagocytes and non-phagocytes are presented separately. In the vast majority of cases, model and data matched well, resulting in a high explained variance (0.8 and higher, see Table S 6.2). For one study, the model did not fit the data for the two tested conditions sufficiently [41]. In the case where cells were exposed to NPs in the presence of serum, the one compartment model resulted in an r^2 of 0.23. In experiments without serum, the original curve is not smooth and cannot be matched well with the model curve. In another case the original curve is not smooth and the deviations between data and model resulted in very high values for u and k_e [39]. Due to the differences between data and model curve, these results were excluded in our calculations. For non-phagocytes, the uptake rates u varied between values of nearly 0 to roughly 27 [hour^{-1}]. First-order elimination rate constants k_e [hour^{-1}] differed from values of nearly zero to approximately 37, the latter of both being exceptionally high and belonging to the unsmooth curve mentioned before. Values of uptake rates u ([hour^{-1}] found in the experiments analyzed are given in Table S 6.1.

For non-phagocytes, approximately one third of the samples had calculated uptake rates $u \leq 0.1$ [hour^{-1}] (Table 6.2, Figure 6.1). The second and third largest amount of data points fell in the range of $u \leq 0.2$ [hour^{-1}] and $u \geq 1.0$ [hour^{-1}]. Therefore, uptake rates were similar in magnitude for different NPs and across various cell lines for approximately 50 % of published data. Yet, 17 % of the data showed rather large uptake rates in comparison.

Neither the fitted normal distribution nor a linear relationship could describe the observed data well, leading to a low r^2 of approx. 0.053 and 0.009, respectively (Table S 6.1).

Table 6.2 Percentage of observed data points per decimal step of the first order uptake rate *u*.

	Observed number of data points [% of total, rounded to full numbers] NP size		Observed number of data points [% of total, rounded to full numbers] NP charge	
Uptake rate u [hour^{-1}]	Non-phagocytes	Phagocytes	Non-phagocytes	Phagocytes
$u \leq 0.1$	37	38	32	32
$0.1 < u \leq 0.2$	21	17	16	9
$0.2 < u \leq 0.3$	4	7	13	15
$0.3 < u \leq 0.4$	4	0	8	9
$0.4 < u \leq 0.5$	6	7	3	3
$0.5 < u \leq 0.6$	2	-	16	18
$0.6 < u \leq 0.7$	-	5	-	-
$0.7 < u \leq 0.8$	4	-	-	6
$0.8 < u \leq 0.9$	2	2	5	-
$0.9 < u \leq 1.0$	4	2	3	3
$u \geq 1$	17	21	5	6

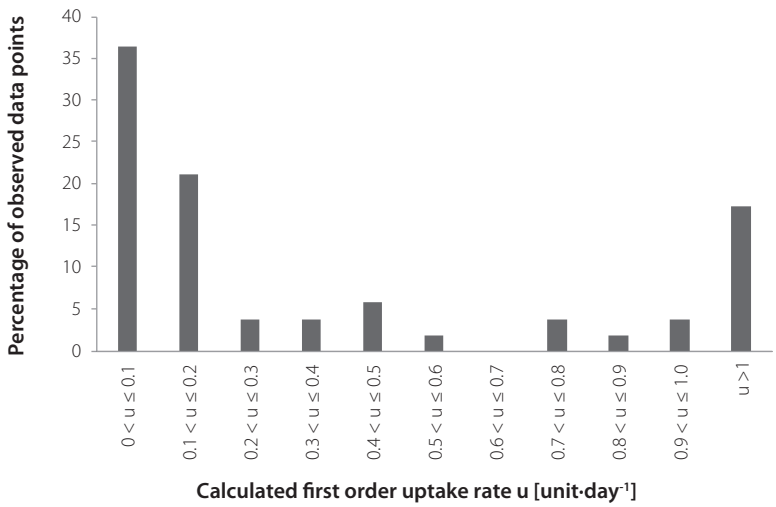

Figure 6.1 Percentage of observed data points per decimal step of the uptake rate *u* [hour^{-1}] for non-phagocytes.

We observed (Figure 6.2) that the same type of NP may lead to different uptake rates in various cell lines [33, 42-44]. This was most pronounced for the tested cell lines of Harush-Frenkel et al. 2007. Uptake kinetics were, therefore, slightly variable between cell lines. The exposure concentration may have a similar effect on uptake rates as demonstrated by several studies [39, 44, 45]. The tenfold higher exposure concentration also lead to a roughly 7-fold increase of the uptake rate [45]. Kim et al. also studied the effect of exposure concentrations on the uptake rate, using a concentration 4 times as large as the low concentration. This lead to an approximately 2.5 fold increase of the uptake rate [44].

The number of studies and number of data point for phagocytes was much smaller than for the non-phagocytes. With the indicated key words only 7 studies with 38 data points were found that fulfil the mentioned criteria. Some of the measurements that lead to this number of data points were counted double because they are compared in different sub groups within one study.

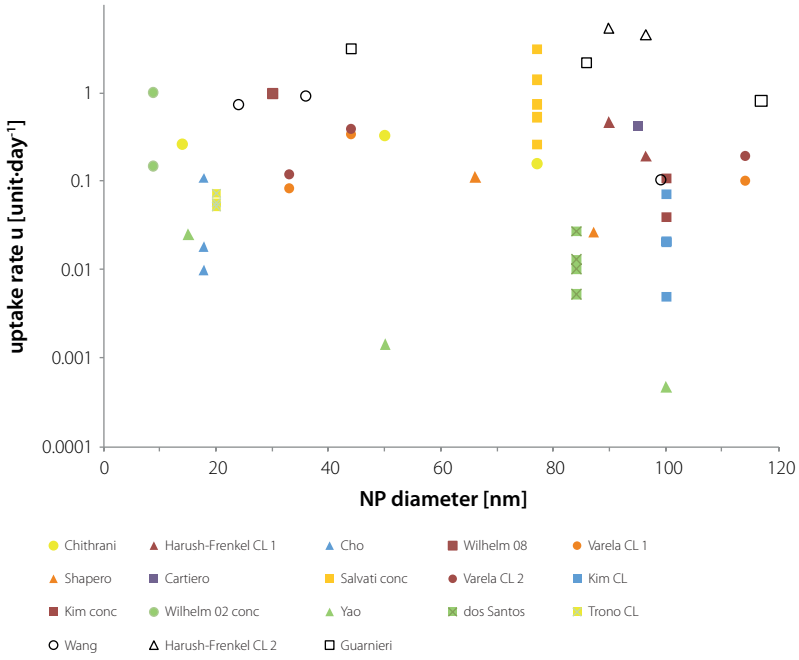

Figure 6.2 Uptake rate *u* [hour^{-1}] for non-phagocytes in dependence of the NP diameter [nm]. Open symbols represent studies with animal cell lines, closed symbols data from human cell lines. The shape of the data points are used to distinguish the applied dose metrics: same NP number (circles), same mass (triangle), unknown/not applicable (squares). Please notice the log scale of the y-axes.

Lunov et al. 2011, for example, studied the effect of the differentiation status of cells, the presence or absence of serum and NP charge [46]. Therefore, the data were divided into three sub groups which results in 24 data points from 8 observations.

Similar to non-phagocytes, roughly one third of the data points for phagocytes had uptake rates $u \leq 0.1$ [hour^{-1}] (Figure 6.3). The group of calculated uptake rates $u \geq 1.0$ [hour^{-1}] is smaller and only comprises roughly 5 percent of the total data points. Phagocytes data were scattered due to variability in the uptake rate for different cell lines but the same NP [46, 47], in dependence of the exposure concentration [35, 45] and the presence or absence of serum [46] (Figure 6.4).

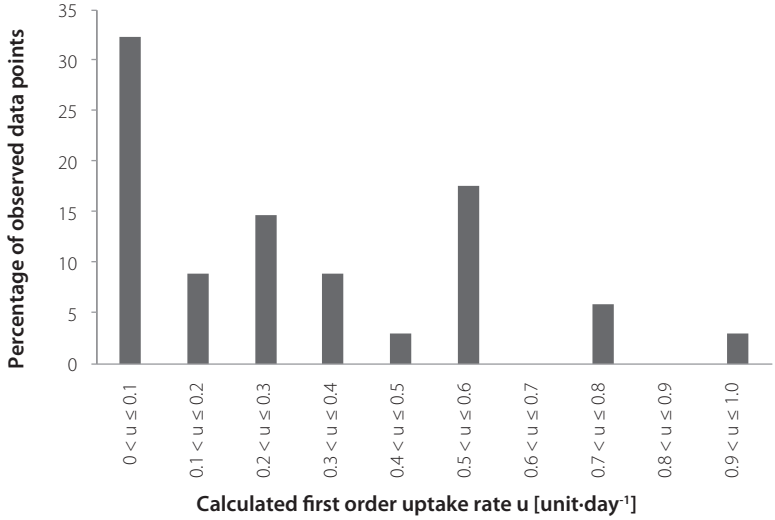

Figure 6.3 Percentage of observed data points per decimal step of the uptake rate *u* [hour^{-1}] for phagocytes.

Little similarity in the distribution of uptake rates of non-phagocytes and phagocytes could be observed when only those studies were considered where the NP's charge was reported (Figure 6.5, Figure 6.6). Not all studies determined the zeta potential, therefore this data set was smaller; 34 instead of 38 data points (phagocytes) and 42 instead of 54 (non-phagocytes).

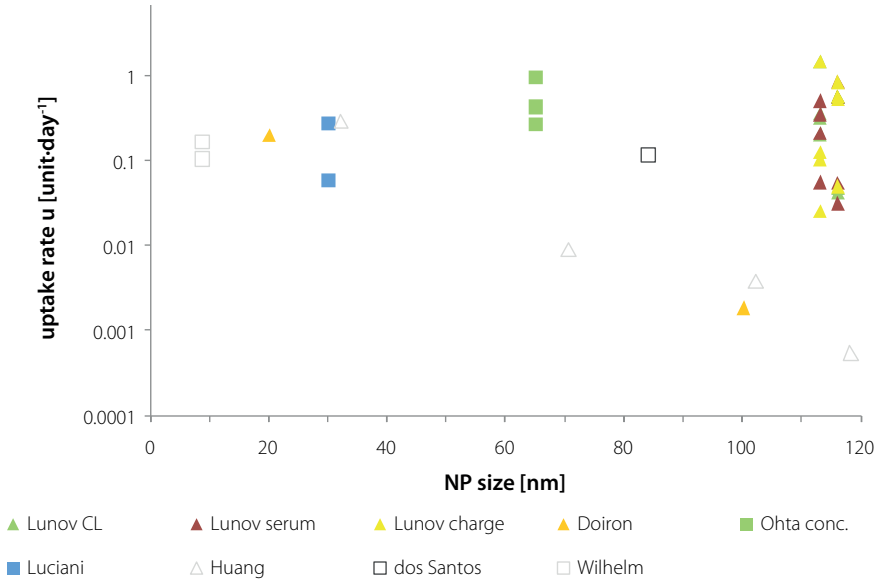

Figure 6.4 Uptake rate *u* [hour^{-1}] for phagocytes in dependence of the NP diameter [nm]. Open symbols represent studies with animal cell lines, closed symbols data from human cell lines. The shape of the data points are used to distinguish the applied dose metrics: same NP number (circles), same mass (triangle), unknown/not applicable (squares). Please notice the log scale of the y-axes.

To test whether other variables might be a better descriptor of uptake rates than the NPs diameter, r^2 was also calculated for the uptake rates in relation to the surface area, volume, zeta potential/charge and combination of diameter and charge (Table S 6.1). Uptake rates could not be explained sufficiently by either of the applied descriptors, neither for phagocytes nor non-phagocytes. There seemed to be no clear relationship between uptake rate and particle size (Figure 6.7, Figure 6.8), as also demonstrated by the overlap of the calculated 95% confidence intervals (Table 6.3).

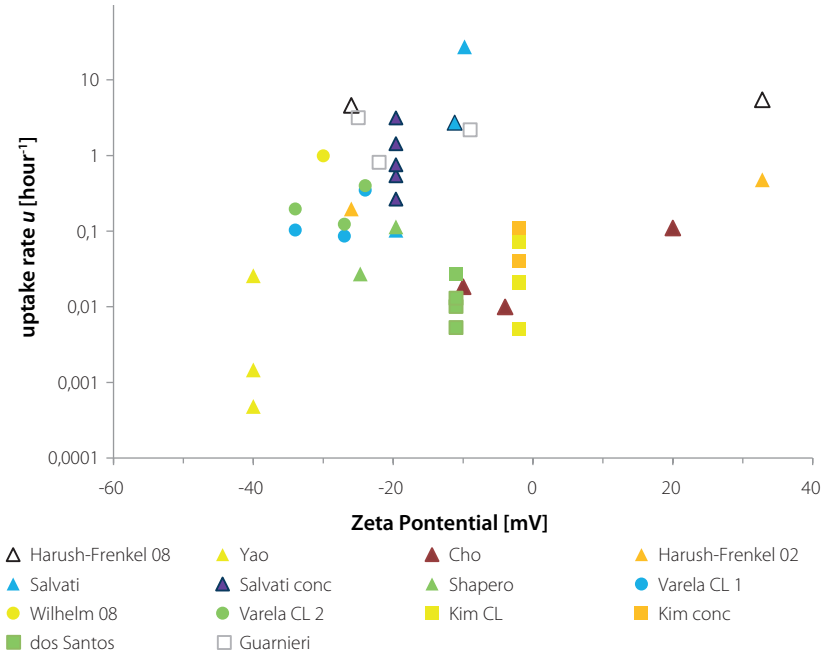

Figure 6.5 Uptake rate *u* [hour^{-1}] for non-phagocytes in dependence of the zeta potential. Open symbols represent studies with animal cell lines, closed symbols data from human cell lines. The shape of the data points are used to distinguish the applied dose metrices: same NP number (circles), same mass (triangle), unknown/not applicable (squares). Please notice the log scale of the y-axes.

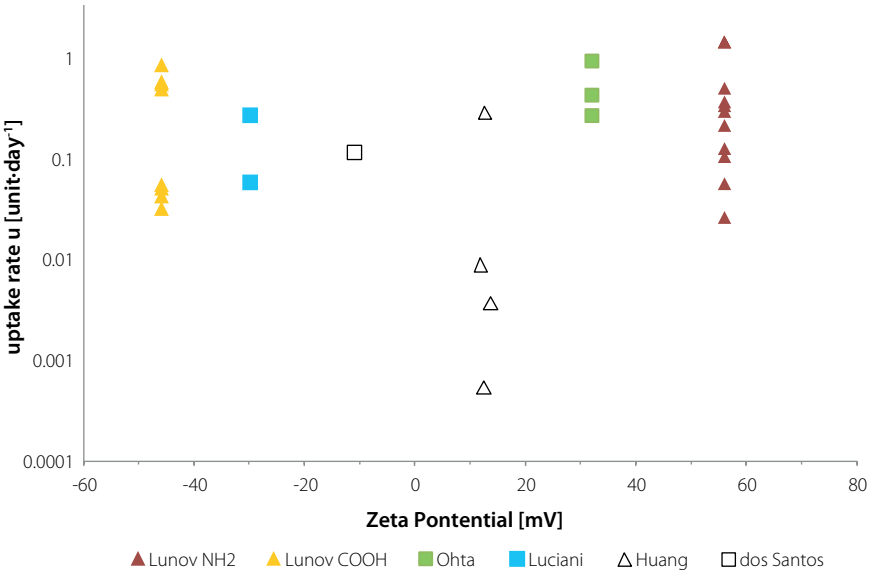

Figure 6.6 Uptake rate *u* [hour^{-1}] for phagocytes in dependence of the zeta potential. Open symbols represent studies with animal cell lines, closed symbols data from human cell lines. The shape of the data points are used to distinguish the applied dose metrices: same NP number (circles), same mass (triangle), unknown/not applicable (squares). Please notice the log scale of the y-axes.

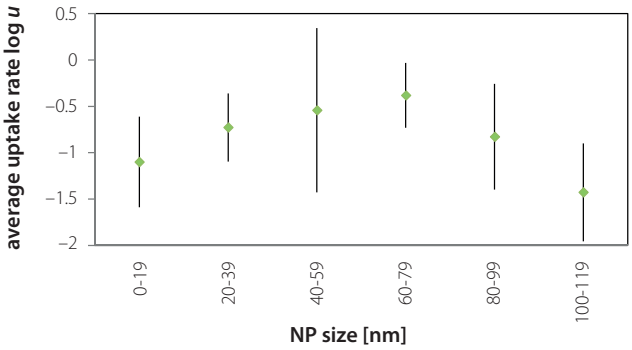

Figure 6.7 Average observed uptake rate log *u* [hour^{-1}] in dependence of NP size for non-phagocytes within 20 nm bins. Error bars represent the 95% confidence interval.

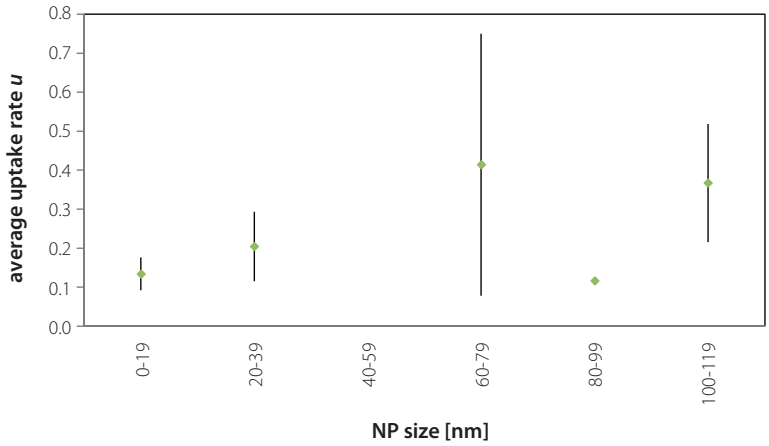

Figure 6.8 Average observed uptake rate log *u* [hour^{-1}] in dependence of NP size for phagocytes within 20 nm bins. Error bars represent the 95% confidence interval.

Table 6.3 95% confidence intervals (CI) of the uptake rate log *u* [hour^{-1}] per NP size class for non-phagocytes and phagocytes.

NP size class	Lower end 95 % CI	Upper end 95% CI	Average
Non-phagocytes			
0-19	-1,587	-0,610	-1,098
20-39	-1,093	-0,360	-0,727
40-59	-1,425	0,344	-0,540
60-79	-0,731	-0,032	-0,381
80-99	-1,397	-0,257	-0,827
100-119	-1,954	-0,898	-1,426
Phagocytes			
0-19	-1,022	-0,744	-0,883
20-39	-1,031	-0,485	-0,758
40-59	-	-	-
60-79	-1,508	0,006	-0,751
80-99	-	-	-0,932
100-119	-1,187	-0,566	-0,877

Discussion

In this study, data from studies on a mass basis were first converted to NP numbers taken up. Next, NP number values were expressed as dimensionless fractions of the theoretical maximum NP number accumulated to test the hypothesis that uptake follows first-order kinetics. The good fit between the converted data and first-order one-compartment model demonstrated that uptake of NP into living cells obeys first-order kinetics. Only in two cases data and model did not fit well [41]. In this case the data points did not result in a smooth curve, likely due to the high standard deviation for some of the data points. In the other case serum was added to the exposure medium, which might lead to the formation of a protein corona on the NPs' surface and aggregation as discussed further later on.

In each data set, values of u and k_e were obtained by fitting a first-order, two-parameter model of equation (6.1) to the normalized amounts taken up. The obtained quotients u/k_e were close to one for the NPs that uptake values were normalized to, indicating that the calculated maximum amounts of uptake had reached the steady-state level sufficiently close. We normalize to the number of NPs internalized at steady state for the NP with highest observed uptake per study. Whether a higher uptake would be possible for a different untested NP was unknown.

Since our work covered different NP core materials, coatings, charges, cell lines, and experimental set ups, such as presence or absence of serum during incubation, we investigated whether uptake kinetics follow a more fundamental mechanism and whether some more general conclusions about NP uptake kinetics can be drawn. Having shown that uptake can be described by first-order kinetics, we attempted to derive QSARs that predictively describe the parameters of first-order uptake as simple functions of NP properties such as size and charge. Large scattering of the data was observed and no predictive QSARs could be derived; there was no clear relationship between the parameters of first-order uptake and the NP properties 'size' and 'charge'.

Several studies suggested that a NP size of approximately 50 nm in diameter leads to the highest NP uptake [13, 25-29]. This is the size range in which many naturally occurring endocytosis targets, such as viruses and lipid carrying proteins, fall [28]. Unfortunately, the size optimum was determined after a fixed time point in those references and did not represent uptake over time. The importance to determine uptake over time to compare uptake efficiencies (between cell lines) was nicely demonstrated by Blechinger et al. [30]. Uptake in HeLa cells started off slowly with low amounts taken up within 4 hours. At 10 h and 24 h uptake increased drastically, reaching much higher intracellular concentrations in the end than HUVEC cells for which uptake kinetics where fast at the beginning. Knowledge on kinetics, in addition to static conditions, generally improves the understanding of uptake mechanisms and enhances the accuracy of risk assessment. Due to the importance of NP safety it is, therefore, of practical importance to explore effects of NP

properties, such as size, on uptake. Uptake and elimination over time is often assessed to determine accumulation of traditional chemicals. Some studies determined uptake of NPs over time and observed that there is a size where the uptake of NPs into cells was maximized [31-33]. Yet, these studies proposed this optimum based on data from their own conducted experiments only. Therefore, they were usually limited either to the use of different particles but only one cell type or vice versa. The combination of both within one study was scarce. The effect of concentration on NP uptake rates was rarely taken into account.

The size-optimum of endocytosis for few studies and a limited set of data points has been confirmed and explained by various models that describe how many NP can be internalized or how fast NPs can be internalized depending on their size, taking into account the competitive binding energy between NPs and receptors and the energy required for the wrapping of the NPs [48-50]. In their theoretical model, Zhang et al. assumed an average receptor density and average area of the plasma membrane. Yet, as discussed later, the size and corresponding surface area of cells might largely vary and it is well known that the amount of expressed receptors is often increased in cancer cell lines [51, 52].

Despite suggestions of 50 nm as an optimal uptake size based on (equilibrium) accumulation, our study suggests that other factors matter more than NP size. The discrepancy might be explained by several factors related to the lack of a straight forward methods to evaluate NP uptake of different sizes or, even more so, standard test protocols and materials.

First, several factors related to the experimental setting may explain why a generalization that uptake is (dominantly) NP size controlled is not possible: Dose metrics differed in the presented studies; either a constant mass was applied or a fixed number of NPs, with mass being the most common one because it is highly practical and convenient. A third, rare option is the application of a fixed volume, which we did not observe here. Exposure concentrations differed from study to study. The amount of NPs taken up after a fixed time point as well as uptake kinetics depended on the exposure concentration [37-39, 44, 45, 47, 53, 54]. Higher exposure concentrations lead to higher uptake until a saturation concentration was reached. The higher uptake at higher exposure concentrations seemed to be related to higher attachment of NPs to the cell membrane [55]. Curves relating uptake after a fixed time point to exposure concentration were non-linear and their slopes differed between cells lines [54]. The attachment efficiency of NPs to the cell membrane and subsequent uptake into cells depended also on the delivery of the NPs to the cells via diffusion and settling in cell culture medium, so called particokinetics, as further described elsewhere [56-58]. Under some conditions the delivery of NPs to the cell was slower than the removal of the particles from the medium through uptake by cells. In this case the low delivery rate would be the rate-limiting factor for uptake [59]. Therefore, incorporation of particokinetics in the study design or as a mean to evaluate experimental

results will further help to get new insights into the NP characteristics influencing NP uptake and intracellular toxicity and the dynamics of NP cell interactions. Uptake data were expressed in numerous units, partly depending on the detection method, and the results can differ depending on the unit used. Levy et al showed that the size optimum varied with the unit in which uptake is expressed [60]. This was also nicely shown graphically by Yue et al. [61].

Second, the choice of cell line influenced uptake and data to unify across cell lines was lacking. Uptake rate and mechanism are cell type specific, and may depend on cell density [44, 62, 63]. Observed differences between various cell lines but the same NP may be attributed to differences in the cell surface area. We assumed that all cell lines were able to take up the same amount of NPs when we normalized the data for each study separately. This was based on a study by Wilhelm et al. [45]. They showed that the iron load per cell after 1 h incubation at 4°C was the same for two cell lines after renormalization of the mass by the cell surface [45]. So the total mass taken up in dependence of the cell surface area could be predicted, but whether similar results could be expected for the first order rate constants is unknown. The binding capacity per unit surface was the same across several cell lines [54], and the efficiency of the adsorption of NPs onto the cell surface prior to uptake depended only on the cell surface. Yet, the characteristic time for internalization ranged from 0.4 to 1.8 hours within the tested cell lines [54], which might lead to different uptake rates. The publications under our investigation usually did not report cell sizes or surface area, therefore it was not possible to normalize NP uptake to cell properties. Values reported in literature differed a lot, e.g. diameters of HeLa cells were reported to range from 15 nm to 30 µm, corresponding to volumes of 500-5000 μm^3 [64]. The small observed differences in rate constants between cell lines could be related to the different intended roles of various cells [65]. In addition to size, the membrane tension can span several orders of magnitude and has been shown to have large effects on the cellular uptake of NPs [50]. As several characteristics of a membrane already vary within one cell type [66], we expected that it might also partly explain the observed differences between cell lines.

Third, besides size and charge, other NP properties may influence their cellular uptake, as previously summarized [9]. Other NP surface properties that influence uptake include surface functional groups, hydrophilicity and lipophilicity, and even surface roughness.

Furthermore, it is questionable whether the reported NP sizes are also those that the cells 'see'. It is well known that the particle size change with the surrounding medium, e.g. by the formation of a so called protein corona [55]. In the presented studies the NP size was not always determined in the exposure medium, or via techniques that don't allow the detection of a protein corona on the NP's surface [43, 53, 67]. The formation of a protein corona may influence the kinetics of membrane binding of NPs rather than the kinetics of the actual uptake process [68].

Besides these data and parameter uncertainties, model uncertainties may contribute to the discrepancy. The chosen equation may not represent the actual process exactly.

Yet, Excel reported a good fit between model and data with high r^2 for the vast majority of data. The given first order rate constants were not absolute but for reasons of comparability between studies relative ones. Comparison of absolute values of those studies that report their results in NP numbers would be desirable, yet impossible in some cases because of a lack of information. Basic information like the number of cells per monolayer for example, were sometimes missing, yet indispensable for such a comparison [69].

Conclusion and recommendations

Besides the increased likelihood of NP exposure through consumer products and medical applications and the fact that uptake kinetics are inherently linked to toxicity assessment, up to now no general approach was conducted to analyze reported uptake data with regard to uptake kinetics. Therefore, we collected data on NP uptake kinetics, which were shown to follow first-order kinetics. Having collected a large data set of uptake rates, it remains difficult to draw general conclusions about the relationship between NP properties and uptake kinetics. Our paper demonstrates that variables commonly thought to govern uptake do not allow for modelling (yet). Predictive QSARs could not be constructed due to heterogeneity of data and a lack of data reported within studies. Our paper will guide future efforts of researchers and demonstrates which bottle necks need to be overcome. Therefore, we recommend to include more information in future studies to enable incorporation within models and to increase their predictive power. We identified the following information to be necessary additions: exposure concentration, NP size and charge in the exposure medium, cell size, surface area or volume. Especially more standardization, e.g. through the use of reference materials would hopefully steer research in the right direction [70].

Supporting Information

Supporting information features r^2 for regressions and all calculated uptake rates u [$hour^{-1}$] from published data presented in this work.

Table S 6.1. Calculated uptake rates u [$hour^{-1}$] from published data for various conditions and NP sizes.

Table S 6.2. r^2 using linear, normal, parabolic, and multivariate regression to relate u [$hour^{-1}$] to the various descriptors.

Acknowledgements

The present study was supported by NanoNextNL, a micro and nanotechnology consortium of the Government of the Netherlands and 130 partners.

Cited Work

1. S.F. Hansen, B.H. Larsen, and S.I. Olsen, *Categorization framework to aid hazard identification of nanomaterials.* Nanotoxicol., **2007**. 1 (3): p. 243-250.
2. A. Dowling, *Nanoscience and nanotechnologies: Opportunities and uncertainties report.* 2004, The royal Socitey and the Royal Academy of Engineering.
3. M. Auffan, et al., *Towards a definition of inorganic nanoparticles from an environmental, health and safety perspective.* Nat Nanotechnol., **2009**. 4: p. 634 - 641.
4. M.G. Lines, *Nanomaterials for practical functional uses.* Journal of Alloys and Compounds, **2008**. 449: p. 242-245.
5. A. Hinther, et al., *Nanometals induce stress and alter thyroid hormone action in amphibia at or below north american water quality guidelines.* Environ Sci Technol, **2010**. 44: p. 8314-8321.
6. F.R. Khan, et al., *Bioaccumulation dynamics and modeling in an estuarine invertebrate following aqueous exposure to nanosized and dilssolved silver.* Environ Sci Technol, **2012**. 46: p. 7621-7628.
7. N.L. Rosi, et al., *Oligonucleotide-modified gold nanoparticles for intracellular gene regulation.* Science, **2006**. 312: p. 1027-1030.
8. P. Fortina, et al., *Applications of nanoparticles to diagnostics and therapeutics in colorectal cancer.* Trends Biotechnol., **2007**. 25 (4): p. 145-152.
9. K. Kettler, et al., *Cellular uptake of nanoparticles as determined by particle properties, experimental conditions, and cell type.* Environ. Toxicol. Chem., **2014**. 33 (3): p. 481-492.
10. D.A. Kuhn, et al., *Different endocytotic uptake mechanisms for nanoparticles in epithelial cells and macrophages.* Beilstein J. Nanotechnol., **2014**. 5: p. 1625-1636.
11. S.D. Conner and S.L. Schmid, *Regulated portals of entry into the cell.* Nature, **2003**. 422: p. 37-44.
12. K. Hirota and H. Terada, *Endocytosis of particle formulations by macrophages and its application to clinical treatment*, in *Molecular regulation of endocytosis*, B. Ceresa, Editor. 2012, InTech: Rijeka, Croatia.
13. J. Rejman, et al., *Size-dependent internalization of particles via the pathways of clathrin- and caveolae-mediated endocytosis.* Biochemical Journal, **2004**. 377: p. 159-169.
14. Y. Xu, T.S. Tillman, and P. Tang, eds. *Pharmacology: Principles and practice.* 1 ed., ed. M. Hacker, W. Messer, and K. Bachmann. 2009, Academic Press: Burlington, USA.
15. L.N. Patel, J.L. Zaro, and W.-C. Shen, *Cell penetrating peptides: Intracellular pathways and pharmaceutical perspectives.* Pharmaceut Res, **2007**. 24 (11): p. 1977-1992.
16. A. Aderem and D.M. Underhill, *Mechanisms of phagocytosis in macrophages.* Annual Review of Immunology, **1999**. 17: p. 593–623.
17. M.V.D.Z. Park, et al., *The effect of particle size on the cytotoxicity, inflammation, developmental toxicity and genotoxicity of silver nanoparticles.* Biomaterials, **2011**. 32 (36): p. 9810-9817.
18. E.J. Park, et al., *Oxidative stress and apoptosis induced by titanium dioxide nanoparticles in cultured beas-2b cells.* Toxicol Lett, **2008**. 180 (3): p. 222-229.
19. T. Xia, et al., *Cationic polystyrene nanosphere toxicity depends on cell-specific endocytic and mitochondrial injury pathways.* ACS Nano, **2008**. 2 (1): p. 85-96.
20. S.M. Hankin, et al., *Specific advice on fulfilling information requirements for nanomaterials under reach (rip-on 2) – final project report.* 2011.
21. G. Oberdörster, E. Oberdörster, and J. Oberdörster, *Nanotoxicology: An emerging discipline evolving from studies of ultrafine particles.* Environ. Health Persp., **2005**. 113 (7): p. 823-39.
22. A.E. Nel, et al., *Understanding biophysicochemical interactions at the nano-bio interface.* Nat. Mater., **2009**. 8: p. 543-557.
23. M. Ferrari, *Cancer nanotechnology: Opportunities and challenges.* Nat Rev Cancer, **2005**. 5: p. 161-171.
24. O.C. Farokhzad and R. Langer, *Impact of nanotechnology on drug delivery.* ACS Nano, **2009**. 3 (1).
25. W. Jiang, et al., *Nanoparticle-mediated cellular response is size-dependent.* Nat Nanotechnol., **2008**. 3: p. 145-150.
26. F. Lu, et al., *Size effect on cell uptake in well-suspended, uniform mesoporous silica nanoparticles.* Small, **2009**. 5 (12): p. 1408–1413.
27. S.-H. Wang, et al., *Size-dependent endocytosis of gold nanoparticles studied by three-dimensional mapping of plasmonic scattering images.* Journal of Nanobiotechnology, **2010**. 8 (33).

28. F. Osaki, et al., *A quantum dot conjugated sugar ball and its cellular uptake. On the size effects of endocytosis in the subviral region.* J am Chem Soc, **2004**. 126 (21): p. 6520–6521.
29. X. Ma, et al., *Gold nanoparticles induce autophagosome accumulation through size-dependent nanoparticle uptake and lysosome impairment.* ACS Nano, **2011**. 5 (11): p. 8629-8639.
30. J. Blechinger, et al., *Uptake kinetics and nanotoxicity of silica nanoparticles are cell type dependent.* Small, **2013**. 9 (23): p. 3970-3980.
31. B.D. Chithrani, A.A. Ghazani, and W.C.W. Chan, *Determining the size and shape dependence of gold nanoparticle uptake into mammalian cells.* Nano Letters, **2006**. 6 (4): p. 662-668.
32. K. Shapero, et al., *Time and space resolved uptake study of silica nanoparticles by human cells.* Mol Biosyst, **2010**. 7 (3): p. 371-378.
33. J.A. Varela, et al. *Quantifying size-dependent interactions between fluorescently labeled polystyrene nanoparticles and mammalian cells.* Journal of Nanobiotechnology, **2012**. 10, DOI: 10.1186/1477-3155-10-39.
34. Oecd, *Oecd guidelines for the testing of chemicals, section 3: Degradation and accumulation test no. 317: Bioaccumulation in terrestrial oligochaetes.* 2010.
35. S. Ohta, S. Inasawa, and Y. Yamaguchi, *Real time observation and kinetic modeling of the cellular uptake and removal of silicon quantum dots.* Biomaterials, **2012**. 33: p. 4639-4645.
36. B.D. Chithrani and W.C.W. Chan, *Elucidating the mechanism of cellular uptake and removal of protein-coated gold nanoparticles of different sizes and shapes.* Nano Letters, **2007**. 7 (6): p. 1542-1550.
37. S. Yu, et al., *Size- and charge-dependent non-specific uptake of pegylated nanoparticles by macrophages.* Int. J. Nanomed, **2012**. 7: p. 799-813.
38. O. Lunov, et al., *Modeling receptor-mediated endocytosis of polymer-functionalized iron oxide nanoparticles by human macrophages.* Biomaterials, **2011**. 32: p. 547-555.
39. A. Salvati, et al., *Experimental and theoretical comparison of intracellular import of polymeric nanoparticles and small molecules: Toward models of uptake kinetics.* Nanomed-Nanotechnol, **2011**. 7: p. 818–826.
40. K. Veltman, et al., *Bioaccumulation potential of air contaminants: Combining biological allometry, chemical equilibrium and mass-balances to predict accumulation of air pollutants in various mammals.* Toxicol. Appl. Pharmacol, **2009**. 238 (1): p. 47–55.
41. A. Lesniak, et al., *Effects of the presence or absence of a protein corona on silica nanoparticle uptake and impact on cells.* ACS Nano, **2012**. 6 (7): p. 5845–5857.
42. O. Harush-Frenkel, et al., *Targeting of nanoparticles to the clathrin-medaited endocytic pathway.* Biochemical and Biophysical Research Communications, **2007**. 353 (1): p. 26-32.
43. J.D. Trono, et al., *Size, concentration and incubation time dependence of gold nanoparticle uptake into pancreas cancer cells and its future application to x-ray drug delivery system.* Journal of Radiation Research, **2011**. 5: p. 103-109.
44. J.A. Kim, et al., *Role of cell cycle on the cellular uptake and dilution of nanoparticles in a cell population.* Nat Nanotechnol., **2012**. 7: p. 62-68.
45. C. Wilhelm, et al., *Interaction of anionic superparamagnetic nanoparticles with cells: Kinetic analyses of membrane adsorption and subsequent internalization.* Langmuir, **2002**. 18: p. 8148-8155.
46. O. Lunov, et al., *Differential uptake of functionalized polystyrene nanoparticles by human macrophages and a monocytic cell line.* ACS Nano, **2011**. 5 (3): p. 1657–1669.
47. N. Luciani, F. Gazeau, and C. Wilhelm, *Reactivity of the monocyte/macrophage system to superparamagnetic anionic nanoparticles.* J Mater Chem, **2009**. 19: p. 6373-6380.
48. H. Yuan and S. Zhanga, *Effects of particle size and ligand density on the kinetics of receptor-mediated endocytosis of nanoparticles.* Applied Physics Letters, **2010**. 96.
49. H. Gao, W. Shi, and L.B. Freund, *Mechanics of receptor-mediated endocytosis.* Proc. Natl. Acad. Sci. USA, **2005**. 102 (27): p. 9469–9474.
50. S. Zhang, et al., *Size-dependent endocytosis of nanoparticles.* Adv Mater, **2009**. 21: p. 419–424.
51. E. Ruoslahti, S.N. Bhatia, and M.J. Sailor, *Targeting of drugs and nanoparticles to tumors.* Journal of Cell Biology, **2010**. 188 (6): p. 759–768.
52. I.H. El-Sayed, X. Huang, and M.A. El-Sayed, *Surface plasmon resonance scattering and absorption of anti-egfr antibody conjugated gold nanoparticles in cancer diagnostics: Applications in oral cancer.* Nano Letters, **2005**. 5 (5): p. 829-834.

53. J. Panyam and V. Labhasetwar, *Dynamics of endocytosis and exocytosis of poly(d,l-lactide-co-glycolide) nanoparticles in vascular smooth muscle cells.* Pharmaceut Res, **2003**. 20 (2): p. 212-220.
54. C. Wilhelm and F. Gazeau, *Universal cell labelling with anionic magnetic nanoparticles.* Biomaterials, **2008**. 29: p. 3161–3174.
55. L. Shang, et al., *Nanoparticle interactions with live cells: Quantitative fluorescence microscopy of nanoparticle size effects*. Beilstein Journal of Nanotechnology, **2014**. 5: p. 2388-2397.
56. J.G. Teeguarden, et al., *Particokinetics in vitro: Dosimetry considerations for in vitro nanoparticle tocixity assessments*. Toxicol Sci, **2007**. 95 (2): p. 300-312.
57. P. Rees, *Uptake and toxicity of nanoparticles*, in *Nanomedicine*, H. Summers, Editor. 2013, Elsvier: Oxforc, UK. p. 123-138.
58. P.M. Hinderliter, et al., *Isdd: A computational model of particle sedimentation, diffusion and target cell dosimetry for in vitro toxicity studies*. Part Fibre Toxicol, **2010**. 7 (36).
59. L.K. Limbach, et al., *Oxide nanoparticle uptake in human lung fibroblasts: Effects of particle size, agglomeration, and diffusion at low concentrations.* Environ Sci Technol, **2005**. 39: p. 9370-9376.
60. R. Lévy, et al. *Gold nanoparticles delivery in mammalian live cells: A critical review.* Nano Reviews, **2010**. 1, DOI: 10.3402/nano.v1i0.4889.
61. H. Yue, et al., *Particle size affects the cellular response in macrophages*. European Journal of Pharmaceutical Sciences, **2010**. 41: p. 650-657.
62. W. Zauner, N.A. Farrow, and A.M.R. Haines, *In vitro uptake of polystyrene microspheres: Effect of particle size, cell line and cell density.* J. Control. Release, **2001**. 71: p. 39–51.
63. A. Vogt, et al., *Interaction of dermatologically relevant nanoparticles with skin cells and skin.* Beilstein Journal of Nanotechnology, **2014**. 5: p. 2363-2373.
64. M.E. Al., *Key numbers for cell biologists.* Nucleic Acids Res, **2010**. 38: p. D750-D753.
65. M.S. Cartiera, et al., *The uptake and intracellular fate of plga nanoparticles in epithelial cells.* Biomaterials, **2009**. 30: p. 2790-2798.
66. A. Diz-Muñoz, D.A. Fletcher, and O.D. Weiner, *Use the force: Membrane tension as an organizer of cell shape and motility.* Trends Cell Bil, **Trends Cell Biol. 2013**. 23 (2): p. 47–53.
67. E.C. Cho, Q. Zhang, and Y. Xia, *The effect of sedimentation and diffusion on cellular uptake of gold nanoparticles*. Nat Nanotechnol., **2011**. 6 (6): p. 385-391.
68. L. Treuel, et al., *Protein corona – from molecular adsorption to physiological complexity.* beilstein Journal of Nanotechnology, **2015**. 6: p. 857-873.
69. M. Yao, et al., *Uptake of gold nanoparticles by intestinal epithelial cells: Impact of particle size on their absorption, accumulation, and toxicity.* J. Agr. Food Chem, **2015**. 63: p. 8044–8049.
70. E. Commission. *Jrc nanomaterials repository.* [cited 2017 21.08.2017]; Available from: https://ec.europa.eu/jrc/en/scientific-tool/jrc-nanomaterials-repository.
165. Guarnieri, D., et al., Effect of serum proteins on polystyrene nanoparticle uptake and intracellular trafficking in endothelial cells. Journal of Nanoparticle Research, 2011. 13: p. 4295–4309.
166. Santos, T.d., et al., Quantitative Assessment of the Comparative Nanoparticle-Uptake Efficiency of a Range of Cell Lines. Small, 2011. 7(23): p. 3341-3349.
167. Harush-Frenkel, O., et al., Surface Charge of Nanoparticles Determines Their Endocytic and Transcytotic Pathway in Polarized MDCK Cells. Biomacromolecules, 2008. 9(2): p. 435-443.
168. Doiron, A.L., B. Clark, and K.D. Rinker, Endothelial Nanoparticle Binding Kinetics are Matrix and Size Dependent. Biotechnology and Bioengineering, 2011. 108(12): p. 2988-2998.

Appendix

Table S 6.1 r^2 using linear, normal, parabolic, and multivariate regression to relate *u* [$hour^{-1}$] to the various descriptors

u [$hour^{-1}$]	descriptor	Diameter [nm]	Surface area [nm^2]	Volume [nm^3]	Zeta potential	Diameter and charge
Non-phagocytes						
Linear	r^2	0.009	0.007	0.011	0.035	0.038
Normal distribution	r^2	0.053	-	-	-	-
	RMSE	0.642	-	-	-	-
Phagocytosing cells						
Linear		0.011	0.028	0.027	0.007	0.018
Normal distribution	r^2	0.030	0.028	0.027	-	-
	RMSE	0.065	0.067	0.065	-	-
parabolic	r^2	-	-	-	0.065	-
	RMSE	-	-	-	0.067	-

Table S 6.2 Calculated uptake rates *u* [hours^{-1}] from published data for various conditions and NP sizes

Ref.	Different conditions (where applicable)	NP size, diameter [nm]	Uptake rate *u* [hour^{-1}]	r^2
Non-phagocytes				
[45]	15 mM	8.7	1.003	0.977
	1.5 mM		0.149	0.992
[31,36]		14	0.265	0.982
[69]		15	0.026	0.995
[67]	PAA	17.7	0.110	0.976
	Citrate		0.018	0.996
	PVA		0.010	0.989
[43]	PK-1	20	0.052	0.969
	PK-45		0.074	0.896
	PANC-1		0.057	0.927
[27]		24	0.702	0.873
[54]		30	0.993	0.978
[33]	A549	33	0.086	0.959
	1321 N1	33	0.123	0.992
[27]		36	0.916	0.975
[33]	A549	44	0.349	0.951
	1321 N1		0.401	0.991
[165]		44	3.172	0.984
[39]		46	27.370	0.706
[31,36]		50	0.327	0.987
[69]		50	0.001	0.991
[39]		56	2.703	0.902
[41]	Serum free	64	0.281	0.981
[32]		66	0.114	0.965
[31,36]		74	0.159	0.990
[39]		77	0.103	0.996
[39]	5 ug/mL	77	0.265	0.784
	15 ug/mL		0.538	0.695
	25 ug/mL		0.753	0.982
	50 ug/mL		1.430	0.888
	90 ug/mL		3.134	0.711

Table S 6.2 Continued

Ref.	Different conditions (where applicable)	NP size, diameter [nm]	Uptake rate *u* [hour^{-1}]	r^2
Non-phagocytes				
[166]	HcMEC D3	84	0.027	0.999
	1321 N1		0.010	0.999
	A549		0.013	0.999
	HeLa		0.005	0.989
[165]		86	2.183	0,995
[32]		87	0.027	0.996
[42]		89.8	0.476	0.987
[167]		89.8	5.444	0.985
[65]		95	0.431	0.985
[42]		96.4	0.197	0.971
[167]		96.4	4.592	0.981
[27]		99	0.104	0.967
[44]	SH-SY5Y	100	0.021	1.000
	1321 N1		0.021	0.967
	hCMEC D3		0.005	0.997
	A549		0.072	0.997
[44]	25 ug/mL	100	0.040	1.000
	100 ug/mL		0.109	0.990
[69]		100	0.001	0.976
[41]	complete medium	105	0.027	0.230
[33]	A549	114	0.103	0.907
	1321 N1		0.197	0.990
[165]		117	0.814	0.986
[45]	1.5 mM	8.7	0.165	0.987
	0.75 mM		0.104	0.995
[168]		20	0.199	0.917
[47]	Monocytes	30	0.059	0.998
	Macrophages		0.273	0.997
[52]		32.2	0.289	0.989
[35]	50 µg/mL	65	0.270	0.993
	100 µg/mL		0.431	0.991
	200 µg/mL		0.948	0.996

Table S 6.2 Continued

Ref.	Different conditions (where applicable)		NP size, diameter [nm]	Uptake rate *u* [hour^{-1}]	r^2
Non-phagocytes					
[52]			70.7	0.009	0.983
[166]			84	0.117	1.000
[168]			100	0.002	0.959
[52]			102.4	0.004	0.952
[38]	PS-NH_2, HBSS, macrophages	Cell line effect	113	0.212	0.924
	PS-NH_2, HBSS, THP-1			0.367	0.923
	PS-NH_2, serum, macrophages	Cell line effect	113	0.322	0.860
	PS-NH_2, serum, THP-1			1.459	0.870
	PS-NH_2, HBSS, macrophages	Serum effect	113	0.212	0.924
	PS-NH_2, HBSS, THP-1			0.509	0.963
	PS-NH_2, serum, macrophages	Serum effect	113	0.056	0.860
	PS-NH_2, serum, THP-1			0.350	0.879
	PS-NH_2, HBSS, macrophages	Charge effect	113	0.106	0.924
	PS-NH_2, HBSS, THP-1			0.126	0.963
	PS-NH_2, serum, macrophages	Charge effect	113	0.026	0.860
	PS-NH_2, serum, THP-1			1.459	0.879
[38]	PS-COOH, HBSS, macrophages	Cell line effect	116	0.575	0.934
	PS-COOH, HBSS, THP-1			0.567	0.885
	PS-COOH, serum, macrophages	Cell line effect	116	0.050	0.999
	PS-COOH, serum, THP-1			0.042	0.827
	PS-COOH, HBSS, macrophages	Serum effect	116	0.841	0.934
	PS-COOH, HBSS, THP-1			0.567	0.885
	PS-COOH, serum, macrophages	Serum effect	116	0.054	0.999
	PS-COOH, serum, THP-1			0.031	0.827
	PS-COOH, HBSS, macrophages	Charge effect	116	0.841	0.934
	PS-COOH, HBSS, THP-1			0.567	0.885
	PS-COOH, serum, macrophages	Charge effect	116	0.050	0.999
	PS-COOH, serum, THP-1			0.531	0.827
[52]			118.3	0.001	0.991

7

General discussion/synthesis

Introduction

NPs represent a new type of chemicals that differ from traditional chemicals with regard to their physico-chemical properties, as well as biological interactions, in particular their uptake mechanism into cells. NPs a particulate in nature, as their name implies, and are therefore not dissolved in water like traditional chemicals. Due to their state the substances obtain different biological activities. In contrast to traditional chemicals, NPs are mainly taken up by endocytosis by the vast majority of cells [1]. Uptake via passive membrane penetration [2], i.e. for red blood cells, which lack the endocytic machinery [3], or via hole formation has been shown to be possible [1, 4]. Yet, uptake into red blood cells is very low with less than one NP per cell on average [5]. Therefore, this type of emerging chemicals requires new models that take this active mechanism into account. In order to achieve this goal, this thesis is focused on the following main points:

- First, to identify factors determining the cellular exposure to NPs, more specifically the extent of NP uptake (Chapter 2)
- Second, to determine uptake kinetics in dependence of NP size into two different cells lines under relevant exposure concentration (Chapter 3, Chapter 4)
- Third, development of an analytical technique for the determination of NP stability and abundance of NPs over time (Chapter 5)
- Fourth, to integrate information on the cellular level into models, possibly enabling predictions for untested NPs through construction of quantitative structure activity relationships (Chapter 6).

In the following, this chapter discusses controversial results between studies, between the chapters mentioned above and possible causes. We point to limitations of NP uptake studies and the resulting uncertainties and variability within the constructed QSARs. We focus on those topics that caused discussion in several chapters, i.e., particle characterization, dose metric and exocytosis. Finally, conclusions and recommendations on how to improve or systematize future studies and experimental set ups to enable the determination of parameters that govern uptake kinetics, are given.

Discussion

Dose metric

In contrast to traditional chemicals, which will usually interact with their environment in their soluble form, it is the NPs particulate nature, and the resulting differences in size and shape between NPs, that govern the complex phenomenon of cellular NP uptake. For traditional chemicals, effects are therefore related to exposure concentration expressed

as mass per volume. This dose metric is also practical and convenient for NPs. For soluble chemicals the total applied mass translates to a defined number of 'subunits', e.g. atoms or molecules, reacting with a cell or the cell surface (receptors). Although NPs are also composed of 'subunits', only part of the mass exposed at the NP surface is able to interact with the membrane for uptake. Due to the increasing surface to volume ratio with decreasing NP size, the portion of mass able to interact differs for the same mass of NPs of different sizes. Therefore, a dose in mass translates in different doses of 'subunits' interacting with the cell membrane for NPs. As a result, there is an ongoing discussion about the most appropriate dose metric with regard to toxicology, also dependent on the endpoint under investigation [6]. Up to today it remains unclear whether the same mass, the same number, the same volume, or the same surface area of NPs represents the proper dose metric for comparison between NPs of different sizes.

The dose metric of studies used in this thesis vary. While some studies are based on the application of the same number of NPs, other researchers expose cells to the same mass of NPs. Since the appropriate dose metric had not been identified yet, we chose to expose cells to the same mass of NPs, the more common dose metric (Chapter 3, Chapter 4). This also enabled comparison with already published data.

Comparison of uptake rates of various studies (Chapter 6) covers publications on both dose metrics. Especially in case of phagocytosing cells the majority of researchers applied the same mass of NPs. In case of non-phagocytosing cells, the data collected from literature cover both dose metrics about equally often. A dose metric can only be applied to studies that compare different NP sizes. For the largest group of studies, no dose metric can be assigned. These study address either only one NP type, the same NP type in different cell lines, or different NP concentrations within one cell line.

Having noticed these differences, the question arises whether differences in dose metrics might cause differences in observed uptake rates and variability within the constructed QSARs. The range of uptake rates for studies based on the same number of NPs is smaller than for mass-based studies (Figure 6.2, Chapter 6). Yet, the range of uptake rates for mass based exposure is similar to those where no metric can be applied. Therefore, variability in uptake rates can be most likely attributed to other differences between studies, as will be further discussed in this chapter.

Understanding NP uptake kinetics in a quantitative way, as intended with this thesis, is a prerequisite to draw meaningful conclusion about nanotoxicology. Instead of evaluating *in vitro* (toxicity) test results based on exposure doses, the NP dose actually taken up by a cell, and therefore reaching intracellular targets, needs to be considered. Ideally, toxicological studies would report the number of NPs reaching the relevant target, e.g. a cellular sub-compartment. Problems related to the determination of the intracellular NP concentration are discussed in the next section.

Determination of intracellular NP concentration

To reach the goal of a quantitative description of NP uptake, the detection of the intracellular particle concentration ideally needs to be improved. Many of the collected studies determined uptake via the measurement of the fluorescence intensity signal of marked NPs, as it is inexpensive and only requires common instruments. The fluorescence intensity is assumed to be proportional to the particle number per cell. Yet, fluorescence intensity cannot be used as absolute value for the particle number, as the images only show a cross section of one cell, i.e. one does not determine the fluorescence of all NPs inside one cell [7]. In addition, different methods may be applied to determine the fluorescence of single NPs and that of cells which took up NPs, e.g. microscopy and flow cytometry. The fluorescence detected by different methods cannot be related to each other [8]. Fluorescence intensity measured by flow cytometry can be normalized to particles of different intensities. However, they cannot be related to actual numbers [8] due to difficulties in the creation of calibration curves; the amount inside of the cells might not be linear in fluorescence as outside of cells [9]. Therefore, it is not possible to convert the fluorescence signal into an absolute measurand. Comparison of absolute amounts of material taken up are therefore not possible.

Chapter 3 indicated that uptake rates of AgNPs into 16HBE14o-cells were higher for 50 nm particles when expressed in mass, but highest for 20 nm particles on number-basis. It stresses the importance of absolute values for NP uptake in order to convert one measurand to another. Our results thus show that not just the uptake expressed as mass should be considered but also the conversion to NP numbers (and vice versa) might need to be considered when studying the mechanism of uptake phenomenon and related fields in order to determine relationships.

Absolute amounts can be detected by a very sensitive detection method called high resolution inductively coupled plasma mass spectrometry (HR-ICP-MS) as applied in Chapter 3, Chapter 4, and Chapter 5. This method was improved by coupling to an asymmetric flow field fractionation (AF4) to allow for separation of NPs in the supernatant according to size and subsequent determination of their abundance (Chapter 5). This newly developed method allows to study particle dissolution or aggregation in the exposure medium during the time course of the experiment. Combination of the total uptake of silver by cells and analysis of the remaining silver in the exposure medium allows one to determine the recoveries. The advantages are applicability to low exposure concentrations of 10 µg/mL and very high sensitivity, as well as the determination of NP stability. Unfortunately the method is expensive and time intensive as the method needs adjustment for each NP. It was therefore only possible to determine silver concentrations in the supernatant of few samples.

Particle concentration

The amount of NPs that cells are exposed to, expressed in either dose metric, is variable across studies largely due to different desired outcomes of studies and available detection techniques. While it might be necessary to expose cells to rather high NP concentrations in order to study and understand toxicological mechanisms, risk assessment should be based on realistic exposure concentrations. Yet, concentrations in uptake studies reach up to 100 µg/mL [10], a manifold of the expected environmental concentration of $8.8 \cdot 10^{-5}$-0,01 µg/mL [11]. We chose the highest expected environmental concentration of 0.01 µg/mL as the exposure concentration for our uptake studies (Chapter 3, Chapter 4). With respect to the origin of the studied cell lines, namely the lung, realistic exposure concentrations for short-term exposure via inhalation might also be of interest. Such exposure concentrations are estimated to be a factor of 10 higher than our chosen exposure concentration [12].

Further complexity is added due to possible differences in the exposure concentration and the amount of particles reaching the cells, which are usually positioned at the bottom of a cell culture plate. Cho et al. found uptake to be higher for cells in the upright configuration, so cells positioned at the bottom of a culture disc in comparison to the inverted configuration [13]. The observed effect was more pronounced for larger and therefore heavier NPs. This effect can be explained by the occurrence of sedimentation. The fraction between the added amount of NPs and those actually reaching the bottom of *in vitro* test systems, and therefore coming into contact with cells, can be estimated via a computational model [14]. This model takes sedimentation and diffusion of particles in the test medium into account. It requires thorough characterization of the NPs within the respective exposure medium.

The effect of NP exposure concentration on cellular uptake (kinetics) remains an open question based on currently available data. It has been shown that higher exposure concentrations lead to increased uptake after a fixed time point. A maximum exposure concentration exists after which no further increase in the maximum intracellular concentration is observed. Higher exposure concentrations also lead to increased uptake rates [15-22]. In addition, slopes differ between cell lines [21]. The observed differences might be caused by differences in the available cell membrane surface area for particle wrapping, the time needed to produce new membrane/membrane recycling, and cell volume, as well as the amount of certain cell surface receptors. These properties go along with the biological function of different cell types. Therefore, it is highly desirable to include additional information about the cells in which uptake is determined, as explained also in more detail later on. As discussed, improved detection of the intracellular particle concentration will aid to determine the relationship of NP exposure concentration and uptake amounts.

Exocytosis

The so called mechanism of exocytosis is an active mechanism to transport (nanoparticulate) substances out of a cell. Exocytosis has been observed in form of decreasing intracellular NP concentrations when the NP in the exposure medium have when removed [10, 15, 23, 24]. This elimination mechanism might be responsible for the observed leveling off of uptake curves. Exocytosis might be the rate limiting factor of NP uptake leading to steady state.

Traditional chemicals that enter cells or organisms by facilitated diffusion, as well as NPs, show increased uptake rates with increasing exposure concentrations, but their transport rates reach a maximum. In case of facilitated diffusion, it is the number of carriers that can be occupied that limit further uptake. For NPs it is likely the amount of available cell surface area for the formation of endocytic vesicles and the speed at which new membrane can be produced.

In order to take endocytosis into account in our work, we calculated parameters for first order uptake kinetics according to a one compartment model that includes a parameter *k* for elimination (Chapter 3, Chapter 4, and Chapter 6). The obtained uptake rates describe simultaneous uptake and elimination. Further studies are needed to determine how long NPs stay in cells, to what extend they are removed and which factors determine their removal. The degree of exocytosis of a non-degradable NP is very important with regard to bioaccumulation.

Size and charge determination

Our literature review showed that NP size is one of the most studied NP property with regard to effects on cellular uptake and first findings supported the hypothesis that a size optimum for NP uptake exists (Chapter 2). The similarity of NP size to biomolecules [25] and viruses [26, 27] resulted in a strong focus on this NP property. Particle size, particle density, agglomeration state and agglomerate characteristics may change when NPs are added to cell culture medium in comparison to stock solutions. The NPs' charge as well as size can be strongly influenced by the surrounding medium [28, 29]. These effects can cause large differences in the size of NPs that the cells 'see'. A critical step for interpretation of uptake (and toxicological) studies is the characterization of the studied NP in the relevant matrix to which it is added. It is important to include critical NP characterization prior to and also after mixing with biological media. Characterization should focus on the physical properties such as aggregation and surface charge. Additional detection of the thickness and composition of adsorbed protein corona would be beneficial. If the size of NPs in the medium of exposure and changes in size over time are not considered and reported, interpretation of data about NPs uptake (and toxicity) become difficult to impossible. In order to understand the influence of NP properties, experimental conditions and cell lines on uptake kinetics and possible accumulation, the starting material, here the NPs and the experimental settings, need to be fully understood, characterized and reported. Otherwise, effects cannot be attributed to one certain factor.

As these characterizations are sometimes not reported in the relevant matrix, we assumed the concept of primary particle size to be valid in the publications under investigation for the construction of QSARs. As the concept of primary particle size may not be relevant due to aggregation and ageing occurring in the medium, the lack of this information results in a limitation of our model. Due to the limited number of available uptake studies containing kinetic information, it was not possible to leave those studies out that lack NP characterization in the relevant media.

In our own uptake studies it became clear that it is not always easy to obtain NP size characteristics as available instrumentation is not always suitable for size detection under given conditions. Dynamic light scattering is an often applied method, yet it is not suitable for the size determination of small NPs with rather low concentrations [30]. Centrifugal particle sedimentation as a second widely applied methods led to unreproducible results in our experiments.

This demonstrates the large discrepancy between requirements for the construction of predictive models, as well as interpretation of uptake and toxicity studies, and the available means. To evaluate whether the concept of primary particle size remains valid under given conditions, easy to use, inexpensive and sensitive detection methods need to be developed. Ideally, they would applicable at low, environmental relevant NP concentrations. One step in this direction was taken at Philips Innovation Services (Chapter 5). The developed method has been shown to allow for the determination of AgNPs stability via the detection of their size in the exposure medium over time, as well as their abundance even at low NP concentrations of 10 µg/mL.

Similar to size, charge can also be altered drastically when the surrounding medium changes. This is especially the case when NPs are added to serum containing cell media. The presence of proteins can influence charge, as well as size, and in turn also uptake, due to the formation of a so called protein corona. Charge of NPs of the same material may already be variable in stock solution (Chapter 3, Chapter 4) and the observed effect might not be only caused by differences in size. The determination of the zeta potential requires higher concentrations than used for our experiments. The determination of the zeta potential under given conditions was therefore not possible [31]. Overall, technical limitations are a major factor that limit systematic studies under environmental relevant concentrations that would close some knowledge gaps.

Cell line

As mentioned earlier, it is desirable to include more information about the cell line under investigation than it is common in publications nowadays. In order to be able to harmonize/normalize published data for modeling purposes it would be beneficial if information about cell sizes, surface area and cell volume would be reported. Wilhelm et al. show that the total NP load per cell is the same when normalized to the cell surface area [20]. The NP binding capacity is proportional to the surface area across different cell lines,

yet the characteristic time needed for NP internalization differs between cell lines [32]. Therefore, according to Wilhelm and Gazeau, the total amount of NPs that can be taken up can be predicted by the cells surface area, but the time needed to achieve this maximum will vary. This contradicts our findings that uptake into 16HBE cells is approximately twice as high as for THP-1 cells besides the similar cell culture dish surface area covered with cells as determined by microscopic inspection. These differences might be explained by other factors such as intended biological role of the cell line and expression of different cell surface receptor (amounts), as discussed in Chapter 2 in detail.

Protocolling

Regretfully, there is also a strong need for the improvement of quality of published data. Fundamental information for the interpretation of results is sometimes lacking. This includes the number of exposed cells, NP concentrations and volumes/numbers applied, as well as information to convert data given in one measurand to another, e.g. molecular mass or the length of the edge of a unit cells in order to convert mass to NP numbers. The latter is of special importance when working with self-made NPs of commonly unknown composition and does not represent any obstacles when working with silver like we did. To improve protocolling we placed importance on the description of the experimental design, reporting not only NP concentrations but also applied volumes, the number of exposed cells and well size. To this end, the provision of NP standards with defined properties and formats for standardized test protocols would greatly improve the further use of studies.

Conclusions

In light of these considerations, we conclude the following:
Size is an important determinant for NP uptake (kinetics) when looking at one uptake study at a time (Chapter 2-4). Results of Chapter 6 contradict these findings; size and uptake kinetics do not correlate when comparing various studies due to observed differences of uptake kinetics for the same NP size in dependence of exposure concentration and cell line.

Similarly, charge was found to play an important role in NP uptake (kinetics) when looking at one study at a time (Chapter 2). Higher charges lead to higher uptake in comparison to less charged NPs. Positively charged NPs are taken up faster than negatively charged ones when the absolute zeta potential is comparable. In contrast, comparison of descriptors of uptake kinetics across various studies do not show a correlation between NP charge and uptake rates (Chapter 6).

Despite the availability of a quite large data set of studies on the effect of NP properties and experimental conditions on NP uptake, the constructed model (Chapter 6)

is considered preliminary. This is due to differences in uptake rates for different exposure concentrations and differences in cell lines, such as available cell surface area or cell volume. Up to now it is not possible to take exposure concentration and cell line effects into account in modeling. Improved models require normalization between studies and experimental conditions. This is not possible up to today due to a lack of systematic studies on concentration and cell (size) effects on NP uptake kinetics.

Overall, accumulation of NPs appears similar to that of traditional chemicals in terms of observed leveling off of uptake curves. While it is the increased elimination of traditional chemicals as a function of time that causes the leveling off, leveling off is likely limited by the rate of production and/or recycling of cell membrane needed to form endocytic vesicles in case of NPs. Similar to traditional chemicals, uptake of NPs into cells also follows first order kinetics.

For traditional chemicals and NPs high concentrations in the medium lead to high concentrations in the cell. Yet, in contrast to traditional chemicals that diffuse through membranes at a rate that increases linearly with the exposure concentration, NPs show saturation of the net transport rate due to either decreased uptake or increased elimination. Similar to traditional chemicals taken up by carriers/channels, NPs show saturation of the transport rate in dependence of the concentration of chemical in the exposure medium. While it is the limited number of carrier proteins for traditional chemicals, it is likely the available cell surface area that can be used to form endocytic vesicles in case of NPs.

Cited Work

1. A. Verma, et al., *Surface-structure-regulated cell-membrane penetration by monolayer-protected nanoparticles.* Nat. Mater., **2008**. 7: p. 588–595.
2. B.J. Teubl, et al., *Interactions between nano-tio2 and the oral cavity: Impact of nanomaterial surface hydrophilicity/hydrophobicity.* Journal of hazardous Materials, **2015**. 286: p. 298-305.
3. L. Shang, K. Nienhaus, and G.U. Nienhaus, *Engineered nanoparticles interacting with cells: Size matters.* Journal of Nanobiotechnology, **2014**. 12 (5).
4. Pascale R. Leroueil, et al., *Nanoparticle interaction with biological membranes: Does nanotechnology present a janus face?* Accounts of Chemical Research, **2007**. 40: p. 335-342.
5. B.M. Rothen-Rutishauser, et al., *Interaction of fine particles and nanoparticles with red blood cells visualized with advanced microscopic techniques.* Environ Sci Technol, **2006**. 40: p. 4353-4359.
6. K. Wittmaack, *In search of the most relevant parameter for quantifying lung inflammatory response to nanoparticle exposure: Particle number, surface area, or what?* Environ. Health Persp., **2007**. 115: p. 187–194.
7. W. Parak, K. Kettler, Editor. 2015.
8. C. Aberg, K. Kettler, Editor. 2015.
9. K.A. Dawson, K. Kettler, Editor. 2015.
10. K. Shapero, et al., *Time and space resolved uptake study of silica nanoparticles by human cells.* Mol Biosyst, **2010**. 7 (3): p. 371-378.
11. M.A. Maurer-Jones, et al., *Toxicity of engineered nanoparticles in the environment.* Analytical Chemistry, **2013**. 85 (6): p. 3036–3049.
12. S. Gangwal, et al., *Informing selection of nanomaterial concentrations for toxcast in vitro testing based on occupational exposure potential.* Environ. Health Persp., **2011**. 119 (11): p. 1539-1546.
13. E.C. Cho, Q. Zhang, and Y. Xia, *The effect of sedimentation and diffusion on cellular uptake of gold nanoparticles.* Nat. Nanotechnol., **2011**. 6 (6): p. 385–391.
14. P.M. Hinderliter, et al., *Isdd: A computational model of particle sedimentation, diffusion and target cell dosimetry for in vitro toxicity studies.* Part Fibre Toxicol, **2010**. 7 (36).
15. B.D. Chithrani and W.C.W. Chan, *Elucidating the mechanism of cellular uptake and removal of protein-coated gold nanoparticles of different sizes and shapes.* Nano Letters, **2007**. 7 (6): p. 1542-1550.
16. S. Yu, et al., *Size- and charge-dependent non-specific uptake of pegylated nanoparticles by macrophages.* Int. J. Nanomed, **2012**. 7: p. 799-813.
17. O. Lunov, et al., *Modeling receptor-mediated endocytosis of polymer-functionalized iron oxide nanoparticles by human macrophages.* Biomaterials, **2011**. 32: p. 547-555.
18. A. Salvati, et al., *Experimental and theoretical comparison of intracellular import of polymeric nanoparticles and small molecules: Toward models of uptake kinetics.* Nanomed-Nanotechnol, **2011**. 7: p. 818–826.
19. J.A. Kim, et al., *Role of cell cycle on the cellular uptake and dilution of nanoparticles in a cell population.* Nat Nanotechnol., **2012**. 7: p. 62-68.
20. C. Wilhelm, et al., *Interaction of anionic superparamagnetic nanoparticles with cells: Kinetic analyses of membrane adsorption and subsequent internalization.* Langmuir, **2002**. 18: p. 8148-8155.
21. N. Luciani, F. Gazeau, and C. Wilhelm, *Reactivity of the monocyte/macrophage system to superparamagnetic anionic nanoparticles.* J Mater Chem, **2009**. 19: p. 6373-6380.
22. L.K. Limbach, et al., *Oxide nanoparticle uptake in human lung fibroblasts: Effects of particle size, agglomeration, and diffusion at low concentrations.* Environ Sci Technol, **2005**. 39: p. 9370-9376.
23. C. Strobel, et al., *Fate of cerium dioxide nanoparticles in endothelial cells: Exocytosis.* J Nanopart Res, **2015**. 17 (206).
24. L. Hu, et al., *Influences of size of silica particles on the cellular endocytosis, exocytosis and cell activity of hepg2 cells.* Journal of Nanoscience Letters, **2011**. 1 (1).
25. S.D. Conner and S.L. Schmid, *Regulated portals of entry into the cell.* Nature, **2003**. 422: p. 37-44.
26. A.E. Smith and A. Helenius, *How viruses enter animal cells.* Science, **2004**. 304: p. 237-242.
27. J. Grove and M. Marsh, *The cell biology of receptor-mediated virus entry.* Journal of Cell Biology, **2011**. 195 (7): p. 1071–1082.
28. A. Lesniak, et al., *Effects of the presence or absence of a protein corona on silica nanoparticle uptake and impact on cells.* ACS Nano, **2012**. 6 (7): p. 5845–5857.

29. D. Guarnieri, et al., *Effect of serum proteins on polystyrene nanoparticle uptake and intracellular trafficking in endothelial cells.* J Nanopart Res, **2011**. 13: p. 4295–4309.
30. K. Sauerova, *Dls measurements*. 2016.
31. Nanocomposix, *Zeta potential analysis of nanoparticles*. 2012.
32. C. Wilhelm and F. Gazeau, *Universal cell labelling with anionic magnetic nanoparticles.* Biomaterials, **2008**. 29: p. 3161–3174.

Summary

Samenvatting

Acknowledgements

About the author

Summary

Introduction (Chapter 1)

The aim of this thesis was to gain a better understanding of NP properties and experimental conditions that determine cellular NP uptake in order to construct a model to describe property-effect relationships. In contrast to traditional chemicals that enter cells or organisms by passive diffusion, most NPs are taken up by cells via active uptake mechanisms. Therefore, this type of emerging chemicals requires new models that take this active mechanism into account. Predictive quantitation of the extent of NP uptake by living cells will enable inexpensive and easy risk assessment of NPs. Relating NP uptake kinetics to easily measurable NP properties can help to overcome the obstacle that not every NP type can be tested for their biological effects separately. On the long run such a correlation facilitates prioritization for toxicity and bioaccumulation testing and allow for the safe implementation of nanotechnology.

Nanoparticle properties and experimental conditions determining cellular nanoparticle uptake (Chapter 2)

A literature review was conducted to determine important factors for NP uptake. This resulted in an inventory of publications that determined the effect of NP properties such as size, charge, aspect ratio, core material, and surface modification and of experimental conditions such as cell type and medium composition on cellular, *in vitro* NP uptake. NP size, charge and medium composition (presence or absence of proteins) are the most well studied factors. We describe emerging patterns, such as the 50 nm size optimum and lower uptake for less charged NPs. We found NP size to play a critical role in the extent of uptake but also in uptake kinetics. We point to contradictory results and explain their possible causes. We give recommendations to overcome some of the observed obstacles, to fill knowledge gaps and resolve apparent contradictions.

Uptake kinetics of differently sized nanoparticles into 16HBE-14o cells (Chapter 3)

Having identified size as the probably most important determinant of uptake, we then explored the effect of NP size and medium composition on uptake kinetics into two different types of cells (Chapter 3, Chapter 4). 16HBE-14o cells, capable of the fundamental mechanism of endocytosis, took up 50 nm NPs to the largest extend in absence of FCS on mass basis. This proposed uptake optimum shifted towards 20 nm NPs when uptake was expressed as NP numbers. These results stress the importance of the measurand in which results of NP uptake studies are presented.

Uptake kinetics of differently sized nanoparticles into THP-1 cells (Chapter 4)

For comparison between different cell lines similar uptake studies, to those with 16 HBE-cells under environmental relevant exposure concentrations, were conducted with THP-1 cells. Macrophages are part of the immune system against invading cells and foreign agents including NPs. These cells have a special uptake mechanism called phagocytosis. The upper size limit for phagocytosis is approximately 10 µm. Therefore, they differ significantly from 16HBE-14o cells. Besides their importance as the first line of defense in organism, there is a considerable lack of NP uptake studies in this cell type. We, therefore, determined uptake rates for three NP sizes (20, 50, and 75 nm) in medium with and without FCS. Uptake in absence of FCS was higher than in the presence of FCS. In contrast to 16HBE-14o cells, THP-1 cells took up the 20 nm NPs faster in absence of FCS on mass basis than the larger NPs.

Method development to determine NP dissolution during the experiments (Chapter 5)

For uptake as well as toxicity studies, the size of NPs within a certain exposure medium over time is of great importance, especially for possibly dissolving NPs such as AgNPs. This is necessary to determine whether observed (toxic) effects might be caused by dissolution and the release of toxic ions. Therefore, a new method was developed to determine the stability and the abundance of Ag nanoparticles in the supernatant after cell exposure at different timings. Asymmetric flow field flow fractionation (AF4) allows for the size dependent particle separation. On-line hyphenation to the sensitive elemental detection by ICPMS results in the determination of the abundance of AgNPs of a certain size. Dissolution of 75 nm AgNPs in cell culture medium without FCS is much faster than in medium supplemented with FCS. The developed method is an important tool to study NP size/dissolution over time in *in vitro* test systems.

Exploring the possibility of read-across via QSARs on the extent of nanoparticle uptake into living cells (Chapter 6)

While fast and inexpensive risk assessment of the ever increasing number of NPs is needed, no general approach to modelling of uptake kinetics has been developed. We therefore tested whether cellular nanoparticle uptake follows first-order kinetics. This was indeed the case across different nanoparticles, cell lines and experimental conditions. Next, we determined whether the values of the parameters of first-order kinetics can be correlated to easily measurable NP properties such as size or charge to derive QSARs. Unfortunately, neither nanoparticle size nor charge correlated well with the parameters of first-order kinetics. This is probably caused by the heterogeneity of published data. Other factors such as exposure concentration and cell properties seem to be more important determinants of NP uptake. As a result, we give recommendations which information

should be included in future studies to prevent the piling up of data that cannot be incorporated into models with increased predictive power.

Samenvatting

Introductie (Hoofdstuk 1)

Het doel van dit proefschrift was het verkrijgen van inzicht in de eigenschappen van nanodeeltjes en experimentele condities die bijdragen aan de cellulaire opname van nanodeeltjes om een model op te kunnen stellen die eigenschap-effect relaties beschrijft. In tegenstelling tot traditionele stoffen, die cellen of organismen binnenkomen door passieve diffusie, worden de meeste nanodeeltjes door cellen opgenomen middels een actief opnamemechanisme. Om deze reden is er behoefte aan nieuwe modellen, die rekening houden met dit type mechanisme. Het kwantitatief voorspellen van de mate waarin nanodeeltjes worden opgenomen in levende cellen maakt goedkope en eenvoudige risicobeoordeling mogelijk. Daarbij kan het relateren van de kinetiek van nanodeeltjes aan hun eigenschappen helpen bij het overwinnen van het feit dat niet elk type nanodeeltje apart getest kan worden op biologische effecten. Op de lange termijn kan een correlatie als deze bijdragen aan de prioritering van stoffen gebaseerd op toxiciteit en bioaccumulatie en zorgen voor een veilige implementatie van nanotechnologie.

Chemische eigenschappen en experimentele condities die bijdragen aan cellulaire opname van nanodeeltjes (Hoofdstuk 2)

Een literatuurstudie is uitgevoerd om de belangrjste factoren gerelateerd aan de opname van nanodeeltjes te bepalen. Deze resulteerde in een inventarisatie van publicaties die het effect van eigenschappen van nanodeeltjes, waaronder grootte, elektrische lading, aspect ratio, kernmateriaal en oppervlakkige modificaties, en van experimentele condities, zoals celtype en mediumcompositie, op cellulaire *in vitro* opname van nanodeeltjes beschrijft. De grootte van nanodeeltjes, elektrische lading en de compositie van het medium (de aan- of afwezigheid van eiwitten) bleken de best bestudeerde factoren. We beschrijven patronen die naar voor komen, zoals het 50 nm optimum en de lagere opname van nanodeeltjes met een lager elektrisch potentiaal. De grootte van het nanodeeltje blijkt een kritische rol te spelen in zowel de mate van opname, als de opnamekinetiek. Verder wijzen wij op tegenstrijdige resultaten en gaan wij in op de mogelijke oorzaken. Tenslotte geven wij aanbevelingen om enkele van de waargenomen obstakels te overwinnen, kenniskloven te dichten en ogenschijnlijke tegenstrijdigheden op te lossen.

Opnamekinetiek van nanodeeltjes van verschillende groottes in 16HBE-14o cellen (Hoofdstuk 3)

Na het identificeren van grootte als (waarschijnlijk) de belangrijkste factor voor opname, onderzochten wij het effect van nanodeeltjesgrootte en mediumcompositie op de opname-kinetiek in twee celtypen (Hoofdstuk 3, Hoofdstuk 4). In 16HBE-14o cellen, die in staat zijn tot fundamentele endocytose, werden 50nm-deeltjes bij de afwezigheid van FCS op gewichtsbasis in de grootste mate opgenomen. Dit voorgestelde opname- optimum

schoof echter naar 20nm-deeltjes wanneer opname werd uitgedrukt in aantallen deeltjes. Deze resultaten benadrukken dan ook het belang van de manier waarop nanodeeltjes-opname wordt uitgedrukt.

Opnamekinetiek van nanodeeltjes van verschillende groottes in THP-1 cellen (Hoofdstuk 4)

Om een vergelijking te kunnen trekken tussen verschillende cellijnen zijn opname-experimenten, uitgevoerd op 16HBE-cellen, herhaald op THP-1 cellen. Macrofagen zijn onderdeel van het immuunsysteem tegen binnendringende lichaamsvreemde cellen, waaronder nanodeeltjes. Deze cellen maken gebruik van een speciaal opnamemechanisme, fagocytose genaamd. De bovengrens voor fagocytose is vastgesteld op ongeveer 10 µm, wat significant afwijkt van 16HBE-14o cellen. Naast het belang van deze cellen als eerstelijns afweermechanisme in organismen is er een aanzienlijk gebrek aan onderzoek aan de opname van nanodeeltjes in dit celtype. Om deze reden hebben wij voor drie verschillende deeltjesgroottes (20, 50, and 75 nm) de mate van opname vastgesteld in medium met en zonder FCS. De deeltjesopname was hoger in afwezigheid van FCS dan in het medium met FCS. 20nm-deeltjes werden sneller opgenomen in THP-1 cellen in afwezigheid van FCS (op gewichtsbasis) dan grotere deeltjes: Dit in tegenstelling tot 16HBE-14o cellen.

Methodeontwikkeling om desintegratie van nanodeeltjes tijdens experimenten te bepalen (Hoofdstuk 5)

In zowel opname- als toxiciteitsstudies speelt de grootte van nanodeeltjes in een bepaald blootstellingsmedium over tijd een belangrijke rol, zeker wanneer het potentieel oplosbare deeltjes betreft, zoals Ag-nanodeeltjes (nanozilver). Het is van belang om te bepalen of de waargenomen (toxische) effecten mogelijkerwijs veroorzaakt zijn door desintegratie en het vrijkomen van toxische ionen. Een nieuwe methode is ontwikkeld om op diverse tijdstippen de stabiliteit en abundantie van nanozilver te bepalen in het supernatant nadat de cellen zijn blootgesteld. Asymmetrische-stroom-veldstroomfractionering (AF4) zorgt voor grootte-afhankelijke separatie van nanodeeltjes. Deze techniek, gekoppeld aan analyses middels ICPMS resulteert in het vaststellen van de abundantie van nanozilver van een bepaalde grootte. De desintegratie van deeltjes nanozilver van 75 nm in een celcultuurmedium zonder FCS verliep veel sneller dan in een medium verrijkt met FCS. De ontwikkelde methode is een belangrijk hulpmiddel in het bestuderen van nano-deeltjesgrootte/desintegratie over tijd in *in vitro* testsystemen.

Het verkennen van de mogelijkheid tot "read-across"-aanpak via QSARs met betrekking tot de mate van opname van nanodeeltjes in levende cellen (Hoofdstuk 6)

Terwijl snelle en goedkope risicobeoordeling van nanodeeltjes nodig is, bestaat er nog geen algemene aanpak met betrekking tot het modelleren van opnamekinetiek. Om deze reden hebben wij getest of de cellulaire opname van nanodeeltjes wordt gekenmerkt door eersteordekinetiek. Dit was inderdaad het geval voor meerdere nanodeeltjes, cellijnen en experimentele condities. Hierop volgend hebben wij bepaald of de parameters gerelateerd aan eersteordekinetiek gecorreleerd kunnen worden aan makkelijk meetbare eigenschappen van nanodeeltjes, zoals grootte of elektrische lading, met als doel het opstellen van QSARs. Helaas bleek noch de deeltjesgrootte, noch de elektrische lading gecorreleerd te zijn aan deze parameters, wat hoogstwaarschijnlijk is veroorzaakt door de heterogeniteit in gepubliceerde data. Andere factoren, zoals de blootstellings-concentratie en celeigenschappen, lijken belangrijkere determinanten voor de opname van nanodeeltjes. Als gevolg hiervan geven wij aanbevelingen met betrekking tot welke informatie studies in de toekomst moeten bevatten. Dit om de ophoping van data te voorkomen, die niet gebruikt kunnen worden in modellen.

Acknowledgements

This work could never have been finished without the help and support of many people, whom I would like to thank.

First of all, I would like to thank my promotors Jan and Dik. Jan, I am deeply grateful that you helped me in so many different ways to finish my thesis. Without your patience in reviewing my manuscripts and asking the right questions to guide me to my own solution to a problem, I wouldn't be standing here. You helped with constructive and valuable feedback to improve my work. I appreciate that you were always available for input of new ideas, despite sometimes difficult circumstances, no matter how many times things needed to be discussed and revised. Thank you Jan for a positive, inspiring work atmosphere. Dik, thank you for your guidance and discussions to achieve the best possible results, for providing numerous suggestions to complete my thesis and for critical, yet encouraging, feedback. I appreciate your time spent reviewing and improving my manuscript, even beyond your retirement, giving constructive and invaluable comments for the success of my study.

Furthermore, I would like to express my appreciation to Dr. Wim H. de Jong for the opportunity to conduct experiments in the laboratories of RIVM and valuable suggestions for the resulting manuscripts. Wim, your expertise was always very helpful when it came down to toxicology and lab work in general. The collaboration was very inspiring and fruitful. I learned so much in a short period of time! On the same line I would like to thank Christina Giannakou for her help in the labs of RIVM and cheerful lunchbreaks.

Petra, thank you for your support! Not just with the actual lab work at Philips, but also the emotional support thereafter, even until today. I am glad that I had the chance to work with you and appreciate what I learned from you. I highly appreciate your advice.

My thanks are extended also to all staff members and colleagues at the Department of Environmental Science, Radboud University Nijmegen. Special thanks go to you, Gina, for your support with organizational things and all your answer to whom to contact, where, when and what… Thanks to all PhD students at our department for nice company at lunch breaks and conferences over the last years. My special thanks go to Leonie, Lisette, and Renske for the support, friendship and good times that we shared together in the office. It helped me tremendously to be able to discuss work related issues with somebody that has overcome similar obstacles, and even more so issues not related to work. Thank you Leonie and Renske for your support as my paranymphs on such an important day! I think without your support I would have gone insane.

And last but not least I would like to express my heartfelt thanks to my whole family and friends.
Mein ganz besonderer Dank an Mama, Papa, Verena und Agnes, aber auch meine Großeltern, Iris, Jessy, Jenny, Sandy, Rowena und Kerstin. So recht weiß ich gar nicht so ich anfangen soll weil es so viele Dinge gibt, für die ich dankbar bin: dass mich jeder von euch auf seine ganz eigene Art und Weise unterstützt hat. Mama, Papa, ich bin dankbar dass ihr mich immer dazu ermutigt habt meine eigenen Vorstellungen zu verwirklichen und mir geholfen habt mich beruflich zu entfalten und weiter zu entwickeln. Ich danke meiner Familie und Freunden für ihre unendliche Unterstützung und Ermunterung um dieses Kapitel erfolgreich abschließen zu können. Ihr habt mich bestärkt wenn ich zweifelte, eine Richtung aufgezeigt wenn ich planlos war, mir gezeigt dass ich euch wichtig bin und euch mit mir über die kleinen und größeren Erfolge gefreut, welche umso schöner wurden. Ich bin glücklich so eine Familie zu haben!
Thomas, danke dir für die vielen glücklichen Stunden seitdem ich dich kenne, für deine Geduld und dein Verständnis, für deine Unterstützung und dass du an mich glaubst und immer ein offenes Ohr für mich hast. Danke aber vor allem dass du einfach da bist, bei mir, und mein Leben somit glücklicher machst.

About the author

Curriculum vitae

Katja was born in Duisburg, Germany, on January the fifth 1986, where she also grew up. After participating in a student exchange in Michigan, USA, she graduated in Germany in 2005. The same year, she started her studies of 'Water Science: Microbiology, chemistry and analytics' at the University Duisburg-Essen. During her study, she conducted her Bachelor thesis at the Norwegian University of Science and Technology with focus on the epimerization of alginates. She conducted her Master thesis at 'IHE, Unesco Institute for water education' in Delft. Her master thesis focused on copper and zinc immobilization by Cupriavidus metallidurans CH34.

In 2012, she started as a PhD at the Radboud University Nijmegen where she investigated the nanoparticle properties and experimental conditions that determine nanoparticle uptake into living cells and to assess their suitability for modeling to describe such a relationship. During this research period she conducted lab work at the National Institute for Public Health and the Environment (RIVM, Bilthoven, the Netherlands), focusing on nanoparticle uptake studies in different cell lines and toxicity testing.

Since 2017 she is working at the German federal institute for risk assessment on two different projects. One project focusses on the hazard of nanomaterials and aims to develop new grouping approaches based on the mechanism of action of nanomaterials. It involves extensive lab work such as nanoparticle toxicity screening in different cell lines. It also includes modern systems biology approaches such as transcriptomics, metabolomics and proteomics studies. The other project aims at the development of criteria for the grouping of nanomaterials with regard to exposure-, hazard-, and risk-potential with the focus on consumer protection.